

# Hyperbaric Conditions

David J. Doolette<sup>\*1,2</sup> and Simon J. Mitchell<sup>3</sup>

## ABSTRACT

Exposure to elevated ambient pressure (hyperbaric conditions) occurs most commonly in underwater diving, during which respired gas density and partial pressures, work of breathing, and physiological dead space are all increased. There is a tendency toward hypercapnia during diving, with several potential causes. Most importantly, there may be reduced responsiveness of the respiratory controller to rising arterial CO<sub>2</sub>, leading to hypoventilation and CO<sub>2</sub> retention. Contributory factors may include elevated arterial PO<sub>2</sub>, inert gas narcosis and an innate (but variable) tendency of the respiratory controller to sacrifice tight control of arterial CO<sub>2</sub> when work of breathing increases. Oxygen is usually breathed at elevated partial pressure under hyperbaric conditions. Oxygen breathing at modest hyperbaric pressure is used therapeutically in hyperbaric chambers to increase arterial carriage of oxygen and diffusion into tissues. However, to avoid cerebral and pulmonary oxygen toxicity during underwater diving, both the magnitude and duration of oxygen exposure must be managed. Therefore, most underwater diving is conducted breathing mixtures of oxygen and inert gases such as nitrogen or helium, often simply air. At hyperbaric pressure, tissues equilibrate over time with high inspired inert gas partial pressure. Subsequent decompression may reduce ambient pressure below the sum of tissue gas partial pressures (supersaturation) which can result in tissue gas bubble formation and potential injury (decompression sickness). Risk of decompression sickness is minimized by scheduling time at depth and decompression rate to limit tissue supersaturation or size and profusion of bubbles in accord with models of tissue gas kinetics and bubble formation and growth. © 2011 American Physiological Society. *Compr Physiol* 1:163-201, 2011.

## Background

This article describes gas exchange at ambient pressures substantially greater than that at sea level. Moon et al. (200) observe that “the performance of the human lung in the diving environment is remarkable” and point out that adequate gas exchange has been achieved at pressures up to 71 atmospheres absolute (atm abs) and at inspired gas densities of up to 25 g/liter. Nevertheless, despite this adaptability, the exchange of metabolic gases can be perturbed under hyperbaric conditions, particularly when combined with immersion, the use of underwater breathing apparatus (UBA), and exercise, as is the case in underwater diving. Moreover, the uptake of inert gases under hyperbaric conditions may cause problems not seen at normal pressure. Although a narrow and highly specialized subject, the physiological changes and perturbations in gas exchange associated with hyperbaric exposure are a fascinating extension to knowledge of normal physiology.

The article begins with a brief background on pressure measurement and hyperbaric environments. This is followed by discussion of selected practical, environmental, and medical issues of diving that are relevant to the subsequent discussion of gas exchange. The remainder of the article is organized around the gases themselves. Though not usually discussed in the context of gas exchange in normal physiology, exchange of nitrogen is particularly relevant in hyperbaric environments. Thus, the exchange of carbon dioxide, oxygen, and nitrogen<sup>4</sup> (and other diving diluent gases) is each treated separately in its own section.

Most human exposures to hyperbaric conditions occur during underwater diving where the water column above the diver exerts a hydrostatic pressure that is additive to the atmospheric pressure. Hyperbaric exposures also occur in certain occupational environments that are pressurized, such as the cavity formed in front of a drill head during modern tunneling projects (18), and caissons that allow underwater access to work sites by construction workers who remain dry (156). Similarly, patients undergoing hyperbaric oxygen therapy (HBOT) and attending staff inside “multiplace” hyperbaric chambers are exposed to a compressed gas environment. Rarely, unintentional exposure to hyperbaric conditions may occur, such as in the case of sunken submarines where water ingress compresses remaining air spaces (112).

Any discussion of hyperbaric conditions requires quantification of pressure (force per unit area). The SI unit of pressure is the pascal (Pa), where 1 Pa = 1 newton per square meter. However, because of the relationship of this subject

\*Correspondence to david.doolette.as@navy.mil

<sup>1</sup>Navy Experimental Diving Unit, Panama City, FL

<sup>2</sup>Department of Anesthesiology, Duke University Medical Center, Durham, NC

<sup>3</sup>Department of Anesthesiology, University of Auckland, Auckland, New Zealand.

Published online, November 2010 ([comprehensivephysiology.com](http://comprehensivephysiology.com))

DOI: 10.1002/cphy.c091004

Copyright © American Physiological Society

<sup>4</sup>Throughout this article, “nitrogen” and “oxygen” are used to mean nitrogen gas (N<sub>2</sub>) and oxygen gas (O<sub>2</sub>), respectively.

area to diving, much of the relevant physiological literature expresses pressure in terms more familiar to workers in that field. Thus, pressure is often expressed as multiples of standard atmospheric pressure at sea level (1 standard atmosphere = 101.325 kPa) or even as depths of sea water. Atmospheres are usually given as absolute pressures (atm abs), whereas meters of sea water (msw) or feet of sea water (fsw) are generally gauge pressures referenced to zero at 1 atm abs (sea level). Thus, a diver at 10.13 msw is exposed to an ambient pressure of 2 atm abs, 1 imposed by the atmospheric pressure and 1 imposed by hydrostatic pressure. Commonly used units of pressure are given here:

$$\begin{aligned} 1 \text{ atm abs} &= 101.325 \text{ kPa} = 1.01325 \text{ bar} = 10.13 \text{ msw} \\ &= 33.08 \text{ fsw} = 760 \text{ mmHg} \end{aligned}$$

## An Introduction to Diving and Diving Equipment

Divers can be classified into a variety of communities based on diving practice, purpose, and to some extent, demographics. The largest such community are “recreational divers” who are occasional participants performing relatively brief, shallow dives primarily to appreciate the ocean’s wonders. Recreational divers are a diverse group spanning a wide age range. Several large training agencies provide courses that make open water diving available to children as young as 10 years, albeit with covenants on depth and supervision. There is no upper age limit and some dive until well into their sixth decade or later. In contrast, occupational divers are a more homogeneous group. They are usually young males between the ages of 20 and 45 who are fit and well (197).

The sobriquet “recreational” also embraces focused enthusiasts such as photographers, cave divers, wreck divers, and others. A recent and significant trend in recreational diving is the use of gases other than air and other advanced diving techniques, previously the province of military and certain occupational diving groups, in order to explore deeper depths for longer periods. These divers refer to themselves as “technical divers.” Some of the advanced exponents are performing more challenging and aggressive dives than any occupational diving organization, yet they remain recreational divers nonetheless.

“Occupational diving” embraces a number of diverse groups. The traditional occupational groups were “construction” or “commercial” divers working on projects such as underwater building, drilling, dredging, and ship’s husbandry. Although some of the tasks performed by these divers have been devolved to unmanned remote operated vehicles, there remains a large construction diving industry, especially in relation to offshore oil fields. Military divers perform not only many of the same construction, repair, and salvage tasks as commercial divers but also other distinctive tasks such as explosive ordinance disposal and covert special operations. The



**Figure 1** Recreational “scuba” (self-contained underwater breathing apparatus) diver using a standard single-cylinder and open-circuit demand valve regulator configuration.

term *occupational diving* is also used to embrace other groups of regulated divers such as police divers, scientific divers, public safety divers, and recreational diving instructors.

The vast majority of dives are air-breathing “bounce dives” (dives lasting minutes or hours) to less than 5 atm abs made by recreational or in-shore occupational divers. Bounce dives breathing various helium-nitrogen-oxygen mixtures are commonly conducted to 10 atm abs and occasionally deeper. “Saturation dives” (dives of sufficient duration that all tissues are in equilibrium with the elevated inspired gas pressures) to a maximum of 30 atm abs are relatively routine in the off-shore oil industry. Saturation divers live in a dry, pressurized helium-nitrogen-oxygen atmosphere, typically in a “deck decompression chamber,” and commute in a pressurized “diving bell” to an underwater worksite where they work, immersed, for several hours. A few shallow, air-breathing saturation dives take place in sea-floor habitats, typically as part of scientific programs.

Virtually all recreational diving and a significant proportion of occupational diving are undertaken using self-contained underwater breathing apparatus (SCUBA). This most commonly consists of a pressure regulator and demand valve attached to one or more compressed gas cylinders (Fig. 1). These “open circuit” configurations release exhaled gas into the water and make inefficient use of a finite gas supply, particularly at deeper depths, because the mass of gas supplied to achieve a normal tidal volume is directly proportional to the ambient pressure. Less commonly, scuba divers breathe from a closed-circuit UBA that incorporates a counterlung and CO<sub>2</sub> absorbent canister (Fig. 2). Gas is added only to maintain the volume and oxygen content of this breathing loop. Such devices are known as “rebreathers” since respired gas is recycled. They have the advantages of consuming much smaller amounts of gas during a dive and, because they emit

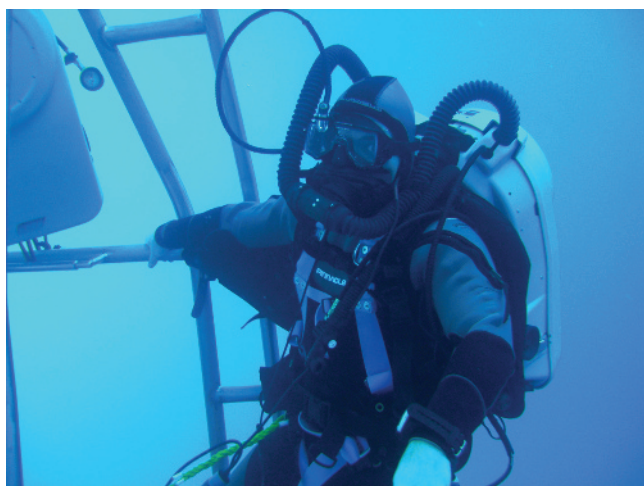


**Figure 2** Diver using a closed-circuit rebreather. U.S. Navy Experimental Diving Unit photograph.

few bubbles, making a covert diver difficult to detect from the surface. Occupational divers may utilize “surface supply” breathing apparatus in which gas is supplied from a surface platform or diving bell to which the diver is tethered by an “umbilical” (Fig. 3). The use of an umbilical has



**Figure 3** Divers in surface supply diving equipment. Each diver has an umbilical supplying gas from the surface and an emergency “bailout” cylinder of gas. Note the oronasal mask visible behind the helmet faceplate of the diver facing the camera. U.S. Navy photograph by Chief Petty Officer Andrew McKaskle.

the advantage of providing a large gas supply and conduits for heating, voice and video communication, and power for lights.

All of these forms of underwater breathing equipment are designed to supply the diver with gas at ambient pressure (which usually corresponds to the pressure at the depth of the mouth) or very close to it. If the inspired gas pressure (and therefore the gas pressure in the lungs) were not kept equivalent to the increasing ambient pressure during descent, then a negative static lung load and negative pressure breathing would rapidly develop (183). If the negative transmural pressure exceeded 150 cmH<sub>2</sub>O (which would be expected after a descent of only approximately 1.5 m), then it would exceed the average adult’s ability to generate inspiratory pressure (229) and inhalation would rapidly become impaired and then impossible.

### Medical complications of diving

The pressure changes of descent and ascent can cause changes in the volume of anatomical or equipment air spaces as predicted by the ideal gas law:

$$PV = nRT \quad (1)$$

where  $P$  = absolute pressure,  $V$  = volume,  $n$  = number of moles of gas,  $R$  = universal gas constant, and  $T$  = temperature.

Divers attempt to prevent injury that might result from volume changes in these air spaces by equalizing the pressure in those spaces with gas at ambient pressure. In the middle ear, this is achieved by the movement of gas through the eustachian tube, and in the lungs, pressure equalization is achieved by breathing a gas supplied at ambient pressure by the UBA. Failure to compensate pressure in these ways may result in injury or “barotrauma”; most commonly middle ear barotrauma during descent; and most seriously, pulmonary barotrauma (which can cause arterial gas embolism) during ascent.

Since breathing gas must be supplied at ambient pressure, it follows that the deeper the dive, the greater the inspired gas pressure. This has several very important implications.

First, all other factors being equal, the deeper the dive then, the greater the density of the gas being breathed. This increases resistance to flow of gas through airways and breathing apparatus, increases work of breathing, and reduces ventilatory capacity in a manner that will be discussed in detail later. Divers can mitigate these changes by reducing the density of the respired gas. This is one of several reasons for the use of gas mixes containing a light gas such as helium (see Table 1) as a diluent for oxygen.

Second, breathing gases at elevated partial pressure will provoke effects whose onset and severity may be variable but essentially inevitable given sufficient pressure. For example, the nitrogen in air produces anesthesia if breathed at very high partial pressures (190). The incipient anesthetic effect, called nitrogen narcosis, is first evident in humans breathing

**Table 1** Gas Densities Measured at 1 atm abs

Gas	Molecular weight	Density <sup>a</sup>
H <sub>2</sub>	2.016	0.090
He	4.003	0.179
Ne	20.183	0.901
N <sub>2</sub>	28.016	1.251
O <sub>2</sub>	32.0	1.428
Air	28.966	1.293
SF <sub>6</sub>	146.066	6.521

From Miller (186).

<sup>a</sup>Density (g/liter) = Molecular weight/22.4 liter.

air at about 4 atm abs (15) and is characterized by emotional changes, impaired higher mental processes, and impaired neuromuscular control. Above 10 atm abs, air breathing can result in unconsciousness (131). Avoidance of narcosis is another argument for the use of helium, which is not anesthetic, instead of nitrogen in gas mixtures for deeper diving. Another example is cerebral oxygen toxicity as a consequence of breathing oxygen at a high-inspired  $P_{IO_2}$  ( $P_{IO_2}$ ). The most feared manifestation is the unheralded onset of a generalized seizure (38). Risk rises with both the  $P_{IO_2}$  and duration of the oxygen exposure. Most diver training agencies impose a maximum  $P_{IO_2}$  for divers at work underwater, typically 1.4 atm or less. Limited duration exposure to a higher  $P_{IO_2}$  may be allowed if breathing a high inspired oxygen fraction ( $F_{IO_2}$ ) in shallow water.

Third, breathing inert diluent gases such as nitrogen and helium at increased pressure results in their uptake into blood and tissues. During ascent (or “decompression”) to sea level, bubbles often form from this excess dissolved gas and potentially cause harm (93). Clinical manifestations of bubble formation are not inevitable but if present, decompression sickness (DCS) is diagnosed. Severity ranges from mild to catastrophic. Musculoskeletal pain is the most common symptom, whereas spinal cord involvement with sensory deficits and muscle weakness is the most common permanently incapacitating variant. Massive intravascular bubble formation can cause fatal cardiopulmonary collapse (92). Divers are taught to minimize the risk of DCS by utilizing tables or dive computers that prescribe time and depth combinations and ascent protocols with decompression stops when necessary. These issues will be explored in more detail later in the article.

### Hyperbaric oxygen treatment

After diving, the second most common form of hyperbaric exposure is in pressure chambers for the purpose of HBOT, which is indicated in a number of medical problems that include selected nonhealing wounds (244), radionecrosis in soft tissue or bone (84), and DCS or arterial gas embolism in divers (201).

Hyperbaric chambers may be “monoplace” or “multiplace”. Monoplace chambers (see Fig. 4) accommodate only



**Figure 4** Monoplace hyperbaric chamber. The patient is the only occupant. The chamber may be pressurized with air and 100% oxygen delivered via a demand valve and oronasal mask, or the chamber may simply be pressurized with oxygen.

the patient undergoing treatment, and are often pressurized with oxygen. The patient simply breathes from the chamber atmosphere. Multiplace chambers (see Fig. 5) accommodate multiple patients who are accompanied by one or more attendants during the compression. These chambers are pressurized with air, and the patients breathe oxygen via either a demand valve analogous to a diver’s scuba regulator, or a hood and neck seal system through which oxygen freely flows at a rate designed to prevent carbon dioxide accumulation.

### Carbon Dioxide

Carbon dioxide (CO<sub>2</sub>) is a product of cellular metabolism. It is a volatile acid by virtue of its reaction with water to produce bicarbonate and hydrogen ions, and pathophysiologic effects may arise from changes in *pH* resulting from low or high  $PCO_2$  in blood and tissues. Consequently, in normal physiology, the  $P_{aCO_2}$  is controlled around a mean of 38.3 mmHg (5.1 kPa) ( $\pm 7.5$  mmHg = 2 SD) (180) by regulation of alveolar ventilation. Ideally, neither the arterial nor the alveolar  $PCO_2$  should change as a result of hyperbaric exposure, though the concentration of alveolar CO<sub>2</sub> (but not its partial pressure) will fall as the pressure of the inspired gas rises with ambient pressure. However, derangement of CO<sub>2</sub> homeostasis is one of the most important disturbances of gas exchange associated with diving and the use of UBA. Specifically, as will be explained, there is a particular predisposition to hypercapnia.

### Production and transport of CO<sub>2</sub>

The production, transport, and elimination of CO<sub>2</sub> in normal physiology have been described in detail elsewhere in *Comprehensive Physiology*. CO<sub>2</sub> is produced in the citric acid



**Figure 5** Multiplace hyperbaric chamber. The chamber is pressurized with air, and delivery of 100% oxygen may be achieved either by the use of a hood sealed around the neck through which oxygen free flows or by a demand valve and oronasal mask.

cycle in the mitochondria. At equivalent levels of work and metabolism, production of  $\text{CO}_2$  is not altered by hyperbaric exposure *per se* (5). However, the work demands of diving can increase  $\dot{V}\text{O}_2$  and  $\dot{V}\text{CO}_2$ , as may other aspects of the particular diving or hyperbaric environment such as increased thermal stress (231). It is also possible that because of multiple factors that may increase the work of breathing (see the section titled “Hypoventilation by perturbation of respiratory control”) ventilation itself may be responsible for a greater proportion of total oxygen consumption (and therefore  $\text{CO}_2$  production) in some hyperbaric scenarios (81, 194, 232), though the significance of this has been debated (259) on the basis of experiments at 1 atm abs demonstrating no increase in submaximal  $\dot{V}\text{O}_2$  as external respiratory load was increased by more than would be expected in diving (33, 57).

Once liberated in mitochondria,  $\text{CO}_2$  diffuses down partial pressure gradients into cytoplasm, tissue, and blood. The three means of transport of  $\text{CO}_2$  in blood (in solution, as bicarbonate, and in carbamino compounds) can be reviewed elsewhere in *Comprehensive Physiology*. A potential difference in this transport paradigm may arise during hyperbaric conditions from a small fall in the solubility of  $\text{CO}_2$  in venous blood that results from a decrease in carbamino compound formation. At higher  $\text{P}\text{I}\text{O}_2$ , an increasing fraction of the total arteriovenous oxygen extraction can be met from dissolved oxygen alone (see the “Oxygen” section later), and the arteriovenous difference in hemoglobin (Hb) saturation falls accordingly. The  $\text{S}_{\text{vO}_2}$  is elevated, and the Haldane effect is correspondingly attenuated causing the venous  $\text{P}\text{CO}_2$  to rise slightly. Using standard blood gas parameters, Forkner et al.

(88) predicted that the  $\text{P}_{\text{vCO}_2}$  would rise by only 0.5 mmHg during 100% oxygen breathing at 1 atm abs (corresponding with a  $\text{S}_{\text{vO}_2}$  of 85%), and 1.2 mmHg if the  $\text{S}_{\text{vO}_2}$  remained 99%. In fact, Whalen et al. (292) measured venous and arterial gases in dry, resting, healthy humans breathing air or 100% oxygen at 1 or 3.04 atm abs. During oxygen breathing at 3.04 atm abs, the  $\text{S}_{\text{vO}_2}$  was 100% in 8 of 10 subjects, and there was a 4-mmHg increase in the mean  $\text{P}_{\text{vCO}_2}$ . There was also a small drop in venous  $\text{pH}$  associated with the reduced buffering capacity of oxyhemoglobin.

References to this phenomenon occasionally appear on Internet diving forums, framed in claims that a high  $\text{P}\text{I}\text{O}_2$  may contribute to hypercapnia in diving by “blocking” the carriage of  $\text{CO}_2$  from tissue to lung in venous blood. In fact, the significance of the issue in hyperbaric environments remains uncertain. The disturbance in  $\text{CO}_2$  carriage imposed by an increased  $\text{S}_{\text{vO}_2}$  appears easily compensated in experimental studies at 1 atm abs by an increase in ventilation thought to be induced by changes in  $\text{pH}$  at the central chemoreceptors (13). Indeed, mild hypocapnia recorded in air-breathing divers resting at 190 fsw ( $\text{P}\text{I}\text{O}_2 = 1.42$  atm) compared to 15 fsw ( $\text{P}\text{I}\text{O}_2 = 0.30$  atm) was attributed to just such compensation (129). Even in Whalen’s subjects with an  $\text{S}_{\text{vO}_2}$  of 100% at 3.04 atm abs, the  $\text{P}\text{aCO}_2$  did not change; however, the minute ventilation was not measured in these experiments (292). Notwithstanding these reassuring findings, the possibility remains that disturbance of  $\text{CO}_2$  carriage by attenuation of the Haldane effect could be more significant in certain hyperbaric conditions if there was difficulty in mounting a compensatory increase in minute ventilation. Piantadosi (218) acknowledged

this possibility in respect of patients with respiratory disease undergoing HBOT. This caveat may also apply to divers operating under conditions where ventilatory capacity is reduced by mechanisms that we describe in detail in the following sections (173). However, out of concern for oxygen toxicity, divers do not normally expose themselves to  $P_{iO_2}$  that would result in an  $S_{vO_2}$  of 100%, so the impairment of the Haldane effect would be less complete than during HBOT.

## Elimination of $CO_2$

Elimination of  $CO_2$  may be impaired under hyperbaric conditions, and  $CO_2$  may be retained. In one of the earliest relevant investigations, Lanphier studied the effect of breathing oxygen at 26 fsw (1.8 atm abs) and helium-oxygen and nitrogen-oxygen mixtures at 99 fsw (4 atm abs) during both work and rest on end-tidal  $CO_2$  levels in immersed divers (171). In his classic report published in 1955, he revealed a general tendency to retain  $CO_2$ , particularly by exercising divers breathing the denser nitrogen-oxygen gas mix at the deeper depth. The consequences of hypercapnia in diving are further discussed later, but since it may contribute to disabling dyspnoea (298), and predispose to oxygen toxicity (39), nitrogen narcosis (126) and blackout (203), it is not surprising that the issue has subsequently occupied many prominent minds in the field. There are now multiple studies that have confirmed the general tendency to retain  $CO_2$ , particularly when breathing dense gas while exercising at higher ambient pressure (36, 39, 129, 149, 152, 182, 231-233, 251, 298, 299). Some of these studies, and others, have also provided insight into the mechanisms of this phenomenon. Although Lanphier (171) singled out nitrogen breathing as an important contributor during his experiments, his method exposed the divers to several factors that were later considered potentially relevant by various researchers, including immersion; the use of breathing apparatus; dense gas; and higher partial pressures of both nitrogen and oxygen.

The relative importance (or lack thereof) for these factors will be discussed below, but at this point, it is important to be clear that the final common pathway by which they may contribute to hypercapnia is relative hypoventilation. This is hardly surprising given the well-understood dependence of  $CO_2$  elimination on alveolar ventilation in normal physiology, as described by the simple equation (31):

$$P_{ACO_2} \text{ (mmHg)} = 863 \times \frac{\dot{V}_{CO_2} \text{ (liters/min STPD)}}{\dot{V}_A \text{ (liters/min BTSP)}} \quad (2)$$

Thus, as pointed out by Camporesi and Bosco (31) at a constant work rate the  $\dot{V}_{CO_2}$  will remain approximately constant across the usual diving depth range and  $P_{ACO_2}$  will then be dependent on alveolar ventilation. A fall in  $\dot{V}_A$  relative to  $\dot{V}_{CO_2}$  represents hypoventilation and will result in a proportional rise in  $P_{ACO_2}$ . There is no definitive unifying explanation for alveolar hypoventilation under hyperbaric conditions (and diving in particular), but relevant studies sug-

gest potential contribution from three mechanisms: limitation of ventilatory capacity; perturbation of control of breathing; and an increase in dead space.

## Hypoventilation by limitation of ventilatory capacity

Hypercapnia could occur during underwater work if the diver's ability to eliminate  $CO_2$  was exceeded by its production. As suggested by Miller (195), when exercise ventilation intercepts maximum breathing capacity (MBC), the exercise limit for normocapnic ventilation is reached. In healthy subjects breathing air at atmospheric pressure, ventilation does not limit exercise in this way (180). Indeed, it has been shown that exercise at 80% of aerobic capacity utilizes 50% to 60% of MBC (239), and that  $P_{ACO_2}$  does not rise (and may in fact fall) during maximal exercise in both trained and untrained subjects (32). In contrast, Anthonisen et al. (5) exercised subjects breathing oxygen-nitrogen mixes at a constant  $P_{O_2}$  of 0.2 atm in a dry hyperbaric environment at 4 and 6 atm abs to show that at these pressures the maximal exercise ventilation may closely approach or equal the MBC, which falls significantly at the higher pressures. Similar findings were reported by Wood and Bryan (299) and Miller (195). The obvious implication, put simply, is that a given level of exercise will produce the same amount of  $CO_2$  and mandate the same volume of alveolar ventilation to maintain normocarbica irrespective of ambient pressure, yet as ambient pressure increases, the MBC decreases markedly (Fig. 6); potentially to a point that equals or falls below the required exercise ventilation.

Why does the MBC fall under hyperbaric conditions? As pointed out by Camporesi and Bosco (31), one explanation in diving would be the imposition of substantial external airway resistance in poorly configured breathing apparatus. But the phenomenon is also seen in carefully controlled experiments where low resistance breathing circuits are used (Fig. 6) and a physiological explanation is required. This is provided in large part by the increasing density of the respired gas (31). Density-related reduction in MBC occurs because of the increased resistance to flow and augmentation of the pressure drop that occurs during nonlaminar flow of a denser gas through the airways. While fully developed laminar flow is unaffected by changes in gas density, the development of parabolic laminar flow in the repeatedly bifurcating architecture of the respiratory tree is impeded by unfavorable entrance length characteristics as comprehensively described by Clarke and Flook (45). They strongly argue that laminar flow is unlikely during respiration of gas at equivalent density to air at 4 atm abs or more, even during quiet breathing in distal airway generations where it is usually predicted to occur. It follows that resistance to flow ( $R$ ) (45) and pressure drop ( $\Delta P$ ) (215) along the lower airway can be described by equations that include terms for density and viscosity.

$$\Delta P = K(\mu\rho)^{\frac{1}{2}} \dot{V}^{\frac{3}{2}} \quad (3)$$

$$R = K(\mu\rho\dot{V})^{\frac{1}{2}} \quad (4)$$

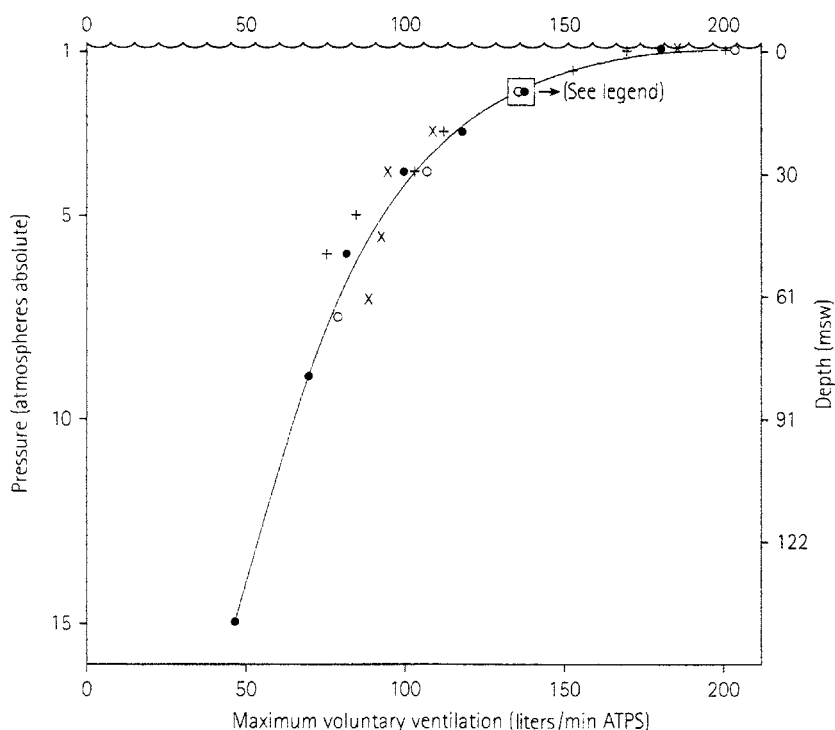


**Figure 6** Pooled data demonstrating the fall in maximum breathing capacity as ambient pressure increases. The studies were conducted using nonimmersed subjects breathing air. Reproduced with permission from Camporesi and Bosco (31).

where  $K$  is a constant dependent on lung anatomy and volume;  $\mu$  = viscosity;  $\rho$  = density; and  $\dot{V}_A$  = flow.

Increases in  $\Delta P$  and resistance potentially affect both inspiratory and expiratory flows, and both appear to make approximately equal contributions to reduction of MBC at high gas density (188). It is appropriate at this point to consider inspiration and expiration separately.

Expiratory flow limitation due to dynamic airways compression (186) is well described in normal respiratory physiology and is discussed in detail elsewhere in the “Respiratory” section of *Comprehensive Physiology*. During a forced expiration the pleural pressure rises and is transmitted to the alveoli where it is additive to the static recoil pressure of the lung. As gas flows outward along the airways the pressure within the airway falls [Eq. (3)]. In the distal airways, particularly beyond generation 11 where structural rigidity is diminished (180), the airway is prone to collapse at a point proximal to that where the intrathoracic pressure equals the airway pressure (the “equal pressure point”). Any further increase in pleural pressure contributes to the Starling resistor effect and achieves no increase in flow. Expiration is therefore said to be effort independent. At higher lung volumes the airways are dilated and elastic recoil is greater, so achievement of effort independence requires higher flow rates. This gives rise to the distinctive shape of the maximal expiratory flow-volume loop (Fig. 7). The mechanics underpinning expiratory flow limitation have received more

contemporary analysis in the form of “wave-speed theory” (54), but the fundamental relationships with key parameters such as flow velocity and gas density remain similar to those assumed by the more traditional explanation outlined above and which has been used to interpret the relevant hyperbaric studies.

Since the pressure drop during flow of gas through the airway will be greater during respiration with dense gas, it might be expected that dynamic airway compression would supervene at lower pleural pressures and flow rates than usual when a dense gas is respired (195). This can be demonstrated under normobaric conditions by comparing exhalation of nitrogen and helium gas mixes of differing density (191) and also under hyperbaric conditions by progressively increasing ambient pressure, which will increase the density of whatever gas is respired. Wood and Bryan (298) measured flow-volume loops and generated isovolume pressure-flow curves during air breathing at ambient pressures between 1 and 10 atm abs. The results at these pressure extremes for one of their subjects are shown in Figure 7. At 10 atm abs, equivalent increases in flow required a greater increase in pleural pressure and maximal flow rates were dramatically limited by the plateau of the isovolume pressure-flow curve. This, in turn, would limit MBC and the authors predicted that “a vicious circle could be established during exercise by an increased work of breathing without an attendant increase in ventilation leading to carbon dioxide accumulation.” In other words, if gas of sufficient

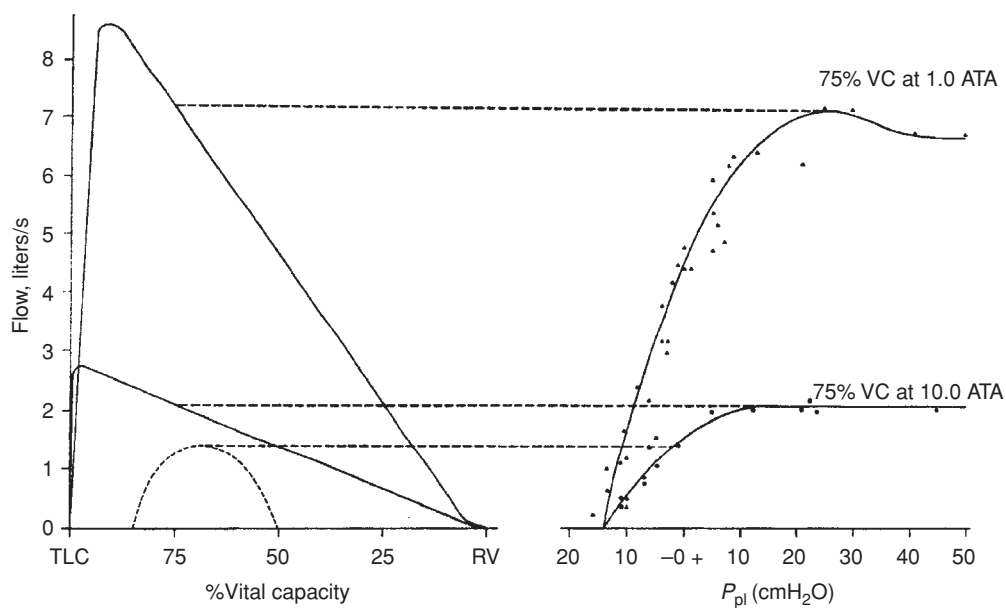


**Figure 7** Maximum expiratory flow-volume curves and isovolume pressure-flow curves at 75% vital capacity (VC) for a single subject breathing air at 1 and 10 atm abs. In the 1 atm abs condition, a small increase in pleural pressure results in a substantial increase in flow. At 10 atm abs, a small increase in flow requires a much greater increase in pleural pressure, and further increases are limited by the plateau of the isovolume pressure-flow curve at relatively low flow rates. TLC, total lung capacity. Reproduced with permission from Wood and Bryan (298).

density were breathed during exercise, then expiratory flow limitation might impair breathing capacity to the point where it is impossible to maintain normocapnia. Greater respiratory effort by the respiratory muscles driven by rising CO<sub>2</sub> levels would serve only to generate more CO<sub>2</sub>, and the vicious circle would be established.

It was recently suggested that this scenario may have explained a unique fatal accident during a rebreather dive at 264 m of fresh water (26 atm abs) where the diver wore a video camera that recorded the circumstances of his death (198). Although the diver appears to be performing little external work, the video reveals progressive tachypnoea, ultimately ending with the “choking dyspnoea” previously described as becoming limiting during studies of maximal exercise under hyperbaric conditions (299). At the maximum depth where the respiratory problems occurred, the inspired gas mixture containing oxygen, helium, and nitrogen had a density of 10.2 g/liter (approximately 8.5 times the density of air at 1 atm abs). While moderate exercise has been performed without similar problems by subjects breathing gas of similar (and greater) density in experimental settings, it is notable that this diver was using a rebreather with a back-mounted counterlung. This will impose a negative transrespiratory pressure (or “static lung load”) because the pressure of gas delivered at the mouth is lower than the external hydrostatic pressure at the centroid of the lung (see Fig. 8). The implications of hydrostatic lung loads are discussed further in the section on “hypoventilation by perturbation of respiratory control,” but it has been shown that negative transrespiratory pressure can predispose to dynamic airway compression during exhalation

(160), arguably making the scenario predicted by Wood and Bryan (298) more likely.

In contrast to expiration, during inspiration there is no Starling resistor effect and distension of the intrapulmonary airways as the lung expands reduces resistance and facilitates flow (195). Nevertheless, Maio and Farhi (188) demonstrated a similar decline in both peak inspiratory and peak expiratory flows during MBC measurements at progressively higher gas densities. Similarly, in an experiment in which subjects exercised maximally while breathing air at 6 atm abs, the subjects hypoventilated (i.e., they became hypercapnic) and inspiratory flows were seen to decrease relatively more than expiratory flows (128). In part, the limitation of inspiratory flow under these conditions of increased gas density must simply reflect a declining flow for a given level of inspiratory muscle effort as the resistive component of inspiratory work increases (177). In addition, it is notable that patients with mild chronic airflow limitation (9), healthy subjects breathing air during exercise (191), and healthy subjects breathing dense gas (127, 128, 267) all exhibit a tendency to increase the expiratory reserve volume when expiratory flow limitation is either imminent or occurring. This aids expiration because the stored elastic energy in the expanded lung is greater and the higher lung volume places traction on airways, thus reducing the tendency to collapse and increasing expiratory flow (128). However, the increasing lung volume shifts inspiration to a less favorable portion of the compliance curve. The elastic work of inspiration increases and the inspiratory transpulmonary pressure produced by a given stimulus decreases (128). This problem may be amplified by a reduction

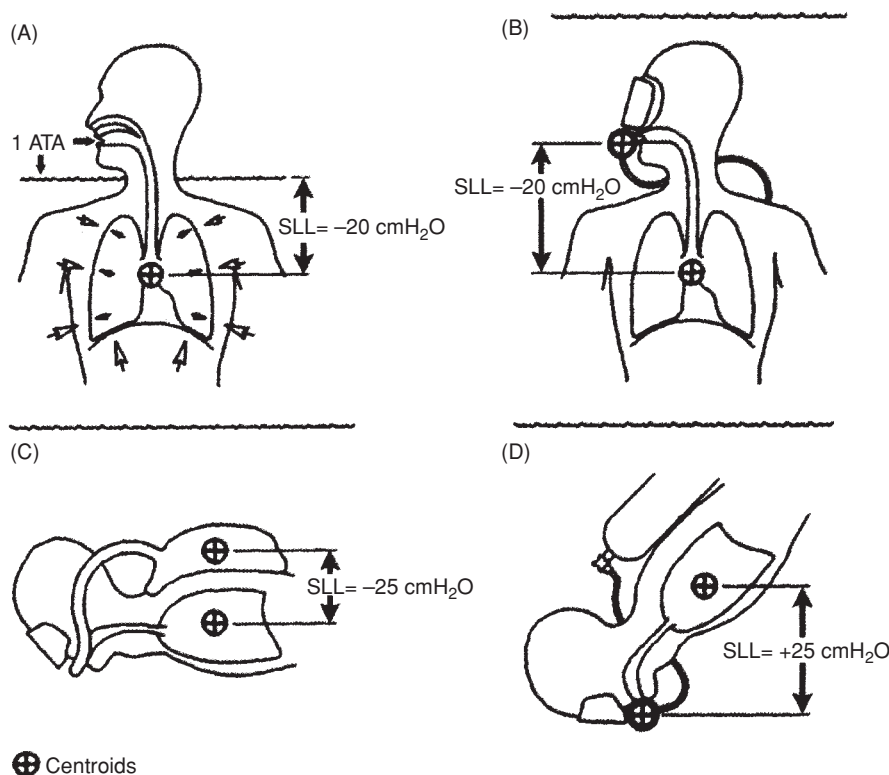


**Figure 8** Schematics to represent static lung loading (or transrespiratory pressure) during immersion. Panel A depicts upright head-out immersion in which there is a negative static lung load of approximately  $-20$   $\text{cmH}_2\text{O}$ . Panel B depicts an upright scuba diver breathing from a regulator in which there is a similar negative static lung load of approximately  $-20$   $\text{cmH}_2\text{O}$  irrespective of depth. Panel C depicts a closed-circuit rebreather diver with a back-mounted counterlung. All of the scenarios depicted in panels (A), (B), and (C) produce a negative static lung load because the airway is in continuity with a gas supply at lower pressure than the hydrostatic pressure acting at the lung centroid. In contrast, Panel D depicts a scuba diver in the head-down position where there is a positive static lung load because gas supply pressure (measured at the depth of the regulator mouthpiece) is now greater than the hydrostatic pressure acting at the lung centroid. SLL, static lung load. Reproduced with permission from Lundgren (183).

in the specific compliance of the lung during immersion with a negative hydrostatic lung load (226), as is discussed in the section titled “Hypoventilation by perturbation of respiratory control.”

In summary, the MBC is significantly reduced at progressively higher pressures and gas densities. This reduction is mediated through decrements in both inspiratory and expiratory functions. The extent to which respiratory muscle fatigue might contribute to hypercapnia by reducing MBC during sustained exercise under hyperbaric conditions is not known, although it is a plausible contributor to the problem. The immutable nature of effort-independent exhalation prompted Camporesi and Bosco (31) to comment that “the most stringent of inescapable limits are primarily expiratory,” but these authors also observed that the ability of the inspiratory muscles to generate flow in the face of the progressive impediments discussed above may, in fact, “be considered the ultimate limiting factor.” Irrespective of the distribution of impairment between expiration and inspiration, it is plausible that hypoventilation and hypercapnia could occur under hyperbaric conditions because exercise ventilation intercepts

a markedly impaired MBC under conditions of increased gas density and immersion.

While this notion is conceptually appealing and may have occasional practical relevance, it seems likely that under usual circumstances divers will not tolerate conditions where the exercise load is high enough, or the impediment to ventilation great enough (or combinations of both) for this mechanism to be relevant. Even with motivated subjects, some researchers have struggled to replicate the scenario. For example, Fagraeus and Linnarsson (82) showed that heavy work during air breathing at pressures up to 6 atm abs (inspired gas density 7.74 g/liter) was only tolerated for very short periods and resulted in severe hypercapnia when ventilation was approximately 80% of MBC. Dwyer et al. (71) compared  $\dot{V}_{\text{Emax}}$  and MBC during immersed exercise at 43.4 atm abs (inspired gas density 7.34 g/liter) and showed no consistent tendency for the two parameters to converge in comparison with measurements made at 1.6 (inspired gas density 1.82 g/liter). Finally, as discussed below (in the “Hypoventilation by perturbation of respiratory control” section), it seems clear that physical limits of ventilation do not need to be

met in order for hypercapnia to occur under hyperbaric conditions.

### *Hypoventilation by perturbation of respiratory control*

Studies have demonstrated hypercapnia under hyperbaric conditions during submaximal exercise (36, 129, 149, 152). The relative hypoventilation implied by these studies therefore appears related primarily to a perturbed ventilatory response to rising CO<sub>2</sub> levels rather than to limitation of ventilatory capacity *per se*. The obvious question, then, is why is the PaCO<sub>2</sub> allowed to rise during sub-maximal ventilation under hyperbaric conditions (and particularly during exercise) when normocapnia is preserved during exercise under normobaric conditions? A number of explanatory hypotheses have been proposed, including the effects of hyperoxia, inert gas narcosis, and pressure; and an alteration in control of ventilation under conditions of increased respiratory load.

It is known that increases in PaO<sub>2</sub> achievable by increasing the FIO<sub>2</sub> under normobaric conditions can depress the ventilatory response to CO<sub>2</sub> (49, 95), although the effect on ventilation is most marked in the hypoxic range and relatively subtle in hyperoxia (171). A much greater increase in PaO<sub>2</sub> is possible under hyperbaric conditions and this might depress ventilation by direct suppression of respiratory drive or by a reduction of metabolic acidosis during exercise, or both (214). The significance of such effects in causation of hypercapnia under hyperbaric conditions remains uncertain. In a reevaluation of the data presented by Lanphier (171), Lanphier and Bookspan (173) reported a small increase in mean end-tidal CO<sub>2</sub> levels in divers exercising at 1.8 atm abs breathing oxygen in comparison with air at 1 atm abs but were unable to separate the relative effects of the simultaneous exposure to higher P<sub>IO<sub>2</sub></sub> and increased gas density in the 1.8 atm abs condition. Similar difficulty is encountered in interpreting other relevant studies. For example, Lambertsen et al. (169) reported a fall in ventilation (and a small rise in arterial PCO<sub>2</sub>) when subjects exercised at 2 atm abs breathing 100% oxygen compared to the same exercise at 1 atm abs breathing air, but again, increased gas density may have been a factor. Fagraeus et al. (81) demonstrated a fall in the  $\dot{V}_E/\dot{V}_{CO_2}$  response and a small rise in end-tidal CO<sub>2</sub> during moderate exercise at 1 atm abs when oxygen was breathed in comparison with air. The hyperbaric limb of their experiment (the same exercise at 4.5 atm abs breathing air; P<sub>O<sub>2</sub></sub> ≈ 1 atm) showed an additional reduction in  $\dot{V}_E/\dot{V}_{CO_2}$  and an increase in end-tidal CO<sub>2</sub> apparently due to gas density, PN<sub>2</sub>, or pressure itself, but this design did not allow comparison of the effect of different inspired and arterial P<sub>O<sub>2</sub></sub>s on ventilation at pressures greater than 1 atm abs. In only a few studies does the design isolate the effect of inspired and arterial P<sub>O<sub>2</sub></sub>s on ventilation and PaCO<sub>2</sub> under hyperbaric conditions. One such study by Taunton et al. (250) compared exercise hyperpnea and postexercise PaCO<sub>2</sub> at 1 atm abs and 2 atm abs during air breathing, and at 2 atm abs during oxygen breathing. In

contrast to air breathing at 2 atm abs, which resulted in PaCO<sub>2</sub> falling after exercise, oxygen breathing at 2 atm abs usually caused a rise in postexercise PaCO<sub>2</sub>. However, this rise was small and neither of the subjects in this study exhibited hypercapnia. Another relevant study conducted at 4.7 atm abs with immersed subjects breathing oxygen-nitrogen mixes showed that increasing the P<sub>IO<sub>2</sub></sub> over a range between 0.7 and 1.3 atm had no effect on PaCO<sub>2</sub> during exercise at 60% and 80% of V<sub>O<sub>2</sub></sub>max (36). In contrast, in a second study by the same group (214) involving work at 100 W during immersion at 4.7 atm abs, the PaCO<sub>2</sub> did increase by 5 mmHg on average (from a mean of 42 to 47 mmHg) when the P<sub>IO<sub>2</sub></sub> was increased from 0.21 to 1.75 atm. This range of P<sub>IO<sub>2</sub></sub> is broader than investigated in their previous study (36), in which the range of P<sub>IO<sub>2</sub></sub> corresponded to the default low and high P<sub>O<sub>2</sub></sub> set points in the most popular diving rebreathers and in which the upper limit (1.3 atm) corresponded to a widely adopted convention on the safeupper limit for P<sub>IO<sub>2</sub></sub> in recreational diving. That study (36) thus seems highly relevant in the context of “routine” diving.

It follows from the above that while the effect of hyperoxia on ventilation and PaCO<sub>2</sub> is interesting, it is unlikely to account for significant hypercapnia in studies where the P<sub>IO<sub>2</sub></sub> is more modest and the gas density higher, and it is unlikely to be the most important cause of hypercapnia in practical diving applications. As pointed out by Cherry et al. (36), this is a reassuring finding for divers who utilize a high P<sub>IO<sub>2</sub></sub> to minimize inert gas uptake. If high P<sub>IO<sub>2</sub></sub> did predispose to hypercapnia, this could induce a sequence of adverse events in which hyperoxia provoked hypercapnia that, in turn, would increase the risk of cerebral oxygen toxicity. One potential caveat is proposed by Lanphier and Bookspan (173), who point to studies, for example, of Wasserman (287), showing that the depressive effect of hyperoxia on ventilation may be greater when exercise approaches or exceeds the anaerobic threshold. They speculate that this mechanism may therefore become more important in divers working very hard underwater while breathing an elevated P<sub>O<sub>2</sub></sub>.

It has been suggested that when air is inspired under hyperbaric conditions, the narcotic effect of nitrogen might predispose to hypoventilation and hypercapnia. Having raised this possibility, Linnarsson and Hesser (177) then compared ventilation and central inspiratory activity (using the P<sub>100</sub> measure (293) as an index of total inspiratory drive) during progressive hypercapnia induced by rebreathing in subjects breathing oxygen at 1.3 atm abs (controls) and air at 6.1 atm abs (hyperbaric condition). The P<sub>IO<sub>2</sub></sub> was 1.3 atm in both conditions. The critical differences between these conditions were the increase in gas density and an inspired PN<sub>2</sub> of 4.8 atm in the hyperbaric condition. Compared to the controls, there was an increase in central inspiratory activity (of approximately 40% when the end-tidal CO<sub>2</sub> was 50 mmHg) at 6.1 atm abs, yet at the same time the slope of the ventilation-CO<sub>2</sub> response curve was reduced by 39%. The authors concluded that narcotic depression of neural structures involved in control of respiration was not the cause of reduced ventilatory responsiveness to hypercapnia. The same conclusion has been drawn by others

based on experiments in which nonnarcotic gases (96) or manipulations of pressure and inspired gas nitrogen content (80) were utilized.

Pressure *per se* might alter control of ventilation. In one study in which resting participants were subject to a variety of gas mix-pressure combinations that yielded inspired gas densities between 0.384 and 7.73 g/liter, the  $P_{aCO_2}$  was positively correlated with ambient pressure but not gas density (231). The authors recognized that this result was at odds with those of others who had found a relevant effect of gas density and were unable to offer an explanation for the finding. To confuse matters, another group demonstrated a small increase in ventilation in resting subjects breathing dense gas on compression to pressures between 36 and 48 atm abs (97). This actually corrected an initial rise in  $P_{aCO_2}$  that occurred during compression, and the authors hypothesized that central nervous system excitation associated with exposure to these very high hydrostatic pressures might explain this apparent stimulation of ventilation. This explanation is difficult to evaluate, and it is notable that another study also recorded a small increase in resting ventilation on compression from 1 to 2.8 atm abs, which the authors attributed to a compensation for an increase in dead space (see later) (205). When moderately exercised at 2.8 atm abs, these same subjects exhibited the more familiar reduction in ventilation associated with breathing denser gas.

Arguably, the most convincing study that aimed specifically to distinguish between the effects of pressure and density on exercise ventilation under hyperbaric conditions was that of Linnarsson et al. (178). Using different combinations of ambient pressure and gas species (including helium and sulfur hexafluoride), the authors created conditions of low pressure-high density, high pressure-high density, and high pressure-low density. Pressure *per se* was not found to reduce exercise ventilation, whereas increased density did, although the design of this study did not exclude an effect of inert gas narcosis.

The potential for perturbation of control of ventilation during exposure to increased resistive and elastic respiratory loads has attracted considerable interest. This has been extensively studied during rest and exercise under normobaric conditions and is discussed in detail elsewhere in *Comprehensive Physiology*. There is a complex interplay between various inputs to control of ventilation during exercise and concomitant respiratory loading that is yet to be fully elucidated. These issues become even more complex when attempts are made to interpret them in the context of exposure to hyperbaric conditions. A key starting point in this regard is an appreciation that hyperbaric conditions (and diving in particular) potentially cause an abnormal increase in all important components of respiratory load (resistance, elastance, and inertance), as is discussed below prior to consideration of the perturbed ventilatory response.

Both inspiratory and expiratory internal resistive loads may be increased by greater respired gas density and an associated increase in airways resistance (46), as was previously discussed in relation to limitation of maximum breathing ca-

capacity under hyperbaric conditions. An increase in airways resistance may also arise due to a decrease in airway caliber as discussed below in relation to immersion and hydrostatic lung loads. An additional external source of increased inspiratory and expiratory resistive loads is the UBA. These resistances are frequently asymmetrical, with most open-circuit SCUBA equipment providing greater inspiratory than expiratory resistance (44). Unfortunately, of the two external resistive loads, inspiratory resistance appears more likely to cause hypoventilation and dyspnea during diving (284). Since respiratory impairment can impact significantly on underwater performance and safety, much effort has gone into the evaluation of acceptable resistance limits for UBA, and a comprehensive account of this is provided by Warkander et al. (286).

Elastance is a property of the lungs and chest wall and of closed-circuit UBA. Work of breathing is proportional to the elastic load, and, as with resistive load limits, the tolerances of equipment-related elastic loads have been studied and standards recommended (282).

A potentially important influence on both resistive and elastic components of work of breathing is exerted by hydrostatic lung loads that arise during immersion when the pressure of the gas delivered to the mouth differs from the external hydrostatic pressure measured at the lung centroid (200). A negative hydrostatic load occurs during head-out immersion (Fig. 8A), and the use of UBA may result in both negative and positive loads (Figs. 8B, 8C, and 8D) While much of the relevant literature describes experiments involving negative loads imposed by head-out immersion, the physical conditions of this state are largely replicated in the upright diver using open-circuit SCUBA and the horizontal rebreather diver using a back-mounted counterlung (Fig. 8). Negative hydrostatic lung loads significantly decrease the expiratory reserve volume by causing cephalad displacement of the diaphragm (183). This has been associated with an increase in airways resistance because of narrowing or collapse of intrapulmonary airways (2, 140), a decrease in lung compliance (at lower lung volumes) (252), and an increase in static inspiratory muscle work in defending an expiratory reserve volume greater than the immersed relaxation volume (252). There is also a decrease in vital capacity, which is greater in cooler water (162), which Lundgren (183) argues is explained by engorgement of the pulmonary circulation with blood. This congestion of the pulmonary circulation also contributes to a decrease in lung compliance (50, 226). Not surprisingly, negative static lung loads are associated with increased dyspnoea during exercise. This can be alleviated by supplying the inspired gas at a pressure equivalent to the hydrostatic pressure at the lung centroid (129, 252), and a positive load appears better tolerated than a negative one (129, 259).

Inertance is mentioned for completeness. Inertia arising from the mass of the respired gas, the chest wall, and the lungs imposes impedance to the change in direction of gas flow, which increases with frequency of breathing (180). In diving, inertance can be increased by increased density (and

mass) of respired gas, the presence of water around both the chest wall and breathing bag (in the case of closed-circuit SCUBA), and the acceleration and deceleration of the UBA components with each breath. In experiments in which the inertance characteristics of a breathing circuit were artificially exaggerated, Fothergill et al. (91) showed that divers will subconsciously adjust their breathing frequency to match the resonant frequency of the breathing system (at which inertial impedance is minimized). Nevertheless, as pointed out by Moon et al. (200), exercising divers normally breathe at a frequency considerably less than the resonant frequencies of the breathing systems, and “inertial impedance has only a limited role in determining respiratory effort.”

Thus, there are a number of ways in which respiratory loading is abnormally increased under hyperbaric conditions, particularly when there is concomitant immersion. This is frequently reported to be associated with hypoventilation and hypercapnia, especially during exercise (36, 39, 127, 129, 149, 152, 178, 182, 231–233, 251, 284, 286, 298, 299). In contrast, under normobaric conditions, the imposition of moderate resistive or elastic loads has frequently been shown to result in little or no tendency to hypoventilation either at rest (138, 223) or even during moderate exercise (70, 85, 306). It can be difficult to compare respiratory loads imposed under normobaric and hyperbaric conditions. Not infrequently, hyperbaric exposure (particularly during immersion) involves more than one loading modality, and their effects are additive (282, 283). Thus, in explaining the frequent finding of hypoventilation and hypercapnia during exercise under hyperbaric conditions, it is tempting to suggest that combined respiratory loads may simply overwhelm any compensatory increase in respiratory neural output, thereby allowing the subject to hypoventilate and become hypercapnic. Camporesi and Bosco (31) alluded to this when they wrote: “While there is good correlation between  $P_{CO_2}$  and inspiratory work performed, the actual ventilation achieved depends not only on  $CO_2$  response but on the volume of ventilation that a given amount of ventilatory work can produce under existing circumstances.”

Nevertheless, questions remain about the adequacy of the response of the respiratory controller in these situations. It remains uncertain why many experiments demonstrate hypercapnia under hyperbaric conditions involving submaximal ventilation, when a greater respiratory neural and ventilatory response seems possible. In describing hypercapnia in their subjects exercising at 6 atm abs, Anthonisen et al. (5) expressed the issue, thus: “since all subjects hypoventilated at depth, those who did not reach their MBC must have *chosen* to retain  $CO_2$  rather than attain ventilations involving dynamic airway compression.” Cain and Otis (27) were among the first to describe this as a tendency of the respiratory controller to sacrifice tight  $CO_2$  homeostasis in the face of an increased respiratory load in order to avoid expending more energy in maintaining or increasing ventilation, and this general theme has been supported by others (149).

A relevant series of investigations performed under normobaric conditions was described by Poon (221). He mea-

sured the slopes of the  $\dot{V}_E - \dot{V}_{CO_2}$ ,  $\dot{V}_E - ET_{CO_2}$ ,  $P_{100} - \dot{V}_{CO_2}$ , and  $P_{100} - ET_{CO_2}$  curves in human subjects exposed to either no load or an inspiratory elastic load during graded exercise performed while the subjects were either eucapnic or hypercapnic (the latter achieved by adding  $CO_2$  to the inspired gas). The slope of the  $\dot{V}_E - \dot{V}_{CO_2}$  curve was depressed in the loaded state, but more so in the hypercapnic condition than in the eucapnic condition (−28.7% vs. −16.0% respectively, compared to the unloaded state). The steady state  $\dot{V}_E - ET_{CO_2}$  curve was also depressed in the loaded condition (−32% compared to the unloaded state). The  $P_{100}$  response to exercise ( $P_{100} - \dot{V}_{CO_2}$  curve) was significantly enhanced in the loaded state during eucapnia (+88.7% compared to the unloaded state) but not during hypercapnia (−11.2%). Qualitatively similar results were obtained in the experiments in which a resistive load was imposed (222), and these findings are consistent with those of earlier related experiments (12, 35, 76). On the basis of these results, Poon suggested that the potency of ventilatory compensation for elastic and resistive loads is greatest at rest and during eucapnic exercise and is diminished or abolished by  $CO_2$  inhalation. He related these findings to his previously published “optimization hypothesis,” which holds that ventilatory output is determined by a balance between the chemical drive to breathe and a propensity of the respiratory controller to minimize respiratory effort (220). In this context,  $CO_2$  inhalation reduces the efficiency of  $CO_2$  elimination by the lung and in the loaded state  $CO_2$  retention is a more economical response than the increase in respiratory effort required to lower it. If Poon’s findings can be extrapolated to respiratory loading during exercise under hyperbaric conditions, then the frequently observed hypoventilatory response may not only be a matter of the load overwhelming neural compensation but also an attenuation of this compensation.

Finally, one aspect of the altered ventilatory response to increased respiratory load and rising arterial  $CO_2$  in diving that deserves mention is the marked degree of individual variability that has been reported by some authors. Lanphier (171, 172) was among the first to report this in the context of diving-related experiments. While he reported a tendency to retain  $CO_2$  in virtually all working subjects breathing dense gas underwater, it was significantly greater in some individuals than others and divers appeared to retain  $CO_2$  more readily than nondivers. Similar variability has subsequently been reported by others under both normobaric (86, 165) and hyperbaric conditions (149, 169, 286). The Israeli Navy group has further investigated the issue of greater  $CO_2$  retention by divers as compared to nondivers (152, 153, 240). Divers appear less sensitive to rising  $CO_2$  levels, although sensitivity among divers does not correlate well with diving experience or current diving activity. Indeed, ex-divers appear to retain the characteristic. In a subset of their experiments in which the  $P_{100}$  occlusion pressure was measured during  $CO_2$  re-breathing, it was shown that the central response to  $CO_2$  was reduced in the divers. This measurable reduction in central respiratory drive suggests that the difference between divers

and nondivers is not explained simply by conscious adoption of a hypoventilatory breathing pattern (e.g., to conserve gas) that becomes habituated. It is also notable that there appears to be some plasticity in the respiratory response to CO<sub>2</sub> among divers, which might be subject to manipulation. For example, Pendergast et al. (216) showed that respiratory muscle training tended to normalize the ventilatory sensitivity to increasing inspired CO<sub>2</sub> in divers who exhibited either high or low sensitivity prior to the training.

### Increase in dead space

Standard physiology texts (180) divide dead space into apparatus dead space (potentially imposed by airway instrumentation or any external breathing apparatus) and physiological dead space. The physiological dead space is divided into anatomical and alveolar components, with the latter potentially having several contributory components as described below. Virtually, all these components of dead space are potentially increased under hyperbaric conditions and particularly during diving.

Apparatus dead space warrants only a brief mention here. The traditional style diving helmets that enclosed the diver's head with no other mechanism of isolating the airway contained a dead space of over 4 liters (44). This necessitated high rates of fresh gas flow through the helmet to minimize rebreathing of exhaled CO<sub>2</sub>, as remains the case in respect of hood systems used to deliver oxygen to patients in multiplace hyperbaric chambers. Most modern diving helmets incorporate an oronasal mask that excludes the airway from the main volume of the helmet. The mask is connected to a demand valve regulator similar to those used by SCUBA divers (Fig. 3), which reduces the apparatus dead space to approximately 200 ml (44). Apparatus dead space is further reduced in the typical demand regulator with a mouthpiece used by SCUBA divers. In this setting there is no oronasal mask and the dead space is less than 100 ml. Similarly, low volumes are found in the mouthpieces of circle circuit rebreather devices in which one-way valves direct flow and isolate the airway from the much larger volume of the circuit. However, failure in one of these valves can cause a catastrophic increase in dead space.

Physiological dead space may be increased under hyperbaric conditions. Salzano et al. (233) measured  $V_D/V_T$  during rest and graded exercise in nonimmersed subjects breathing air at 1 atm abs and breathing helium-oxygen mixes at 47 atm abs (inspired gas density 12.3 g/liter) and 66 atm abs (inspired gas density 17.1 g/liter). There was an insignificant difference between the two hyperbaric exposures, but resting  $V_D/V_T$  was greater in both high-pressure conditions than at 1 atm abs; and more importantly, it decreased only marginally during exercise in comparison with a much greater fall at 1 atm abs (see Fig. 9). Mummery et al. (205) performed an experiment at pressures more relevant to routine hyperbaric exposures and everyday diving. They measured  $V_D$  during rest and graded exercise in dry subjects breathing air at 1 and

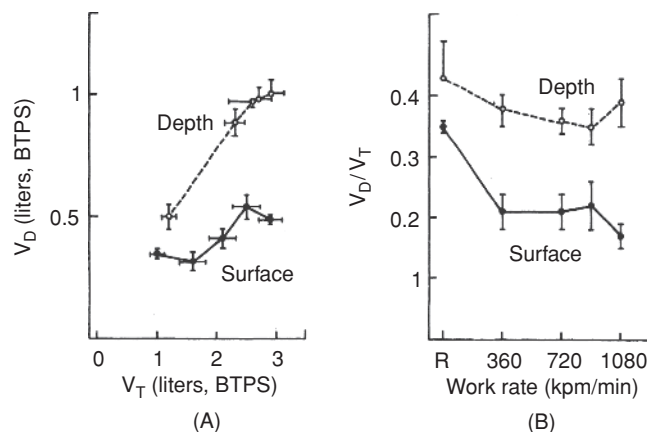


**Figure 9** (A) Dead space ( $V_D$ ) as a function of tidal volume ( $V_T$ ) in nonimmersed subjects breathing air at 1 atm abs ("surface") and during experimental hyperbaric chamber exposures ("depth") to between 47 and 66 atm abs (inspired gas densities between 12.3 and 17.1 g/liter). (B) The  $V_D/V_T$  ratio during increasing levels of exercise at the "surface" and at "depth." At the surface during exercise at 360 kpm, the ratio decreases by 43% of the resting value in comparison with a 10% decrease at depth. Reproduced with permission from Salzano et al. (233).

2.8 atm abs (inspired gas density 3.1 g/liter) and recorded significant increases during rest (+0.06 liter BTPS), light exercise (+0.11 liter BTPS), and heavy exercise (+0.06 liter BTPS) at the higher pressure. The increased  $V_D$  was compensated by an increase in ventilation at rest such that  $\dot{V}_A$  did not change, but during heavier exercise, the increase in  $V_D$  together with a concomitant decrease in ventilation resulted in a significantly reduced  $\dot{V}_A$  at 2.8 atm abs. Others have reported similar trends in  $V_D$  during dense gas breathing in humans (193,300) or liquid breathing in dogs (164). Data from these studies have been compiled into a single figure by Moon et al. (200) (see Fig. 10). In the most recent relevant experiment

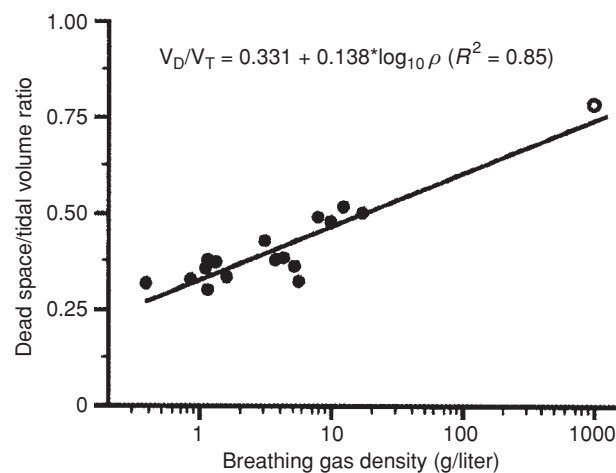


**Figure 10** Pooled data from human studies (closed circles) illustrating the effect of gas density ( $\rho$  in the formula) on the  $V_D/V_T$  ratio as respired gas density increases. The extremely high-density datapoint (open circle) comes from a liquid-breathing experiment in dogs. Reproduced with permission from Moon et al. (200).

conducted in a depth (pressure) range relevant to recreational diving, Cherry et al. (36) measured various respiratory parameters during rest and exercise in immersed subjects breathing air at 1 and 4.7 atm abs while challenging the subjects with hydrostatic and external resistive loads. They reported a 6% average rise in  $V_D/V_T$  during exercise at 4.7 atm abs and commented that compensation of the associated decrease in effective  $\dot{V}_A$  would have required a 6.4-liter/min increase in ventilation, which instead decreased by 14.7 liter/min.

Dead space reduces the efficiency of ventilation. For a given minute volume,  $\dot{V}_A$  will fall as  $V_D$  rises. The obvious corollary is that an increase in dead space does not cause alveolar hypoventilation and hypercapnia unless there is a concomitant failure to compensate by increasing ventilation. Such failure was considered to explain the increase in  $P_{aCO_2}$  measured during exercise at 2.8 atm abs in the experiment by Mummery et al. (205). Indeed, the authors proposed that "increased  $V_D$  is the primary perturbation that leads to a compensatory increase in ventilation at rest or light exercise levels, but that inadequate  $\dot{V}_A$  results when the respiratory drive inadequately compensates for the increased  $V_D$  during heavy exercise." Their results seem confluent with Poon's hypothesis (discussed earlier) that there is diminished respiratory drive under conditions of increased respiratory load if ventilation is inefficient. "Inefficiency" in Poon's experiments was induced by  $CO_2$  rebreathing, and it is difficult to compare this directly to an increase in  $V_D$ . Nevertheless, an increase  $V_D$  undoubtedly renders ventilation less efficient at depth (233) and a marriage of Mummery's observation and Poon's hypothesis provides a plausible explanation for the genesis of alveolar hypoventilation and hypercapnia during submaximal exercise under hyperbaric conditions where multiple factors can increase respiratory load.

It remains to comment briefly on the possible causes of increased dead space under hyperbaric conditions. The components of dead space calculated by the Bohr equation include anatomic dead space, ventilation-perfusion mismatching, impaired diffusion in distal gas exchange units, and any defect in  $CO_2$  transport between erythrocytes and alveoli (233). Many factors may influence these components in normal and abnormal physiology, and they are considered in detail elsewhere in *Comprehensive Physiology*. Only those specifically relevant to hyperbaric conditions are mentioned here.

The anatomical dead space may be increased if subjects distend the conducting airways by shifting their tidal excursions to higher lung volumes (238), which is known to occur during breathing of a dense gas (127, 128, 267). It is also theoretically possible (but not proven) that a positive static lung load during immersion could increase anatomical dead space by distending the conducting airways (200).

The alveolar dead space may be increased during ventilation with hyperoxic gas. Hyperoxia may cause pulmonary vasodilation and diversion of blood flow from well-ventilated to hypoventilated lung units (192, 214). In a recent study, this appeared to be the most plausible mechanism for an increase in  $V_D/V_T$  seen during respiration of hyperoxic but

not normoxic gas during immersed exercise at 4.7 atm abs (214).

Alveolar dead space may also be increased during ventilation with dense gas in several ways. First, impairment of  $\dot{V}/\dot{Q}$  matching might occur if respiration of dense gas induced nonuniform alteration of turbulent flow and airway resistance, which could exaggerate heterogeneity in the time constants of different lung units (200). This would result in less efficient gas exchange unless parallel adjustments in perfusion were to occur (200). Second, since diffusivity of a gas is inversely proportional to gas density, it is plausible that respiration of dense gas under hyperbaric conditions may impair  $CO_2$  diffusion in the distal gas exchange segments of the airway (272, 300). Interpretation of both these hypotheses is complicated by the finding that respiration with dense gas appears to decrease the alveolar-arterial partial pressure difference for oxygen (37, 87, 104, 231, 300). This seems at odds with the proposal that dense gas increases alveolar dead space by causing either  $\dot{V}/\dot{Q}$  mismatch or a diffusion impairment since both phenomena could be expected to increase the A-a $DO_2$ . However, in an experiment utilizing the multiple inert gas washout technique (279) in dogs, Christopherson and Hlastala (37) identified a partial dissociation between oxygen exchange and the  $\dot{V}/\dot{Q}$  distribution when a denser gas was respired. Their explanation draws on work by Paiva and Engel (213) and focuses on the position of the gas concentration "front" that arises in intermediate airways from the interaction between convection and diffusion. It holds that a respired gas (such as oxygen or CO) may be distributed differently from overall alveolar ventilation if the breathing of a denser carrier gas shifts the front to a position in the airway from which lung units with heterogeneous ventilation arise. With the front in this position, the inspired gas concentration entering the distal units is more uniform despite their differing volume-flow characteristics. The important implication for the present discussion is that improvement in oxygen exchange remains compatible with a slight worsening in  $\dot{V}/\dot{Q}$  matching when a denser gas is respired.

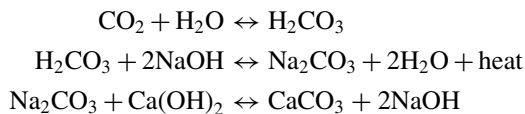
Thus a derangement of  $\dot{V}/\dot{Q}$  matching is generally favored by contemporary commentators as the explanation for an increase in physiological dead space under hyperbaric conditions (200, 205, 233). In support of this hypothesis, Moon et al. (200) presented preliminary data from a single subject in whom the multiple inert gas elimination technique identified a clear trend toward an increase in high  $\dot{V}/\dot{Q}$  units during respiration of a denser gas under hyperbaric conditions. The  $P_{iO_2}$  was kept constant in both conditions to exclude any effect on hypoxic pulmonary vasoconstriction.

## Rebreathing of $CO_2$

The preceding discussion of the causes of hypercapnia under hyperbaric conditions has focused on the impairment of  $CO_2$  elimination. For completeness, the possibility of  $CO_2$  rebreathing should be mentioned, particularly as a cause of hypercapnia in diving. The risk has been reduced in modern

diving equipment by the use of a low-dead-space breathing apparatus such as diving helmets with oronasal masks. Nevertheless, the increasing use of rebreather devices, in which exhaled gas is recycled through a CO<sub>2</sub> absorbent, remains associated with a significant risk of CO<sub>2</sub> rebreathing.

Anecdotally, CO<sub>2</sub> rebreathing events in modern diving occur most commonly during the use of rebreathers when the absorbent canister fails to remove all CO<sub>2</sub> from the gas passing to the inspiratory limb of the loop. This may occur either because the canister is packed or installed incorrectly or, more commonly, because the absorbent material becomes partly or completely exhausted allowing CO<sub>2</sub> to “break through.” The most frequently used CO<sub>2</sub> absorbent in diving is “soda lime,” a mix of calcium hydroxide, sodium hydroxide, water, and small amounts of potassium hydroxide and silica. Its components react with CO<sub>2</sub> according to the following reactions:



The absorbing capacity of soda lime for CO<sub>2</sub> is thus finite. Measurements made in a recent anesthesia study for a soda lime preparation similar to that used by divers suggested an absorbing capacity between 12 and 15 liters CO<sub>2</sub>/100 g (130). However, the absorbent performance is also context-sensitive and may vary with environmental temperature, the density of the respired gas, absorbent granule size, the quality of the canister packing, and dispersion of the flow paths within the canister (257). Assuming that the canister is well designed and properly packed, the worst possible combination of circumstances for high risk of CO<sub>2</sub> breakthrough is a small absorbent canister containing coarse granules of absorbent, used under conditions of hard work (high CO<sub>2</sub> production) in a cold environment at deep depths with high gas density. Given that most divers simply renew their absorbent material in accordance with manufacturer’s estimates of safe duration, the susceptibility of canister performance to these multiple variables, some of which are unpredictable, represents a significant hazard that is difficult to manage. At the time of writing, no commercially available rebreathers incorporate systems that allow the user to monitor CO<sub>2</sub> levels in the inspired gas, although such systems are known to be in development. There are, however, devices that monitor the progress of the CO<sub>2</sub> absorbent reaction front through the scrubber material by measuring temperature changes along an axial probe passing through the center of the canister. This provides an indication of the remaining absorbent capacity for CO<sub>2</sub> and possibly a warning of impending CO<sub>2</sub> breakthrough (281).

Where CO<sub>2</sub> is inhaled, determination of the PACO<sub>2</sub> is no longer a simple function of metabolic CO<sub>2</sub> production and alveolar ventilation but must take account of the inspired CO<sub>2</sub>

load. Thus, PACO<sub>2</sub> is predicted by a variation of Eq. (2):

$$\text{PACO}_2 = 863 \times \frac{\dot{V}_{\text{CO}_2}}{\dot{V}_A} + \text{PiCO}_2 \quad (5)$$

Camporesi and Bosco (31) provide an excellent perspective on the implications of inspired CO<sub>2</sub> during diving. They point out that PACO<sub>2</sub> cannot remain lower than the PiCO<sub>2</sub> and that “all alveolar ventilation can do is to decrease the difference between PiCO<sub>2</sub> and PACO<sub>2</sub>.” They go on to demonstrate that during moderate work ( $\dot{V}_{\text{CO}_2} = 1.5$  liter/min STPD) maintenance of a PACO<sub>2</sub> of 40 mmHg would require a  $\dot{V}_A$  of 32.4 liter/min (BTPS) in the absence of inhaled CO<sub>2</sub> and 43.2 liter/min if the PiCO<sub>2</sub> were 10 mmHg. Such compensations are clearly possible during air breathing at 1 atm abs (193). However, in diving, CO<sub>2</sub> rebreathing might arise in a setting of increased respiratory work and impaired respiratory drive as extensively discussed above. Of particular relevance in this regard are the previously discussed experiments by Poon (221, 222), who showed that CO<sub>2</sub> inhalation diminished the potency of ventilatory compensation for elastic and resistive loads, or abolished compensation altogether. It can be appreciated that under these circumstances, there may be a failure to maintain CO<sub>2</sub> homeostasis and that hypercapnia might easily result.

### Consequences of CO<sub>2</sub> retention

In order to place this detailed discussion of CO<sub>2</sub> retention in context, it is appropriate to briefly enumerate the adverse effects of CO<sub>2</sub> retention in diving.

Hypercapnia may produce uncomfortable dyspnea, which can precipitate panic and drowning. In addition, on dives utilizing self-contained gas supplies and open-circuit breathing apparatus, dyspnea may result in rapid exhaustion of the gas supply. On dives utilizing rebreather devices where the reason for the hypercapnia may be CO<sub>2</sub> scrubber failure in the device itself, severe dyspnea may prevent the diver from switching to an alternative gas supply (which requires removal of the rebreather mouthpiece and replacing it with a scuba regulator) (265). This is of particular concern because “getting off the loop” is the only way to retrieve such situations. For this reason, many modern rebreathers incorporate a “bailout valve” that allows switching to an open-circuit gas supply without removing the mouthpiece. Not surprisingly, there are data demonstrating that those divers who are less responsive to CO<sub>2</sub> are also less likely to suffer significant dyspnea if hypercapnic (286), but this may expose them to a greater risk of the other adverse consequences of hypercapnia described below.

Hypercapnia may increase the risk of cerebral oxygen toxicity. This conclusion is drawn from the well-established relationship between underwater exercise and the risk of oxygen toxic convulsions (43), although direct evidence that hypercapnia underpins this link is somewhat sketchy. One highly plausible explanation is the increase in cerebral blood flow

that accompanies hypercapnia, which may result in delivery of a larger oxygen dose to the cerebral tissues (39). Indeed, Lambertsen et al. (166) found that adding 2% CO<sub>2</sub> to oxygen inhaled at 3.5 atm abs caused an average increase of internal jugular venous PO<sub>2</sub> of nearly 1000 mmHg above the level found during breathing of oxygen alone. The authors also noted that this effect virtually eliminated the well-recognized inter- and intraindividual variability in latency of oxygen toxicity among their subjects, leading them to suggest that interindividual differences in CO<sub>2</sub> tolerance and related differences in PaCO<sub>2</sub> during diving might underpin differences in susceptibility to oxygen toxicity.

Hypercapnia may cause narcosis, which may be additive to any narcotic effect produced by nitrogen in air diving. Indeed, there have been supporters of the notion that all narcosis is caused by CO<sub>2</sub>, but the current consensus holds that nitrogen narcosis and CO<sub>2</sub> effects are simply additive (126) albeit with some qualitative differences (90). There is evidence that in severe hypercapnia, a narcotic effect may cause or contribute to unconsciousness (198, 203), with obvious severe consequences when this occurs underwater. Of significant concern is the possibility that divers with low sensitivity to CO<sub>2</sub> who suffer hypercapnia may become unconscious or severely disabled without suffering noticeable premonitory symptoms such as dyspnea (285).

Finally, there is speculation that fluctuating CO<sub>2</sub> levels might increase the risk of DCS (31). Hypothetically, if CO<sub>2</sub> levels are high during the early working phase of a dive, this might enhance inert gas uptake by tissues whose vascular beds dilate in response to hypercapnia. In contrast, during the decompression phase when the diver is typically resting and when any hypercapnic vasodilation might be expected to have resolved, the tissue perfusion and therefore off-gassing might be reduced. To the best of our knowledge, there are no data supporting this notion. Indeed, Anderson et al. (4) cast doubt on the significance of CO<sub>2</sub>-induced hemodynamic effects on inert gas exchange when they failed to show acceleration of nitrogen elimination during induced hypercapnia in human subjects.

Because of the potentially deleterious effects of CO<sub>2</sub> retention in diving, and the recognized interindividual variability in the tendency to retain CO<sub>2</sub> (described earlier), there has been much interest in the exclusion of candidates with a predilection for "CO<sub>2</sub> retention" from diver training. To this end, Lanphier (172) demonstrated that a low ventilatory response to inspired CO<sub>2</sub> was predictive of a tendency to retain CO<sub>2</sub> during underwater work. However, his attempts to define a selection procedure based on CO<sub>2</sub> response testing were frustrated by poor specificity of the test and the difficulty in defining an appropriate "cutoff" threshold in the response. Kerem et al. (153) investigated using the end-breath-hold PaCO<sub>2</sub> as an indicator of any tendency to CO<sub>2</sub> retention under diving conditions but found it a weak predictor. The desirability of an appropriate screen for a tendency to retain CO<sub>2</sub> in diving candidates has subsequently been discussed by others (77, 117), but to date there is no consensus on an appro-

priate technique. This likely reflects the previously discussed multifactorial etiology of CO<sub>2</sub> retention in divers (216) and the consequent difficulty in developing a broadly applicable single test.

## Oxygen

Animal life depends on energy production by mitochondria, which utilize oxygen as an electron and a proton receiver in the final step of oxidative phosphorylation. The processes of oxygen uptake in the lungs, transport in blood, and uptake and utilization in tissues are well understood and described in detail elsewhere in *Comprehensive Physiology*. We restrict our commentary here to issues relevant to oxygen exposure under hyperbaric conditions. Under hyperbaric conditions, humans generally inspire a higher PO<sub>2</sub> than that for which the mechanisms of oxygen utilization and protection against damaging reactive oxygen species evolved.

### Oxygen exposure under hyperbaric conditions

For compressed gas divers and patients undergoing HBOT, there are good reasons to inspire a PO<sub>2</sub> greater than encountered during air breathing at 1 atm abs (P<sub>IO<sub>2</sub></sub> = 150 mmHg BTPS). In diving, the corollary to a greater P<sub>IO<sub>2</sub></sub> is a lower inspired inert gas partial pressure and, potentially, a lower risk of DCS. In HBOT, at least some of the beneficial effects are dose dependent and the motivation for exposure to a high P<sub>IO<sub>2</sub></sub> is self-evident. However, in both diving and HBOT, there are accepted limits of P<sub>IO<sub>2</sub></sub> that are usually not exceeded because of the risk of oxygen toxicity.

### Oxygen exposure in diving

The toxic effects of oxygen depend on the P<sub>IO<sub>2</sub></sub> and the duration of the exposure. Saturation divers inspire a PO<sub>2</sub> between 0.3 and 0.5 atm since long-term exposure to a higher PO<sub>2</sub> may result in pulmonary oxygen toxicity. Different communities of bounce divers limit P<sub>IO<sub>2</sub></sub> to between 1.0 and 1.4 atm, primarily to reduce the risk of cerebral oxygen toxicity. For various purposes, a higher P<sub>IO<sub>2</sub></sub>, up to about 2.5 atm, may be inspired for brief periods with adequate precautions. Calculation of P<sub>IO<sub>2</sub></sub> depends on the nature of the breathing apparatus. For instance, closed-circuit rebreathers are generally designed to maintain a constant PO<sub>2</sub> in the breathing circuit, and this breathing circuit gas is warmed and humidified by the diver's body and the exothermic CO<sub>2</sub> absorbent canister reactions described in the "Rebreathing of CO<sub>2</sub>" section. Open-circuit breathing apparatus deliver a fixed fraction of oxygen and a dry gas (since compressed gas is purposely dehumidified). For instance, when breathing air from open-circuit apparatus, the F<sub>IO<sub>2</sub></sub> remains constant at 0.209 and the P<sub>IO<sub>2</sub></sub> is obtained by multiplying with the prevailing ambient pressure. Thus, at 30 msw (100 fsw) where the ambient pressure is 4 atm abs,

the  $P_{IO_2}$  is given by  $0.209 \times 4 = 0.836$  atm. This is a dry gas  $P_{IO_2}$  and would require correction to BTPS for use in, for instance, the alveolar gas equation, but the small contributions of water vapor pressure and temperature are ignored with respect to oxygen toxicity limits. Since  $P_{IO_2}$  increases with depth, it follows that any open-circuit breathing gas will have a “maximum operating depth” [MOD (atm abs) =  $P_{O_2\max}/F_{IO_2}$ , where  $P_{O_2\max}$  is the maximum safe  $P_{IO_2}$ ]. Substituting a maximum safe  $P_{IO_2}$  of 1.3 atm, and the  $F_{O_2}$  for air into this formula, it can be seen that in order to avoid a  $P_{IO_2}$  of more than 1.3 atm, air should not be used at depths greater than 42 msw (5.2 atm abs). It follows that for deeper diving, the  $F_{O_2}$  of the respired gas must be reduced below that found in air. The choice of an optimal  $F_{O_2}$  in this setting can be guided by the simple formula,  $Ideal\ F_{IO_2} = Target\ PO_2\ (atm)/P_{amb}\ (atm\ abs)$ , where  $P_{amb}$  is the ambient pressure at the planned depth. Thus, for a dive to 90 msw (10 atm abs) in which the diver wishes to breathe a  $P_{IO_2}$  of 1.3 atm, the  $F_{IO_2}$  of the respired gas mix should be 0.13. As briefly mentioned in the introduction to this article, the composition of the remaining inert gas fraction of the gas mix will be chosen giving due consideration to the potential for narcosis and the density of the gas. Most divers substitute helium into the mix for dives beyond 50 msw in order to reduce the narcotic effect of nitrogen. Further discussion of such issues is beyond the scope of this article and is reviewed elsewhere (179).

### Oxygen exposure in HBOT

During HBOT treatments, the patients breathe oxygen in an inspired fraction of 1. The dose of oxygen is thereafter determined by the pressure and duration of the hyperbaric exposure. Most treatments for the nondiving indications are conducted at 2.0 to 2.4 atm abs over 1 to 2 h, whereas treatment for DCS is most commonly initiated at 2.8 atm abs for 1.5 to 2.5 h, followed by a further period at 1.9 atm abs for 2.5 to 5 h. The rationale for these different oxygen doses is discussed in chapters dedicated to specific indications in Neuman and Thom (209). Therapeutic oxygen exposures are usually at a considerably higher pressure than considered safe in diving; first, because the dose-response relationship is believed to favor higher pressure exposures in at least some of the relevant indications (75, 148), and second, because the risk of an oxygen toxic seizure is lower in a dry resting occupant of a hyperbaric chamber than in an immersed working diver (43). The reasons for this are not unequivocally proven but probably relate to cerebral vasodilation caused by the elevation of  $P_{aCO_2}$  often seen in divers. The choice of 2.8 atm abs as the widely accepted maximum treatment pressure in HBOT is based, at least in part, on the fact that the risk of cerebral oxygen toxicity increases substantially at greater pressures even in a resting dry subject (202). Although a seizure during HBOT almost invariably resolves spontaneously and causes no sequelae (in contrast to one taking place underwater), it is nevertheless unpleasant and any extra benefit

of HBOT at higher pressures is not considered to justify the risk.

### Uptake of oxygen under hyperbaric conditions

The transfer of oxygen from inspired gas through the airway to blood under hyperbaric conditions can be perturbed (or in some instances enhanced) by effects of increased respired gas density; increased  $P_{IO_2}$ ; immersion; and pressure *per se*. However, we preempt this discussion with an important practical perspective. While these effects can complicate accurate prediction of  $P_{aO_2}$  from  $P_{IO_2}$  or  $P_{AO_2}$ , most (with the conspicuous exception of immersion pulmonary edema) are of academic rather than practical relevance under hyperbaric conditions. As pointed out by Moon et al. (200), in most hyperbaric exposures, the  $P_{IO_2}$  is hyperoxic and often markedly so. This usually overwhelms any subtle physiological disturbances of oxygen uptake that may arise in hyperbaric conditions, and hypoxemia is an unusual problem.

### Effect of respired gas density

As discussed in the introduction to this article, respiration under hyperbaric conditions usually involves respiration of gases whose density is higher than that of air at 1 atm abs. Moon et al. (200) expertly reviewed the theoretical implications for exchange of oxygen between inspired gas and the gas resident in the airway. They point out that under conditions of increased gas density, convective mixing in airways is potentially enhanced because of distal extension of turbulent flow. However, this will substitute convective mixing for mixing by Taylor laminar dispersion [see Piiper and Scheid (219)] and the resulting net effect is uncertain. It is also possible that mixing due to cardiogenic oscillations in airway flow is increased under conditions of increased gas density (243). To further complicate prediction of the effect of increased gas density, the associated impairment of gas diffusivity (272) could impede both Taylor dispersion and diffusion along the acinus beyond the zone of convective mixing.

A related concept that deserves mention in the context of increased gas density is that of “acinar diffusion screening.” Sapoval et al. (234) point out that for the pulmonary acinus to work most efficiently, oxygen must be supplied evenly, or at least “adequately,” to all perfused gas exchanging surfaces. It is proposed that oxygen diffusing along the acinar airway is absorbed on the alveolar surfaces encountered along its path and, assuming that the alveolar membranes are highly permeable, oxygen molecules diffuse into the capillary blood at the first “hits” and are therefore “screened” from reaching those alveoli deeper in the structure. In effect, these alveoli become low  $V/Q$  units. The likelihood of such a process occurring is dependent on the permeability of the alveolar membranes and the geometry of the acinus. Further discussion is beyond the scope of this narrative. However, there are data suggesting that this phenomenon may become more important during

respiration of a dense gas, presumably because of a reduction in oxygen diffusivity (291).

The implications of increased respired gas density described above have, at the very least, hypothetical relevance to the efficient transfer of inspired oxygen to the distal airway and thence into the blood. However, their relative importance and net effect is poorly understood and may not be negative. Indeed, as discussed in the “Carbon dioxide” section, despite the association between dense gas breathing and an increase in dead space that is probably attributable to spatial  $\dot{V}/\dot{Q}$  inequalities, several studies in which subjects (or experimental animals) inspired a  $P_{O_2}$  similar to that in air at 1 atm abs found that the A-a $DO_2$  decreased rather than increased when a denser carrier gas was utilized (37, 87, 104, 231, 300). As was discussed in the “Carbon dioxide” section, one possible explanation is that dense carrier gases may improve the uniformity of distribution of other inspired gases to heterogeneously ventilated areas of lung. This mechanism may also be responsible for the finding that the DLCO may increase, though not invariably (206), during respiration of a denser gas (137, 163). A potential “parallel” contribution to the reduction in the A-a $DO_2$  (and improvement of diffusing capacity) during dense gas breathing may result from exaggerated swings in intrapleural pressure that amplify cyclic changes in blood flow through the lung. This, in turn, might result in better matching of ventilation and perfusion at any instant (6, 7). At face value, this hypothesis might seem at odds with the previously mentioned observation of a partial dissociation between oxygen exchange and  $\dot{V}/\dot{Q}$  distribution when a denser gas was respired (37), but as pointed out by Arieli (6), the reduction in mismatch arising from cyclical pulmonary perfusion would occur over the domains of both volume and time and “therefore differs from the accepted definition of spatial  $\dot{V}/\dot{Q}$ .”

### Effect of inspired oxygen partial pressure

Although an elevated  $P_{IO_2}$  precludes hypoxemia under most hyperbaric conditions, exposure to elevated  $P_{O_2}$ s may, somewhat paradoxically, perturb oxygen transfer between alveoli and blood (28). Perhaps, the most obvious effect is that higher inspired oxygen tensions could slow the rate of uptake of oxygen by alveolar capillary blood if the concentration of unliganded Hb in the returning venous blood was reduced (89). However, this would only occur if Hb was highly saturated with oxygen and is therefore of no physiological significance. Other effects are hypothetically more relevant. For example, Clark and Lambertsen (41) reported an average A-a $DO_2$  of 9.4, 46, 74, and 121 mmHg in healthy dry subjects breathing  $P_{IO_2}$ s of 0.2, 1.0, 2.0, and 3.5 atm, respectively. The authors attributed these findings to a combined effect of several factors. First, based on extrapolations from work published by Whalen et al. (292) and Greenbaum et al. (107), they proposed that the progressive decrease in cardiac output and reciprocal increase in the arterial-mixed venous oxygen content difference that can occur with hyperoxia would increase the shunt

component of the A-a $DO_2$  if the proportion of the cardiac output perfusing extant pulmonary shunts remained constant. A quantitative estimate of this effect based on parameters in the literature suggested that it could account for the majority of the observed increase in the A-a $DO_2$  in their study. Second, they suggested a contribution from the alveolar atelectasis and consequent increase in shunt that has been demonstrated during oxygen breathing (278). It is probable that this effect is primarily related to a high inspired fraction of oxygen rather than to the  $P_{IO_2}$  *per se*, although augmented release of hypoxic vasoconstriction may accelerate atelectasis in hyperoxia (278) and this may be more likely with an increase in the  $P_{IO_2}$  beyond 1 atm. Finally, based on previous observations of an increase in pulmonary vascular resistance during hyperoxia (48, 204), they hypothesized that a pulmonary vasoconstrictive effect might selectively reduce flow to well-ventilated alveoli and thereby increase flow through shunt pathways or perfusion of poorly ventilated alveoli. It should be noted, however, that the pulmonary vasoconstrictive effect of hyperoxia on which this latter hypothesis is based is not a universal finding. Indeed, arguably the most relevant and recent studies suggest that hyperbaric hyperoxia causes pulmonary vasodilation in human subjects (193, 214).

In addition to these essentially physiological effects of high inspired oxygen tensions, it remains possible that pathophysiological changes associated with pulmonary oxygen toxicity might also perturb the exchange of oxygen between alveoli and blood. The mechanisms and consequences of pulmonary oxygen toxicity were recently reviewed by Clark and Thom (43) and Clark (38) and are summarized only briefly here. The process is initiated during cellular metabolism under conditions of hyperoxia by increased production of free radical intermediates such as superoxide and hydrogen peroxide, which undergo further reaction to more reactive species such as peroxynitrite and the hydroxyl radical. These form a “pool” of tissue oxidants whose potentially harmful action is normally opposed by antioxidant defenses such as glutathione. In hyperoxic conditions favoring increased production of reactive species, the defenses may be overwhelmed allowing harmful processes to occur, such as lipid peroxidation, modification of proteins, and enzyme inactivation. In humans, the related pulmonary consequences are first manifest subjectively as substernal discomfort and then objectively as a reduction in vital capacity. Onset of these manifestations is clearly related to the oxygen dose; that is, the  $P_{IO_2}$  and duration of exposure (see Fig. 11). While it is clear from experiments in animals that irreversible and ultimately fatal lung damage can occur if the oxygen dose is large enough (115), the effects encountered in practical situations by humans have been invariably reversible, usually with hours to days but occasionally over “months” (184). There is uncertainty over whether the A-a $DO_2$  might be increased by diffusion limitation arising from the pulmonary toxic effects of hyperoxia. Several studies have demonstrated that very long periods of normobaric or hyperbaric oxygen exposure can reduce the human lung’s diffusing capacity for carbon monoxide (29, 42, 227). This was

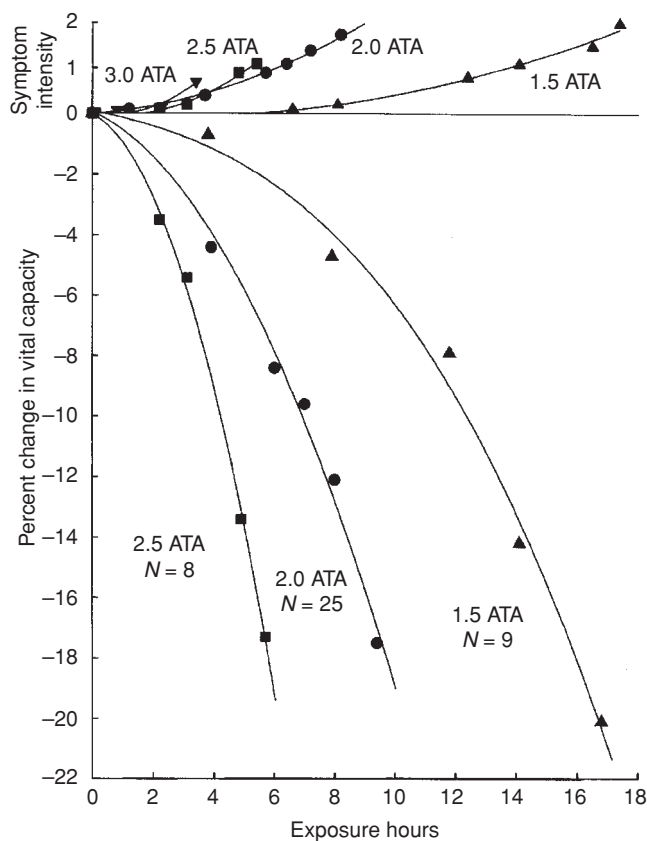


**Figure 11** Rates of development of pulmonary symptoms and decrements in slow vital capacity in human subjects continuously breathing oxygen at increasing inspired pressures (ATA = atm abs). Reproduced with permission from Clark et al. (42).

interpreted as being caused by interstitial or alveolar edema formation in one study involving oxygen breathing ( $F_{IO_2} = 1$ ) at 1 atm abs for 30 to 74 h (29) and by a reduction in capillary blood volume in another involving oxygen breathing ( $F_{IO_2} = 1$ ) at 2 atm abs for 6 to 11 h (227). According to Clark and Thom (43), these differing pathophysiological interpretations may simply reflect “variation in the sequence of toxic effects on the alveolar-capillary diffusion barrier at different oxygen pressures and durations of exposure.” Perhaps not surprisingly, these toxic effects on diffusing capacity are not seen consistently in shorter oxygen exposures. For example, Clark et al. (40) found no change in CO diffusing capacity in human subjects after oxygen breathing ( $F_{IO_2} = 1$ ) at 3.0 atm abs for 3.5 h despite significant changes in spirometric indices. Moreover, despite the significant reductions in DLCO in the study by Clark et al. (42), comparison of pre- and postexposure measurements of the A-aDO<sub>2</sub> revealed no significant differences except after the very long (mean 17.7 h) exposure to a  $P_{IO_2}$  of 1.5 atm and even then the difference was only apparent during exercise when capillary transit time was reduced and any diffusion impairment was more likely to be detectable. It can be safely concluded that widening of the A-aDO<sub>2</sub> due to pulmonary oxygen toxicity is not an early

effect and is unlikely to be of significance in most oxygen exposures in practical diving or hyperbaric conditions.

### Effect of immersion

The pulmonary effects of immersion were discussed earlier in the section on CO<sub>2</sub>. A number of these, particularly in relation to immersion in the upright position, are potentially relevant to oxygen uptake. Derion et al. (59) point out that the associated decrease in functional residual capacity, the decrease in elastic recoil at low lung volumes, and the increase in pulmonary vascular engorgement all favor airway closure and, potentially, an increase in closing volume. Indeed, several studies have demonstrated an increase in closing volume during head-out immersion (60, 225), with one identifying a tendency for closing volume to approach the highest lung volumes reached during tidal breathing in older subjects (60). If airway closure occurs during tidal breathing, this would alter ventilation and perfusion matching in affected lung units, with consequent widening of the A-aDO<sub>2</sub>. Studies designed to test the significance of any such effect during immersion using human subjects have had mixed results. Cohen et al. (47) and Prefaut et al. (225) showed a widening of the A-aDO<sub>2</sub> in the majority of their subjects during head-out immersion. In contrast, Derion et al. (59) did not demonstrate any sustained effect of immersion on  $\dot{V}/\dot{Q}$  mismatch in either young or older subjects, although in some older subjects (age 40–54 years) in whom the closing volume was greater than the ERV, there was a small increase in true shunt that nevertheless did not alter the PaO<sub>2</sub> significantly. It is difficult to compare the results of these studies because of variability between the ages and breathing pattern of the subjects. For example, older subjects studied by Derion et al. exhibited much larger tidal volumes than subjects studied by Prefaut et al., meaning that the former group subjects were ventilating only partially within the closing volume whereas the latter group subjects ventilated completely within closing volume. By combining data from both studies, Moon et al. (200) demonstrated a clear tendency for the A-aDO<sub>2</sub> to increase when the sum of the expiratory reserve and tidal volumes approached the closing volume. This was more likely to occur in older subjects.

For completeness, we mention “immersion pulmonary edema,” a rare pathological event associated with swimming or diving that can markedly derange oxygen exchange. This disorder, whose incidence is unknown, is characterized by the rapid onset of cough, dyspnea, and hypoxemia. In severe cases, there may be coughing of edema froth that may be blood stained. Most commonly, the symptoms arise during the period of immersion and may recover spontaneously and relatively quickly on egress from the water. Nevertheless, some victims require emergency treatment with oxygen, continuous positive airway pressure, and diuretics, and the condition may be fatal (242). The most remarkable aspect of the disorder, given its resemblance to acute left ventricular failure, is its occurrence in individuals who are normally fit and well (108, 114), in fact, who in some cases, are highly trained

athletes (187, 241). The pathophysiology is not definitively described. Mitchell (196) speculated on potential contributing factors that might act in an upright compressed gas diver, these being simultaneous increases in cardiac preload (caused by abolition of venous pooling during immersion) and afterload (caused by peripheral vasoconstriction); an increase in pulmonary artery pressure; a negative transthoracic pressure with an associated engorgement of the pulmonary capillaries; and cyclical worsening of the latter during inspiration of dense gas or inspiration against the resistance of a poorly tuned regulator (or both). Several of these factors could predispose to stress failure in pulmonary capillaries. A number of other risk factors have been proposed including cold water (295), moderate to heavy exercise (which is an almost invariable feature of the swimming cases) (241), excessive fluid loading (241), extant or latent hypertension (295), an exaggerated peripheral vascular response to cold (296), and (anecdotally) treatment with beta-blocker drugs (196).

### Effect of pressure

Several *in vitro* studies (20, 155) and one study using human subjects (248) have demonstrated a small leftward shift in the P-50 for Hb, indicating an increase in its affinity for oxygen at very high pressures. The effect appears to increase with pressure (228), but there are no data for pressures less than 26 atm abs. Thus, it is not clear whether this effect is relevant to the usual pressure range for diving and hyperbaric exposures. The finding is most likely explained by conformational changes in the Hb molecule induced by pressure, with a possible contribution from interaction of the molecule with inert gas (199). In theory, a left shift of the oxygen-Hb dissociation curve can be advantageous to the loading of oxygen into the pulmonary capillary blood (277). However, the magnitude of the change in P-50 seen in hyperbaric conditions would be unlikely to have any significant effect on pulmonary gas exchange (200).

### Carriage of oxygen under hyperbaric conditions

The carriage of oxygen in blood is described in detail elsewhere in *Comprehensive Physiology*. Once again, the focus here is on those aspects of “normal” oxygen transport that

change under hyperbaric conditions. As a basis for this discussion, a brief overview of “normal” oxygen transport is as follows.

Oxygen is transported in two forms: chemically bound to Hb and dissolved in blood. Hemoglobin is contained within erythrocytes at a whole-blood reference concentration of 15 g/dl. Each Hb molecule is a tetramer and each of its constituent protein chains carries a heme group capable of binding a molecule of oxygen. Estimates of percentage oxygen saturation of Hb refer to the percentage of the total oxygen binding sites on Hb that are occupied. The relationship between  $P_{O_2}$  and the oxygen saturation of Hb is described by the oxygen-Hb dissociation curve, which is explained in detail elsewhere in *Comprehensive Physiology*. There is a history of controversy over the volumetric oxygen-binding capacity of Hb that has resulted in different estimates continuing to appear in the literature. We follow the recent example of Piantadosi (218) in utilizing the Huffer constant of 1.34 ml  $O_2$ /g Hb. Thus, assuming a  $P_{aO_2}$  of 100 mmHg, an approximate corresponding Hb saturation of 100%, and a blood Hb concentration of 15 g/dl, the oxygen content of arterial blood ( $CaO_2$ ) that is bound to Hb is given by  $1.34 \text{ ml/g} \times 15 \text{ g/dl} = 20.1 \text{ ml/dl}$ . In contrast, the amount of oxygen dissolved in plasma under these conditions is much smaller. The solubility of oxygen in blood at 37°C is 0.003 ml/mmHg/dl. Once again assuming a  $P_{aO_2}$  of 100 mmHg, the amount of dissolved oxygen is given by  $0.003 \text{ ml/mmHg/dl} \times 100 \text{ mmHg} = 0.3 \text{ ml/dl}$ . Combined with the 20.1 ml/dl  $O_2$  carried by Hb, this gives a total arterial oxygen content of 20.4 ml/dl. The quantitative importance of Hb in oxygen carriage is clearly evident and is brought more sharply into focus when it is considered that the normal arteriovenous difference in oxygen content at rest is approximately 5 ml/dl.

The amount of oxygen dissolved in plasma can increase significantly as a result of the hyperoxia frequently encountered under hyperbaric conditions (see earlier). Table 2 compares theoretical figures for oxygen carriage compiled from simple calculations similar to that described above. The same principles are illustrated in Figure 12, which, in effect, shows the oxygen-Hb dissociation curve on a  $P_{O_2}$  scale extending into the hyperoxic range. Figure 12 demonstrates that the oxygen content of blood increases rapidly within the range

**Table 2** Calculated Arterial Oxygen ( $CaO_2$ ) Carriage by Binding to Hemoglobin and Dissolved in Physical Solution

Pressure, atm abs	Gas	$P_{iO_2}$ , <sup>a</sup> mmHg	$P_{aO_2}$ , mmHg	$P_{aO_2}$ , <sup>b</sup> mmHg	Hb sat, %	$CaO_2$ Hb, ml/dl	$CaO_2$ dissolved, ml/dl
1	Air	149	101	101	~100	20.1	0.3
1	$O_2$	713	673	673	100	20.1	2.0
2	$O_2$	1473	1433	1433	100	20.1	4.3
3	$O_2$	2233	2193	2193	100	20.1	6.6

$CaO_2$  based on parameters in text.

<sup>a</sup>Wet gas.

<sup>b</sup>Assuming no A-a $DO_2$ .

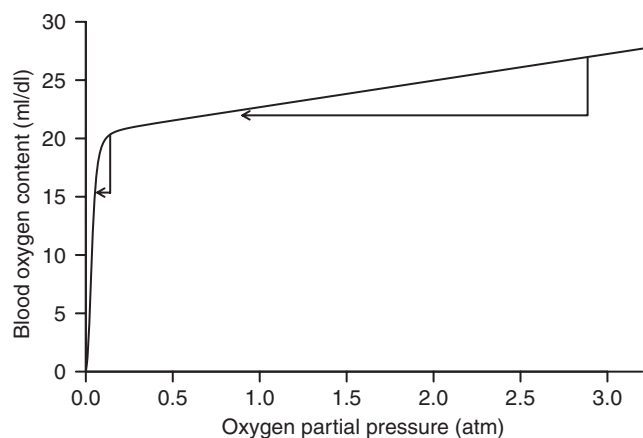


**Figure 12** Blood oxygen content for oxygen partial pressures extending into hyperbaric conditions. The right-angle arrows illustrate oxygen extraction of 5 vol% for air breathing at sea level (left arrow) and for oxygen breathing at 3 atm abs.

of  $P_{aO_2}$  expected during air breathing until Hb is saturated. From that point, and despite large increases in  $P_{aO_2}$ , the  $CaO_2$  increases only slowly because of oxygen's low blood solubility. Nevertheless, it is notable that when breathing oxygen ( $F_{IO_2} = 1$ ) at 3 atm abs, approximately 6 ml/dl of oxygen is dissolved in blood. This exceeds the resting arteriovenous extraction of oxygen and implies that the body's oxygen requirements could be met from dissolved oxygen alone under these conditions. This notion is supported by the finding of a mean venous  $PO_2$  of 424 mmHg and a mixed venous Hb saturation of 100% in 8 of 10 human subjects breathing oxygen ( $F_{IO_2} = 1$ ) at 3.04 atm abs (292). A further implication is that breathing oxygen at such pressures could allow survival without Hb, at least transiently. This was confirmed by Boerema et al. (21), who exsanguinated piglets and replaced their blood with a buffer solution while ventilating them with oxygen at 3 atm abs. This forms the basis for the use of HBOT in the treatment of exceptional blood loss anemia in humans where transfusion is not possible (113), such as in the case of Jehovah's Witness patients.

### Transfer of oxygen to tissues under hyperbaric conditions

There is abundant evidence that delivery of oxygen to tissues is enhanced under conditions of hyperbaric hyperoxia. Indeed, this is a critical goal in most applications of HBOT and the treatment of nonhealing wounds in particular. The use of transcutaneous oximetry to demonstrate correction of tissue hypoxia during hyperoxia is a daily reminder for most hyperbaric physicians of the efficacy of hyperoxia in this regard and one of the cornerstones of their approach to patients with problem wounds (244). In terms of oxygen delivery to individual organs during hyperoxia, the brain is one of the most extensively studied organs. Both direct and indirect measurements of cerebral oxygenation show improved oxygenation during both normobaric and hyperbaric hyperoxia (150, 168, 261) despite a mild vasoconstrictive response to hyperoxia (56).

An increase in oxygen delivery to tissues during hyperoxia is not surprising given the increased  $PO_2$  of oxygen dissolved in plasma and the dependence of oxygen transfer from blood to tissues on diffusion under normal circumstances. In this context, Piantadosi (218) recently discussed the Krogh-Erlang model, which portrays the capillary-tissue unit as a cylinder whose radius varies with the  $PO_2$  in the capillary and defines the diffusion distance for oxygen through the tissue. Since the  $PO_2$  declines along the length of the capillary from the arteriolar to venous ends, the cylinder radius also tapers in the same direction. The effects of hyperoxia on this model were predicted for the brain by Saltzman (230) (see Fig. 13). His calculations were based on a lower limit of tissue  $PO_2$  for adequate metabolic function of 12 mmHg and showed that during air breathing at 1 atm abs, the radii at which this threshold would be crossed were 64 and 36  $\mu\text{M}$  at the arteriolar and venous ends of a capillary, respectively. These radii increased to 247 and 64  $\mu\text{M}$ , respectively, during oxygen breathing ( $F_{IO_2} = 1$ ) at 3 atm abs. It is notable that in the latter condition, the radius of effective oxygen diffusion at the venous end of the capillary has increased to be equivalent to that at the arteriolar end during air breathing. Saltzman also hypothesized that if countercurrent blood flow occurs in the capillary bed (see Fig. 13), then the maximal intercapillary distance consistent with adequate oxygenation of tissue increases even further. The potential benefit of these effects is apparent in the context of diseases in which capillaries are injured or destroyed (such as diabetes and radiation tissue injury) or where there is an increase in interstitial edema that effectively increases intercapillary diffusion distances (218).

Concerns have been raised that oxygen administration may reduce tissue perfusion and thereby negate any potential benefit of an increase in  $P_{aO_2}$  (146). In theory, this might occur because of a more direct vasoconstrictive effect of hyperoxia (55). This issue has been recently reviewed by both Forkner et al. (88) and Piantadosi (218) and is not considered a valid concern under most circumstances. Indeed, tissue oxygen delivery is almost certainly maintained (in the worst case) or enhanced during hyperoxia despite the fact that hyperoxia may reduce blood flow.

## Inert Gases

### Need for diluent gas

Since oxygen becomes toxic to various organ systems at inspired pressure above 0.5 atm, pure oxygen may only be used as a diving breathing gas at shallow depths and for relatively brief periods. Most diving therefore occurs using a breathing gas that is a mixture of oxygen and another gas. Air is the most common breathing gas, but nitrogen-oxygen (nitrox), helium-oxygen (heliox), and helium-nitrogen-oxygen (trimix) mixtures are widely used. In operational diving, if helium and nitrogen are handled separately from oxygen, they may be referred to as diluent gases, but in diving physiology jargon, these gases are "inert" gases, although nitrogen is not

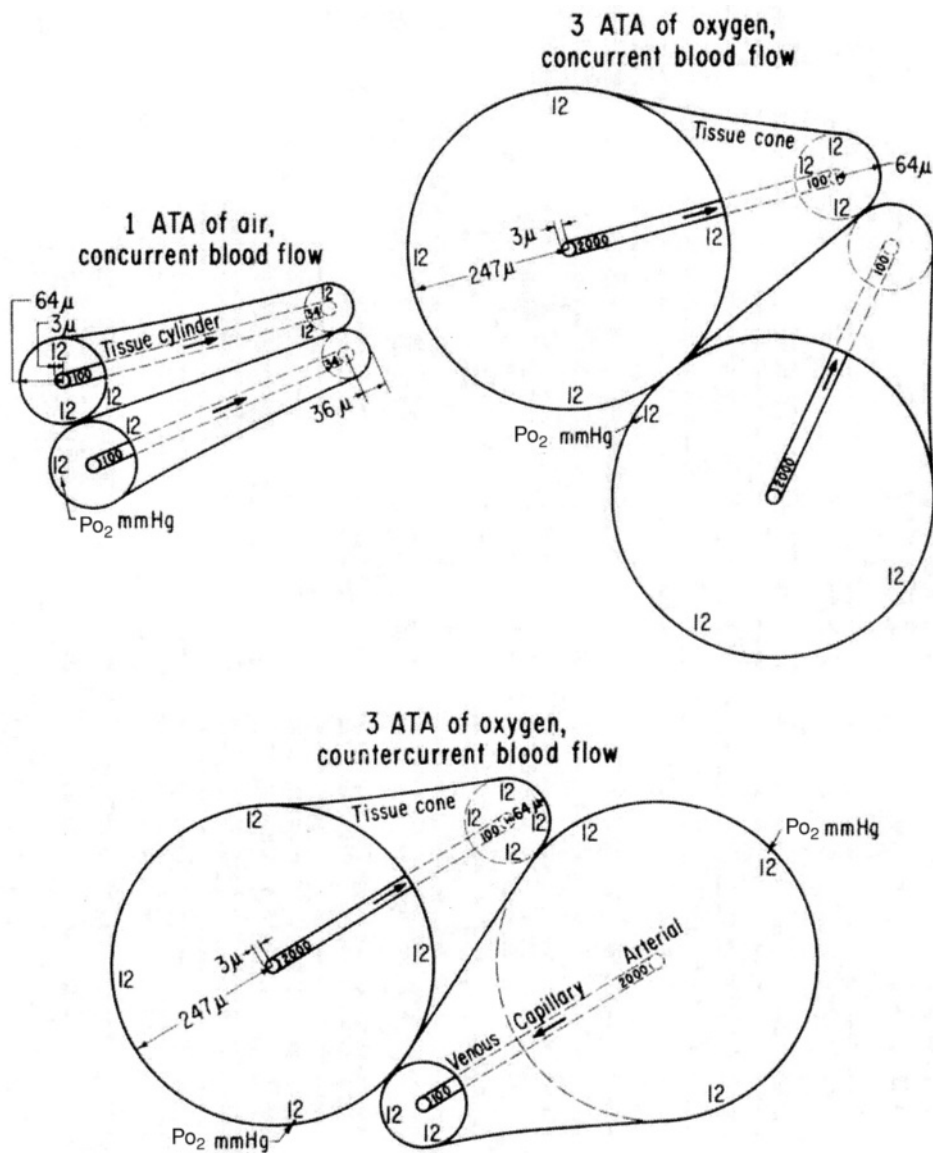


**Figure 13** Intercapillary diffusion distances for oxygen depicted using the Krogh cylinder model under conditions of air breathing at 1 atm abs (top left); oxygen breathing at 3 atm abs (top right); and oxygen breathing at 3 atm abs assuming countercurrent flow in adjacent capillaries (bottom). Cylinder boundaries are defined by the calculated distance from capillary to the point where tissue PO<sub>2</sub> falls to 12 mmHg. The advantage of a high PaO<sub>2</sub>, particularly at the arterial end of the capillary is clearly apparent, as is the potential advantage of a countercurrent flow pattern during hyperbaric oxygen breathing. Reproduced with permission from Saltzman (230).

chemically inert; the term refers to the fact that these gases do not participate in cellular respiration.

### The basic issues

For an air-breathing animal that has not made an excursion from sea level, nitrogen is dissolved in all the body tissues at a concentration proportional to the alveolar nitrogen partial pressure as described by Henry's law.

$$y_j P = H_{lj} x_j \quad (6)$$

where  $H$  is Henry's constant for gas  $j$  in liquid  $l$ ;  $x$  and  $y$  are the mole fractions in the liquid and vapor phases, respectively; and  $P$  is the total gas mixture pressure. The gas partial pressure ( $y_j P$ ) at equilibrium describes the gas activity in either phase and will generally hereafter be denoted more compactly as  $P_j$ .

A change in alveolar nitrogen partial pressure will result in the transport of nitrogen between lungs and tissues, eventually establishing a new equilibrium where alveolar and tissue PN<sub>2</sub> are equal. Such a change in alveolar PN<sub>2</sub> occurs at sea level if the inspired gas mixture is changed, for instance, in a

clinical setting where a patient is administered oxygen or an anaesthetic gas [change in  $y_j$  in Eq. (6)]. The resulting change in tissue nitrogen gas partial pressure is of no consequence at sea level. During a hyperbaric exposure, although changing inspired gas mixture is also common, alveolar inert gas partial pressures change as a result of the change in total pressure [ $P$  in Eq. (6)] and the potential increase of inert gas partial pressures above 1 atm are not inconsequential.

One consequence is nitrogen narcosis, described in the introduction to this article. Nitrogen narcosis can be eliminated by substituting helium for nitrogen in breathing gas mixtures. A consequence of the uptake of diving diluent gases into tissues at increased pressure that cannot be eliminated is the risk of DCS. During ascent to sea level (decompression) following a hyperbaric exposure, the ambient pressure may drop below the sum of the partial pressures of all gases dissolved in tissue:

$$\left(\sum P_{\text{tis}_{\text{inert}}} + P_{\text{tis}_{\text{O}_2}} + P_{\text{tis}_{\text{CO}_2}} + P_{\text{H}_2\text{O}}\right) - P_{\text{amb}} > 0 \quad (7)$$

This state, referred to as supersaturation, is a necessary condition for bubbles to form. Bubbles can then grow from the excess dissolved gas [Eq. (6)]. Excessive bubble formation in body tissues is the putative cause of DCS. Minimizing the risk of DCS is the principal motivation to study the respiratory exchange of helium and nitrogen.

### Decompression models

In diving practice, to minimize the risk of DCS, the rate of decompression is controlled, typically by interrupting ascent with specified “decompression stops” (see Fig. 14). Dives are conducted according to depth/time/breathing gas decompression schedules derived from decompression algorithms that implicitly or explicitly minimize bubble formation through controlling tissue gas supersaturation. The bubble-tissue interactions that result in DCS have not been observed, and the tissues in which bubble injury manifests as DCS are unknown; consequently, the relevant gas uptake and washout, bubble formation, and bubble growth have not been measured and these processes are represented with latent variables in decompression models. Parameters of these latent variables are adjusted in accord with observed DCS incidence resulting from manned-testing. Parameters may be adjusted intuitively and then representative schedules tested, or parameters may be formally estimated by statistical fit of the model to an extensive set of preexisting man-trial data. The resulting decompression models are physiologically structured empirical models and are not intended to investigate these latent processes. Such validated decompression algorithms will be discussed only to the extent that they provide the motivation for the underlying theory. Decompression models are more completely reviewed elsewhere (263).

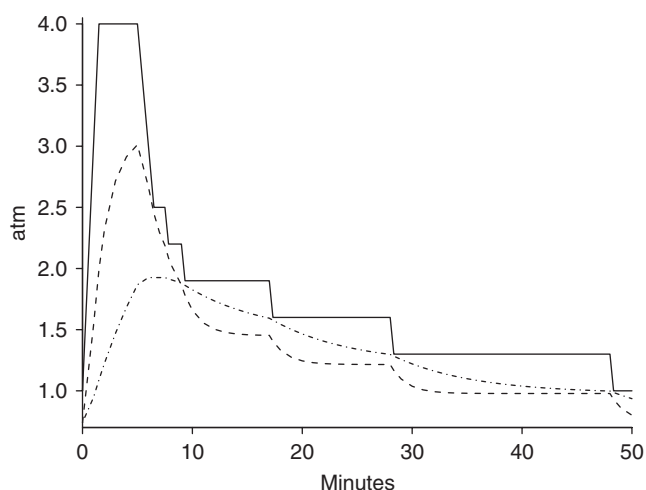


**Figure 14** Ambient pressure (solid line) versus time and the corresponding total gas pressures ( $\sum P_{\text{tis}_j}$ ) in two compartments (half-times of 1 and 5 min) for an air-breathing dive. Classical decompression is scheduled to keep dissolved gas pressure in  $k$  modeled compartments less than or equal to a maximum permissible value,  $P_{\text{tis}_k} \leq a_k P_{\text{amb}} + b_k$ . For simplicity, the above figure shows only two compartments and sets  $a = 1$  and  $b = 0$  so that the “safe ascent depth”,  $P_{\text{amb}} = \max\{(P_{\text{tis}_k} - b)/a\}$ , is equal to  $\max(P_{\text{tis}_k})$ . By convention, decompression stops are taken at increments of 10 fsw (0.3 atm abs) deeper than sea level.

### Ideal gas approximation in human hyperbaric exposures

Normal respiratory physiology uses an equation of state and gas laws, for instance the ideal gas law [Eq. (1)] and Henry’s law in the form given in Eq. (6), that presume ideal gas and are strictly correct only in the limit as  $P$  approaches zero. There has been unfounded concern regarding the applicability of these gas laws in the context of human hyperbaric exposures. However, these gas laws remain good approximations over the range of pressures encountered in human hyperbaric exposures.

Equilibrium with respect to heat transfer, boundary displacement, and mass transfer in a heterogeneous closed system comprising a gas phase and a liquid phase is defined by any of the fundamental equations describing the combined first and second laws of thermodynamics (224). For instance, Eq. (8) defines the change in Gibb’s free energy ( $G$ ) in any of the phases; temperature ( $T$ ), pressure ( $P$ ), and chemical potential ( $\mu_j$ ), each have a uniform value throughout all phases at equilibrium.

$$dG \leq -S dT + V dP + \sum_j \mu_j dn_j \quad (8)$$

The chemical potential defines the contribution of a mass transfer of  $n$  moles of chemical species  $j$ . The chemical potential can be described in less abstract terms as follows:

$$\mu_j = \mu_j^0 + RT \ln \frac{f_j}{f_j^0} \quad (9)$$

where  $R$  is the universal gas constant; superscript 0 refers to an arbitrary standard state; and  $f$  is the fugacity. Fugacity is the pressure corrected for deviation from ideal behavior:

$$f_{\text{gas}_j} = \varphi y_j P \quad (10)$$

where the fugacity coefficient ( $\varphi$ ) = 1 for an ideal gas. Gas departure from ideal is defined by its compressibility ( $PV/RT$ ), which can be used to calculate  $\varphi$  or fugacity. Fugacity at or near body temperature differs from the pure gas pressure by less than 1% (equivalently  $|\varphi| \leq 1.01$ ) for pressures up to at least 20 atm for nitrogen and 30 atm for helium (58, 99, 290). The Lewis rule, implicit in Eq. (10), assumes that the fugacity coefficient is independent of the composition of a gas mixture and is a good approximation at pressures where the gas phase is nearly ideal ( $\varphi \cong 1$ ), if the component gases have similar physical properties or if one species dominates (224). Breathing gas mixtures can be considered ideal for the majority of human exposures, which use mixtures of nitrogen and oxygen (which have similar physical properties), are to pressures less than 10 atm abs, and deeper dives are conducted using mixtures consisting mainly of helium ( $y_j > 0.95$ ).

If standard states for different phases are defined at the same temperature ( $T$ ), chemical equilibrium of species  $j$  between, for instance, a liquid phase and a gas phase is defined as follows:

$$f_{\text{gas}_j} = f_{\text{liquid}_j} \quad (11)$$

or, assuming an ideal gas,  $P_{\text{gas}_j} = P_{\text{liquid}_j}$ . Diffusion will occur down any chemical potential gradient to attain this equilibrium.

The mole fraction ( $x_j$ ) of a gas solute dissolved in liquid is related to the fugacity by a proportionality constant that in the limit of an ideal dilute solution (no solute-solute interactions) is Henry's constant:

$$\lim_{x_j \rightarrow 0} \frac{f_{\text{liquid}_j}}{x_j} = H \quad (12)$$

Substitution of Eq. (10) into Eq. (12) and using the identity of Eq. (11) gives the familiar form of Henry's law [Eq. (6)] that does not account for pressure dependence. The pressure dependence of Henry's constant for temperatures below the critical temperature of the solvent can be given by (161):

$$\ln \frac{f_j}{x_j} = \ln H + \frac{\bar{v}_2^\infty (P - P^s)}{RT} \quad (13)$$

where  $P^s$  is the vapor pressure of the solvent and  $\bar{v}_2^\infty$  is the partial molar volume of the solute. The second term on the right-hand side applies a pressure-dependent correction to what is otherwise Henry's law. Equation (13) fits experimental nitrogen and helium solubilities in water and olive oil up to 300 atm (100) and using the estimated partial molar volumes, the second term on the right-hand side of Eq. (13) results in

**Table 3** Ostwald Solubility Coefficients ( $\alpha$ , Dimensionless) and Diffusivities ( $D$ ,  $10^{-5}$  cm<sup>2</sup>/s) at 37°C\*

	Nitrogen	Helium
$\alpha_{\text{olive oil}}$	0.0736	0.0169 <sup>a</sup>
$\alpha_{\text{yellow marrow}}$	0.073 <sup>a</sup>	–
$\alpha_{\text{aqueous tissue}}$	0.0156 <sup>b</sup>	0.0117 <sup>a,c</sup>
$\alpha_{\text{whole blood}}$	0.0151	0.0094
$D_{\text{skeletal muscle}}$	1.3	3.94 <sup>a</sup>

Compiled from Lango et al. (170). Data are from various species. Solubilities are means of 3-10 values, with coefficient of variation of 8% or less.

\*Olive oil often used as a model for biological lipids.

<sup>a</sup>Single value.

<sup>b</sup>Brain.

<sup>c</sup>Skeletal muscle.

at most a 3% correction to Henry's constant for nitrogen and helium for pressures up to 10 atm. Henry's law in the form of Eq. (2) is applicable to human hyperbaric exposure with trivial error.

In physiological literature, it is more common to describe solubility using a solubility coefficient than using Henry's constant. For instance, the Ostwald solubility coefficient ( $\alpha$ ) relates partial pressure and concentration ( $C$ , in ml gas/ml liquid at 1 atm) at the temperature of the experiment by  $\alpha P = C$  (see Table 3). The Ostwald coefficient and Henry's constant are related by  $\alpha = RT\rho/PMWtH$  for a liquid, with density  $\rho$  and gram molecular weight  $MWt$  at experimental temperature ( $T$ ) and pressure ( $P$ ).

## Lungs

Equilibration of arterial blood to changes in inspired partial pressure of diving diluent gases is rapid as illustrated for nitrogen in Figure 15. Underwater breathing apparatus delivers gas at ambient pressure, so a change in ambient pressure alters inspired and alveolar gas partial pressures in parallel. The equilibration between inspired, alveolar, and arterial nitrogen partial pressures proceeds rapidly as a result of the low solubility of helium and nitrogen in tissues. Therefore, over a time course relevant to decompression physiology, the kinetics of helium and nitrogen reduces to a problem of exchange between the blood and the tissues.

## Tissue kinetics

Compartmental (lumped) kinetic models are generally used to describe blood-tissue exchange of diving diluent gases. In this context, a compartment is represented by a single, time-varying partial pressure. Underlying this notion is the assumption that owing to rapid diffusion, equilibration of inert gas partial pressure gradients across the tissue region represented by the compartment is much faster than transport in and out of the compartment (well mixed). The most commonly used

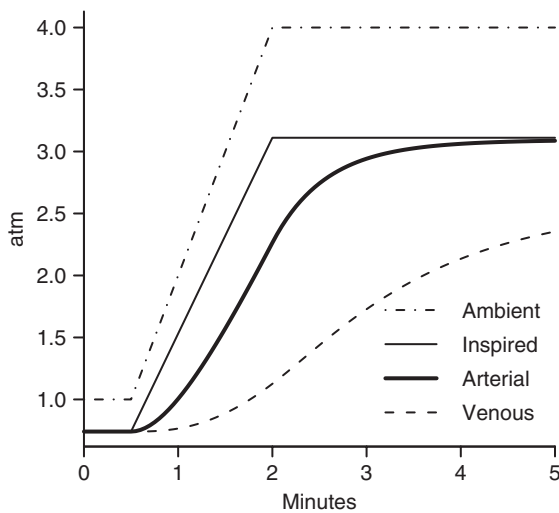


**Figure 15** Simulation of the equilibration of blood with inspired nitrogen with compression breathing air. Simulation is based on the standard, resting 70-kg man (189) with inspired gas, alveolar gas, pulmonary blood, and the body in series, the latter composed of four parallel compartments representing vessel rich, muscle, fat, and vessel poor tissue groups (74). The simulation uses nitrogen tissue solubility coefficients ( $\alpha$ ) of 0.015 (blood), 0.015 (lean), and 0.075 (fat) and an estimated lung nitrogen diffusing capacity of 0.15 liters/min/kPa (170, 180). A ramp in inspired  $\text{PN}_2$  occurs with compression from 101 kPa (sea level) to 404 kPa (4 atm abs) ambient pressure (dashed line). Ninety-nine percent equilibration of arterial blood with inspired  $\text{PN}_2$  (solid line) occurs 2.5 min after reaching depth. Throughout the time course of this simulation, there less than 0.3% difference between arterial blood and alveolar  $\text{PN}_2$ .

tissue model is the single, well-mixed compartment in which perfusion is considered the rate-limiting process, tissue and venous partial pressures are in equilibrium, and arterial-tissue inert gas partial pressure difference ( $P_a - P_{tis}$ ) declines monoexponentially. The rate of change of compartmental partial pressure is given by (suppressing gas subscripts):

$$\frac{dP_{tis}}{dt} = \frac{(P_a - P_{tis})}{\tau} \tag{14}$$

where the time constant  $\tau$  is given by:

$$\tau = \frac{V_{tis}\alpha_{tis}}{\dot{Q}_{tis}\alpha_{blood}} \tag{15}$$

and where  $V_{tis}$  is tissue volume,  $\dot{Q}_{tis}$  is tissue blood flow, and  $\alpha_{tis}/\alpha_{blood}$  is the tissue:blood partition coefficient. In diving physiology, it is common to use the half-time, which is equal to  $\ln(2)\tau$ .

Since the tissue sites relevant to DCS are unknown, it is common to model uptake and washout of inert gases in a collection of such compartments in parallel (i.e., no gas flow between compartments), each with a different time constant spanning some range thought to encompass all relevant tissues. In this regard, DCS has protean manifestations, credibly attributable to bubble formation in many organ systems.

This parallel compartment approach dates to Haldane and colleagues, who produced the first decompression model and decompression schedules in the early 20th century (22) and is similar to pharmacokinetic models that first appeared several decades later (253).

### Application: Ratios and M values

The Haldane decompression model tracked air pressure, with air treated as if a single inert gas, in five parallel compartments with half-times of 5, 10, 20, 40, and 75 min. Decompression was allowed to an ambient pressure of half the maximum air pressure in any compartment (designated a 2:1 tissue ratio). This tissue ratio was established experimentally from DCS in goats. Thus, according to this model, an air-breathing diver could stay an unlimited time at 2 atm abs pressure and return directly to sea level. From deeper depths, a diver would likely have to interrupt ascent to the surface with decompression stops at a depth governed by the 2:1 ratio to allow washout of gas from the tissues. By convention established with these decompression tables, decompression stops are taken at increments of 10 fsw pressure (0.3 atm, 31 kPa) from sea level (see Fig. 14).

The Haldane tables, developed for the Royal Navy, were soon adopted by the U.S. Navy (208), where the approach has been further developed in association with extensive manned-testing. Principal early developments designed to increase the depth and duration of decompression stops following longer, deeper dives included increasing the range of compartmental nitrogen half-times, assigning a different tissue ratio to each compartment, and using different ratios for decompression stops than for surfacing (72, 118, 266). Depth-dependent ratios were found to be well described by a relationship of the form  $P_{tis} = aP_{amb} + b$ , where  $P_{tis}$  is the maximum allowed compartmental inert gas partial pressure at  $P_{amb}$ . If pressures are expressed in feet of sea water, the expression is written as  $M = aD + M_0$ , and these “M” values give the allowed compartment inert gas partial pressure at decompression stop depth ( $D$ ) (301). M values and an algorithm developed by Thalmann (255) form the basis of many current U.S. Navy decompression procedures.

Many decompression procedures employ increased inspired oxygen fraction to reduce the inspired inert gas partial pressure, thereby reducing compartmental inert gas uptake or accelerating inert gas washout and reducing decompression time. Helium diving has been handled by a different set of M values and ignoring nitrogen (256,301) or tracking both gases and applying compartmental-gas-weighted average of the respective M values (24). The latter model, probably owing to publication outside the military technical literature, has seen widespread adaptation for use in diver-carried decompression computers and desktop decompression software used by recreational divers. A century after development, the Haldane approach remains the most prevalent form of decompression algorithm.

## Experimental data

Consistent with the use of multiple compartments with a range of time constants in decompression models, experimental studies of diving diluent gas kinetics have demonstrated differing rates of gas exchange in different tissues. For instance, early measurements of nitrogen in bone marrow (30) indicate an approximate time constant of 4.1 h (time constant from reanalysis of the data by the present authors), whereas brain has nitrogen and helium time constants of 1.2 and 1.0 min, respectively (64). Whole-body elimination of inert gas reflects such a range in time constants. One to three exponentials with time constants ranging from 2.2 to 185 min are extracted by graphical backward projection from lung nitrogen elimination curves of humans during oxygen or helium-oxygen breathing (16, 185, 276). Three time constants (2.1, 16.9, and 153.8 min) have been extracted from arterial-mixed venous nitrogen difference during nitrogen washout in oxygen breathing anaesthetised dogs (109). Two time constants (2.9 and 250 min) are extracted from mixed venous nitrogen concentrations during hyperbaric nitrogen uptake in dogs (51).

Some earlier workers attempted to identify compartment time constants with specific anatomical tissues, for instance, based on symptoms arising from decompression (24). This latter approach supposes that other latent variables in the model are correct and can be misleading, for instance, assigning time constants to the vestibulocochlear apparatus (25) that are an order of magnitude longer than physiologically plausible (62). Also, the time constants of tissues may change substantially during and following a dive, as evidenced by alteration of lung nitrogen elimination curves in humans under conditions relevant to diving. Immersion causes an increase in cardiac output and a more rapid elimination of nitrogen than in the dry, representing a shift of some tissues to a faster time constant (11). Compared to thermoneutral air temperature (28°C), warm ambient temperature (37°C) increases the rate of nitrogen recovery, perhaps as a result of increase blood flow to superficial tissues (10). Exercise causes substantial changes in blood flow in many tissues and has been shown to increase the rate of nitrogen and helium elimination compared to rest (17).

There is no need to identify compartment time constants with specific tissues. Of more relevance is whether any microscopic site at which a DCS-provoking bubble forms is adequately represented by monoexponential gas kinetics. There are relatively few data on the kinetics of diving diluent gases suitable to address this issue because of the limited relevance outside the field of diving. Other inert gases, particularly nitrous oxide, krypton, xenon, and hydrogen, have received considerable attention because of their importance as tracers for calculation of tissue blood flow from the converging arterial and tissue tracer concentrations according to the indirect Fick method (154).

Multiexponential uptake and washout of inert gas is found in even relatively homogenous tissues. For instance, helium

(65), nitrogen (1, 66), xenon (158, 211, 236, 237), hydrogen (8), and nitrous oxide (68) display multiexponential kinetics in skeletal muscle. Similarly, helium (67), nitrogen (64), methane, argon, (212), krypton (174), hydrogen (274, 275), and nitrous oxide (63) display multiexponential kinetics in the brain.

Multiexponential kinetics has been attributed to adjacent tissue regions behaving as separate compartments with differing time constants. Such regions would need to be of millimeter dimensions so that partial pressure gradients between adjacent regions are not equilibrated by diffusion (61, 67, 139). Differing regional time constants could arise from differing blood flows and differing inert gas tissue:blood partition coefficients. Heterogeneity of the latter may arise from differing fat content because inert gases are much more soluble in fat than in blood or aqueous tissues (see Table 3). However, the heterogeneity of blood flow (110, 147, 159, 211, 236) and fat content (34, 158) is not sufficient to account for the difference in inert gas time constants measured in skeletal muscle or brain. Multiexponential kinetics may arise from macroscopic diffusion gradients between compartment-sized tissue volumes, for instance, between distinct tissues (217) or across a few regions with unusual anatomy (see the "Isobaric counterdiffusion" section below).

However, multiexponential washout of gases is also characteristic of tissue regions too small to behave as separate compartments. Using fine polarographic electrodes, multiexponential hydrogen clearance curves are measured in tissue volumes with less than millimetre dimension (274). Diffusion-limited gas exchange at this scale over time courses relevant to decompression calculations is not supported by reported values for diffusion coefficients (170) and the absence of diffusion limitation is the basic assumption of the lumped approximation. A candidate process for multiexponential kinetics at this scale is diffusion of gas from arterioles to venules, allowing some gas to bypass the capillary bed. Such arterial-venous diffusion shunt has been used to explain the observed kinetics of xenon, hydrogen, nitrous oxide, helium, and nitrogen in skeletal muscle (8, 65, 66, 68, 139, 211, 237), helium in cardiac muscle (297), and nitrogen, helium, and nitrous oxide in the brain (63, 64, 67). There is direct evidence for arterial-venous diffusion shunt in brain (23) and muscle (235, 237) where xenon gas from an arterial bolus appears in venous effluent ahead of coadministered intravascular tracers.

## Alternative approaches

The experimental data indicate that the single perfusion-limited compartment is an unrealistic representation of the inert gas kinetics for many tissue regions. Alternative tissue kinetic treatments have been used for decompression models. Distributed treatments of blood:tissue diffusion limitation include a single tissue capillary unit model with annular geometry (132, 133) and diffusion in a tissue slab bathed on both sides by arterial blood, the latter forming the basis of Royal Navy decompression procedures in the 1950s (124). The Canadian

Forces decompression procedures are based on a mathematical model of a pneumatic-mechanical analogue decompression consisting of four gas-filled compartments, connected in series with breathing gas (210). Except for the nonlinear pressure dependence of gas flow between the compartments, this serial model has similarities to a finite difference approximation of bulk diffusion through a slab (125) or to arterial-venous countercurrent diffusion models (65). Other multiexponential compartmental models, similar to those used to model diving diluent gases (65, 67) and other inert gas kinetic data (288), have been used to analyze the incidence of DCS in military decompression data sets (3, 105, 119). Monoexponential and multiexponential compartmental models fit a broad range of such data equally well (3, 119, 264). There is no evidence that any of these approaches represent a significant improvement over the more common multiple, parallel compartments approach for the development of practical decompression procedures.

## Bubble formation

### Theory and experimental data

If gas supersaturation occurs in tissue, bubbles may form to relieve the supersaturation. The sum of all gas partial pressures inside a spherical bubble ( $P_{\text{bub}}$ ) of radius  $r$  exceeds the ambient barometric pressure ( $P_{\text{amb}}$ ) and is given by:

$$P_{\text{bub}} = P_{\text{amb}} + \frac{2\sigma}{r} + \frac{4\pi r^3 B}{3V_{\text{tis}}} \quad (16)$$

The last term on the right-hand side is pressure exerted by displaced tissue, where  $V_{\text{tis}}$  is the volume of tissue affected and  $B$  is the bulk modulus of elasticity of that tissue (98). The second term on the right-hand side is the pressure increase across the gas-liquid interface due to surface tension ( $\sigma$ ). For instance, for a surface tension characteristic of blood of 56 mN/m (141), a bubble with  $r = 1 \mu\text{m}$  must have an internal pressure that exceeds ambient by  $2\sigma/r = 112 \text{ kPa} = 1.11 \text{ atm abs}$ . Ignoring any mechanical pressure due to tissue distortion, a bubble can only persist and grow if  $\Sigma P_{\text{tis}_j}$  exceeds  $P_{\text{amb}}$  by enough to overcome the pressure due to surface tension.

$$\sum P_{\text{tis}_j} - P_{\text{amb}} \geq \frac{2\sigma}{r} \quad (17)$$

*De novo* bubble formation in pure water (nucleation) requires 190 atm supersaturation pressure of nitrogen or 300 atm supersaturation pressure of helium (121). The free energy required to nucleate a bubble is not well defined but must include components for assembly of a sufficiently large cluster of gas molecules and formation of a surface of separation between gas and liquid (121) and then maintaining the bubble surface against surface tension (280).

However, in humans, detectable venous gas bubbles follow decompression to sea level as shallow as 3.6 m (1.36 atm abs, 137 kPa) (73), indicating only very small tissue super-

saturation is required. Susceptibility to bubble formation is not an intrinsic property of biological fluids since very high supersaturation pressures are required to nucleate bubbles inside unicellular organisms (123), erythrocytes (120), blood isolated from the circulation (116, 175), or water in the presence of surfactants larger than 330 Da (122).

It is widely accepted that bubble form at low supersaturation from preexisting gas nuclei (theoretical protobubbles). There is evidence for preexisting gas nuclei in animals, for instance, shrimp can be rendered resistant to decompression-induced bubble formation with a preceding 200 atm abs compression that presumably drives gas nuclei back into solution (79). The origin of gas nuclei is unknown, but one source appears to be from tensile forces induced by movement (79, 192).

### Application

Decompression models have been developed that count the number of bubbles induced to grow from a theoretical distribution of gas nuclei sizes in response to supersaturation. Decompression proceeds allowing a safe number or volume of bubbles (303). This style of decompression model has gained importance recently because of widespread adaptation for use in desktop decompression software by technical divers. This popularity is probably due to easy access in the mainstream scientific literature, Internet publication of source code (305), and because its prescriptions are in keeping with current folklore.

### Influence of bubble growth on inert gas kinetics

Once formed, bubbles will shrink or grow as gas diffuses to or from surrounding tissue. The primary reason to track bubble formation and growth in decompression models is to use some function of bubble size and profusion, typically bubble volumes, as an indicator of the risk of DCS. However, bubbles also alter the kinetics of inert gas in surrounding tissue.

Equation (14) describing tissue gas kinetics must be altered to accommodate transfer of gas between tissue and bubble (suppressing inert gas subscripts):

$$\frac{dP_{\text{tis}}}{dt} = \frac{(P_a - P_{\text{tis}})}{\tau} - \frac{1}{V_{\text{tis}}\alpha_{\text{tis}}} \frac{d(P_{\text{bub}}V_{\text{bub}})}{dt} \quad (18)$$

The impact of formation of a free gas phase on inert gas kinetics can be appreciated by examining a hypothetical worst case following a decompression resulting in sufficiently dense bubble formation such that all tissue gas is in partial pressure equilibrium with an adjacent bubble ( $P_{\text{bub}_j} = P_{\text{tis}_j}$ ) and neglecting surface tension so that  $P_{\text{amb}} = \Sigma P_{\text{bub}_j} = \Sigma P_{\text{tis}_j}$ . This gives for a single inert gas  $P_{\text{tis}_{\text{inert}}} = P_{\text{bub}_{\text{inert}}} = P_{\text{amb}} - \Sigma P_{\text{fixed}}$ , where  $\Sigma P_{\text{fixed}}$  is the sum of any gases assumed to have a constant tissue partial pressure. Although some decompression models have kinetic treatments of oxygen, for simplicity, tissue oxygen and  $\text{CO}_2$  partial pressures are commonly assumed fixed.

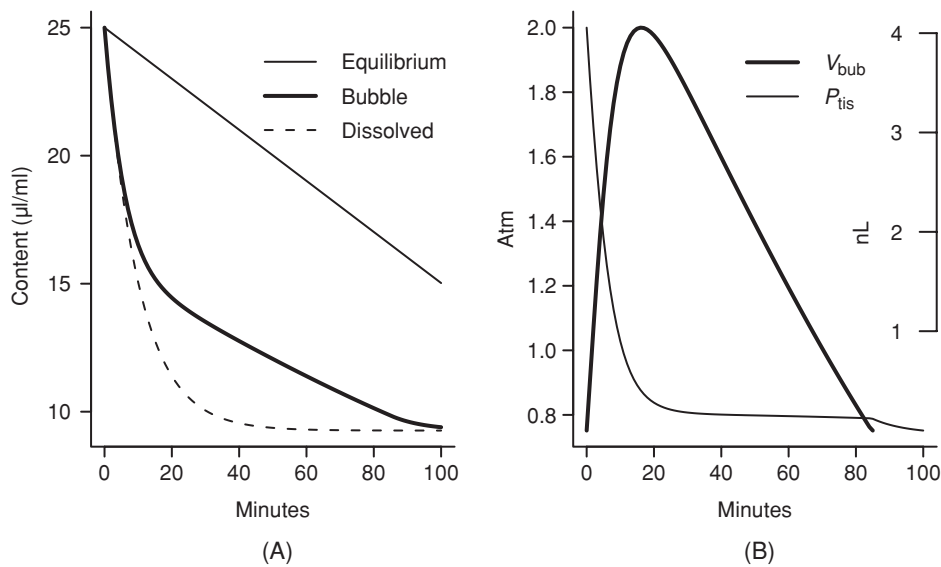


**Figure 16** (A) Washout of nitrogen (sum of dissolved and free gas) from tissue for the cases of all gas remaining dissolved (dotted line) according to Eq. (14), for phase equilibrium between bubble and dissolved gas partial pressures (thin line) according to Eq. (19), and for a single, spherical bubble in a small tissue volume (equivalent to a very high bubble density of  $10^{-6}$  bubbles/ml, thick line) by using a three-region model diffusion-limited bubble growth (245). (B) Dissolved tissue  $P_{N_2}$  (thin line, left axis) and bubble volume (thick line, right axis) for the spherical bubble case illustrated in panel (A).

Furthermore, oxygen and CO<sub>2</sub> along with water vapor are often assumed to equilibrate instantaneously between bubble and tissue ( $P_{\text{fixed}}$ ) (132, 255). These assumptions do not hold during rapid changes in ambient pressure or inspired oxygen partial pressure, but any changes in these “fixed” gas partial pressures inside bubbles are considered transient and small compared to those of the inert gases.

Substituting for  $P_{\text{tis}}$  on the right-hand side of Eq. (18) and collecting together the two differential terms and represented them in terms of a notional partial pressure this gas would represent if it had all remained in solution,  $p'_j = V_j/(\alpha_{\text{tis}} V_{\text{tis}})$  gives (255):

$$\frac{dP'}{dt} = \frac{dP_{\text{tis}}}{dt} + \frac{1}{V_{\text{tis}}\alpha_{\text{tis}}} \frac{d(P_{\text{bub}}V_{\text{bub}})}{dt} = \frac{(P_a - P_{\text{amb}} + \sum P_{\text{fixed}})}{\tau} \quad (19)$$

At constant  $P_{\text{amb}}$  and  $P_a$ , there will be slow, linear gas washout while  $P_{\text{tis}}$  is “clamped” by the bubble (see Fig. 16).

Inert gas washout is less affected in models that include restraints on nucleation and bubble growth. There has been considerable development of diffusion-limited growth of stationary, spherical decompression bubbles in tissue (98, 136, 245–247, 262, 271).

The transfer of gas across the bubble surface is given by Fick’s first law:

$$\frac{d(P_{\text{bub}}V_{\text{bub}})}{dt} = A \sum_{j=1} \left( \alpha_{\text{tis}_j} D_j \left. \frac{dP_{\text{tis}_j}}{dr} \right|_{r=r_A} \right) \quad (20)$$

where  $D_j$  is the bulk diffusivity of gas  $j$  in tissue,  $A$  is the bubble surface area, and  $dP_{\text{tis}_j}/dr$  is the gas partial pressure gradient evaluated at the bubble surface.  $dP_{\text{tis}_j}/dr$  is evaluated using (suppressing gas subscripts):

$$\alpha_{\text{tis}} \frac{\partial P_d}{\partial t} = \alpha_{\text{tis}} D \left( \frac{\partial^2 P_d}{\partial r^2} + \frac{2}{r} \frac{\partial P_d}{\partial r} \right) - \alpha_{\text{blood}} \frac{\dot{Q}_{\text{tis}}}{V_{\text{tis}}} (P_d - P_s) \quad (21)$$

where  $P_d$  is the inert gas partial pressure in the tissue diffusion region surrounding the bubble. The first term in parentheses on the right-hand side is the divergence of the partial pressure gradient for spherical geometry, and the second term allows for a sink or source of gas pressure ( $P_s$ ) owing to tissue perfusion (245, 271). Equation (21) is typically solved using the quasi-static approximation that sets  $\partial P/\partial t = 0$  (98, 245, 271). The quasi-static approximation is used under the presumption that changes in the partial pressure gradient with time are slow compared to the equilibration between bubble and tissue, an approximation that differs little from the nonsteady-state solution (78).

To find bubble radius and surface area ( $A = 4\pi r^2$ ), the differential on the left-hand side of Eq. (20) is expanded, and substituting for  $P_{\text{bub}}$  from Eq. (16) (ignoring the tissue distortion term) and  $V = 4\pi r^3/3$  gives (245):

$$\frac{dr_A}{dt} = \frac{\sum_{j=1} \left( \alpha_{\text{tis}_j} D_j \left. \frac{dP_{\text{tis}_j}}{dr} \right|_{r=r_A} \right) - \frac{r_A}{3} \frac{dP_{\text{amb}}}{dt}}{P_{\text{amb}} - \sum P_{\text{fixed}} + \frac{4\gamma}{3r_A}} \quad (22)$$

The solution for the partial pressure gradient at the bubble surface and the last term in Eq. (18) depends on the modeled structure of the diffusion region. Equation (21) was originally developed as a two-region model comprising the bubble and surrounding tissue, where  $P_s$  was defined as the gas pressure in arterial blood (271) or in tissue too distant to be influenced by the bubble (245). This model has been shown to imply an infinite tissue volume and therefore unsuited for evaluating mass balance of gas in the tissue using Eq. (18) (245). Three-region models separate the bubble from a well-stirred tissue with a thin, unperfused diffusion barrier (98, 245, 262) and Eq. (18) defines the mass balance between the bubble and the well-stirred tissue. Alternatively, the diffusion region may be extensive with diffusion gradient defined by Eq. (21) and no net gas exchange with the well-stirred region, in which case Eq. (18) defines the mass balance between the bubble and the diffusion region (246, 247).

### Experimental data

There are few experimental measurements of tissue bubble dynamics *in vivo*. Oxygen and CO<sub>2</sub> partial pressures in macroscopic subcutaneous gas pockets have been shown to be qualitatively similar to predictions from models of spherical bubble dynamics (26, 269). There are some photomicroscopy data on growth and dissolution of bubbles in rat abdominal adipose tissue arising from decompression from air dives (143), air injected into spinal white matter, muscle, tendon, or eye following decompression from air dives (144, 145), and helium injected into abdominal adipose tissue prior to heliox dives (142). These data will be discussed further in the “Isobaric counterdiffusion” section, but it is interesting to note here that a switch to breathing pure oxygen following decompression caused transient bubble growth, indicating elevation of PO<sub>2</sub> in the vicinity of the bubble, contrary to the common simplifying assumption of a fixed tissue PO<sub>2</sub>. Thereafter, bubbles shrink rapidly presumably as a result of rapid washout of tissue inert gas. A spherical bubble model is qualitatively in accord with these data if a low oxygen metabolism is assumed (136).

None of these experimental data include mass balance of tissue gases, so do not address any slowing of inert gas elimination due to bubble growth, but there is indirect evidence from whole-body inert gas kinetics. In dogs and goats, mixed venous PN<sub>2</sub> falls rapidly following decompression compared to the nitrogen kinetics observed following either compression or isobaric breathing gas switch—the authors attribute this to retention of nitrogen in the tissues following decompression (51, 53). A slight decrease in rate of whole-body nitrogen washout with decompression has been reported for guinea pigs (134). In humans, following air breathing at 4 atm abs, exhaled nitrogen collected during oxygen or heliox breathing was greater with decompression to 2.5 atm abs than for decompression to 1.6 or 1.3 atm abs (157, 294).

In the experiments just described, whole-body nitrogen elimination was greater with decompression to 2.5 atm abs than with an isobaric breathing gas switch at 4 atm abs

(157, 294). Although not measured in these experiments, venous bubbles are routinely detected by ultrasound methods following decompression, raising the possibility that such bubbles may enhance the washout of inert gas from tissue. Inert gases are sparingly soluble in blood (see Table 3) and much more gas can be carried in a bubble than dissolved in an equivalent volume of blood. This concept has been exploited to enhance blood-carrying capacity for gases with intravascular administration of a low-boiling-point perfluorocarbon that forms subcapillary size bubbles as it warms to body temperature. Whole-body nitrogen elimination during oxygen breathing is enhanced in pigs administered with this fluorocarbon (181). Typically, venous bubbles arising from decompression are excreted harmlessly in the lungs. Massive embolization of the pulmonary vasculature impairs respiratory gas exchange (273) and might impair inert gas exchange, but this has not been measured, and such massive pulmonary embolization is rare and often fatal in human diving exposures (92).

### Application

There are well-developed decompression models based on three-region (98) and two-region (102, 103) models of spherical bubble growth. The model parameters of the latter model are estimated by fit to an extensive military decompression data set and a single schedule has been extensively tested and found to have the predicted incidence of DCS (101–103). In neither model do bubbles have significant impact on the kinetics of dissolved gases.

Exponential uptake and potentially linear washout of inert gas [described in Eq. (19)] (255) underlie most decompression schedules in the present U.S. Navy Diving Manual (207). Linear washout arises at a threshold supersaturation and was introduced to slow gas washout and to account for the observed incidence of DCS resulting from long, deep dives and repetitive dives (dives begun with excess tissue inert gas remaining from a preceding dive) (255). Linear gas washout results in a small but significant improvement in fit of models to an extensive military decompression data set (258). However, a recent man-trial calls into question the notion that bubble formation during decompression has any practical influence on washout of inert gas (101). In this large manned evaluation of two decompression schedules that differed only in the depth distribution of decompression stop time, the greater incidence of DCS was observed on the schedule with deeper initial decompression stops. The deeper initial decompression stops must result not only in less initial bubble formation, but, to explain greater incidence of DCS, also in less efficient gas washout in some tissues.

### Inherent unsaturation (oxygen window)

In the course of cellular respiration, oxygen is consumed and replaced with an approximately equal number of CO<sub>2</sub> molecules. Because CO<sub>2</sub> is more soluble than oxygen in biological liquids, the extraction of  $n$  moles oxygen from a liquid

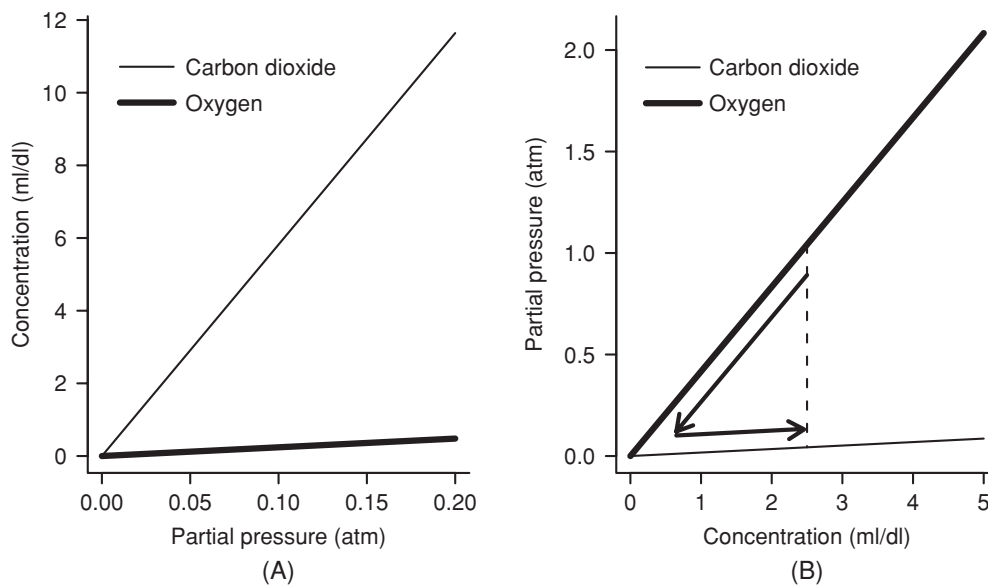


**Figure 17** The oxygen window. (A) Increasing dissolved oxygen and CO<sub>2</sub> concentrations for a liquid at equilibrium with increasing partial pressures of these gases for Ostwald solubility coefficients of 0.024 for oxygen and 0.528 for CO<sub>2</sub>. (B) Relationship similar to panel A, but with axes reversed. Upper arrow indicates extraction of 2.5 vol% oxygen from the liquid, and lower arrow indicates replacement with 2.5 vol% CO<sub>2</sub>; the dotted line indicates the resulting oxygen window that is the net difference for the sum of all gas partial pressures in the liquid. Note that extraction of more oxygen, similarly replaced with CO<sub>2</sub>, would result in a larger oxygen window.

and replacement with  $n$  moles CO<sub>2</sub> results in a larger drop in P<sub>O<sub>2</sub></sub> than the corresponding increase in P<sub>CO<sub>2</sub></sub>. This concept is illustrated in Figure 17. As a result, the sum of tissue oxygen and CO<sub>2</sub> partial pressures will be less than the corresponding alveolar sum under most circumstances,<sup>5</sup> as given by a positive value of the expression on the right-hand side of Eq. (23). Furthermore, at equilibrium between alveolar and tissue inert gases ( $\Sigma P_{A_{\text{inert}}} = \Sigma P_{\text{tis}_{\text{inert}}}$ ), the sum of all alveolar gas partial pressures equals ambient pressure ( $P_{\text{amb}} = \Sigma P_{A_j}$ ) and the sum of all tissue gas partial pressures is less than ambient pressure so that tissue is “inherently” unsaturated<sup>6</sup> and therefore unfavorable for bubble formation as given by (132):

$$P_{\text{amb}} - \left( \sum P_{\text{tis}_{\text{inert}}} + P_{\text{tis}_{\text{O}_2}} + P_{\text{tis}_{\text{CO}_2}} + P_{\text{H}_2\text{O}} \right) = \text{PAO}_2 + \text{PACO}_2 - (P_{\text{tis}_{\text{O}_2}} + P_{\text{tis}_{\text{CO}_2}}) \quad (23)$$

A tissue can be additionally unsaturated as a result of a compression (increasing  $P_{\text{amb}}$ ) (see Fig. 18), so Eq. (23) specifically defines the inherent unsaturation as that portion of tissue unsaturation that is due to the metabolism of oxygen into CO<sub>2</sub>.

In the simple situation illustrated in Figure 17, the magnitude of the inherent unsaturation would depend on the tissue metabolism but be independent of the arterial partial pressures of the gases. However, unless tissue oxygen demand is satisfied entirely from oxygen dissolved in plasma (as il-

lustrated in Fig. 12), tissue P<sub>O<sub>2</sub></sub>, and therefore the magnitude of the inherent unsaturation, is strongly dependent on the nonlinear relationships between oxygen partial pressure and blood oxygen content due to Hb, as illustrated in Figure 19. Calculations indicate the inherent unsaturation increases with increasing P<sub>riO<sub>2</sub></sub> up to a limit that is not generally met in normal diving operations (270,304). This linear increase in the inherent unsaturation with P<sub>riO<sub>2</sub></sub> has been demonstrated in rabbits exposed to various ambient pressures and P<sub>riO<sub>2</sub></sub> by allowing equilibration of gases between tissue and the lumen of an implanted subcutaneous polyvinylchloride tube then measuring the pressure inside the tube (132,135).

The importance of the inherent unsaturation is that it defines a minimum decompression that will not result in bubble formation, since a decompression of no more than the inherent unsaturation will not produce supersaturation. This concept was first proposed by Momson, who defined a “partial pressure vacancy” as  $\Sigma P_{A_j} - \Sigma P_{V_j}$  (199), which under the assumptions of  $P_{V_j} \cong P_{\text{tis}_j}$  and  $\Sigma P_{A_j} \cong P_{\text{amb}}$  is equivalent to Eq. (23), and used it to calculate decompression to a first stop that would not result in venous bubble formation. In a confusing description of Momson’s concept and its potential

<sup>5</sup>The only exception might be a transient reversal of the above inequality in a tissue with low metabolism in response to a precipitous drop in inspired and alveolar P<sub>O<sub>2</sub></sub> such as would occur during a very rapid decompression.

<sup>6</sup>The left-hand side of Eq. (23) is the negative of Eq. (7), by convention in the literature, continued here, both unsaturation and supersaturation are expressed as absolute values.

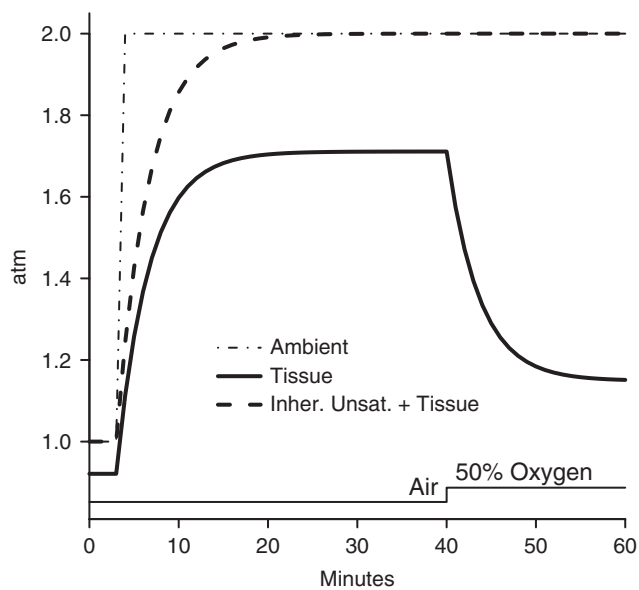


**Figure 18** Change in the sum of all dissolved tissue gas partial pressures (heavy solid line) in response to a compression (dot-dash) and subsequent change in inspired oxygen fraction (thin solid line, arbitrary scale). The inherent unsaturation (oxygen window) is equal to the vertical distance between the dashed line and the tissue gas partial pressure. Prior to compression, the tissue is inherently unsaturated. For a period following the compression, the total unsaturation (ambient – tissue) exceeds the inherent unsaturation until the alveolar and tissue PN<sub>2</sub> reequilibrate. Increasing the inspired oxygen fraction causes washout of tissue nitrogen and a corresponding increase in the inherent unsaturation. Inher. Unsat., inherent unsaturation.

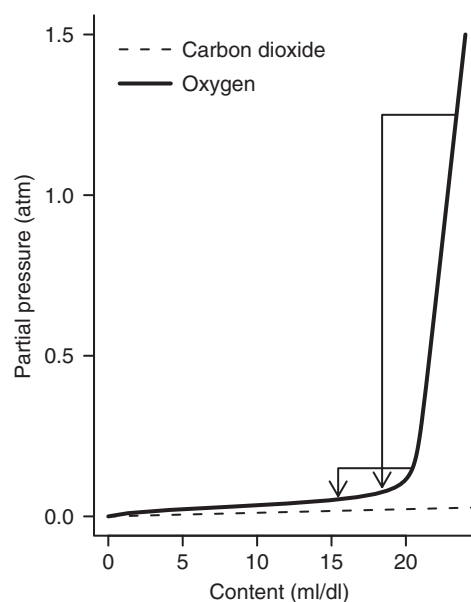


**Figure 19** The oxygen window increases with increase inspired PO<sub>2</sub> because of the nonlinear relationship between blood oxygen content and PO<sub>2</sub> due to oxygen-hemoglobin dissociation (x- and y-axes reversed from the familiar presentation, such as in Fig. 12). The two right-angle arrows indicate the arterial-venous PO<sub>2</sub> differences resulting from 5 vol% oxygen extraction for inspired PO<sub>2</sub> of 1.3 or 0.2 atm abs. Since the corresponding increase in PCO<sub>2</sub> will be approximately equal in both cases, and assuming equilibrium between tissue and venous blood gases, the difference between the vertical segments of the arrows illustrates the difference in magnitude of the oxygen window for the two cases.

application for calculating entirely bubble-free decompression from saturation dives, Behnke coined the term “oxygen window,” which is usefully evocative of the underlying mechanism (14). Hills, who appears to have been unaware of Momson’s work, independently defined the concept of “inherent unsaturation” as it appears in Eq. (23) and used it to schedule bubble-free decompression until the final decompression stop (132). Final ascent to surface is scheduled to liberate insufficient free gas to provoke symptoms of DCS.

There is probably no diving physiology concept more misunderstood that the oxygen window and confusion probably arises because of a related concept. Van Liew and colleagues (269) examined gas exchange in artificial, compressible, subcutaneous gas pockets created by subcutaneous injection of air in rats. After compression to 2 or 4 atm abs ambient air pressure, gas pocket PO<sub>2</sub> and PCO<sub>2</sub> stabilize at levels consistent with those expected in surrounding tissue. Since the sum of alveolar gases must equal the sum of pocket gases because both are at ambient pressure ( $\sum P_{A_j} = \sum P_{\text{pocket}_j} = P_{\text{amb}}$ ), after equilibration of tissue and pocket gases, there must be a pocket-alveolar PN<sub>2</sub> gradient of the same magnitude as the left-hand side of Eq. (23):

$$P_{\text{pocket}_{N_2}} - P_{A_{N_2}} = P_{A_{O_2}} + P_{A_{CO_2}} - (P_{\text{pocket}_{O_2}} + P_{\text{pocket}_{CO_2}}) \quad (24)$$

Similarly, Hills theorized that a diffusion gradient described by the right-hand side of Eq. (23) dissolves the gas phase arising from decompression. This diffusion gradient was relevant to his model of the critical site for decompression, where he envisioned that the gas phase initially formed not as bubbles but as films not subject to surface tension or mechanical compression and therefore at ambient pressure, that tissue and separated gas phase PN<sub>2</sub> were in equilibrium, that owing to a blood:tissue diffusion limitation, capillary blood was in equilibrium with alveolar gases, and only a single inert gas was considered (132). Unfortunately, Hills used the term “inherent unsaturation” indiscriminately for this diffusion gradient as for the conditions relevant for phase transition. Subsequently, the term “oxygen window” has also been used in the same sense but to describe the nitrogen diffusion gradient between spherical bubbles and tissue when tissue and alveolar PN<sub>2</sub> are equal, analogous to Eq. (24) (268, 270). This is only approximately correct because spherical bubbles are not at ambient pressure [see Eq. (16)]. This approximate relationship does not hold if tissue and alveolar inert gas pressures are not in equilibrium or for multiple inert gases. Potential ambiguity is resolved if the oxygen window is defined uniquely as the difference expressed by the right-hand side of Eq. (23), which gives rise to the inherent unsaturation and a component of the bubble-tissue inert gas partial pressure gradient.

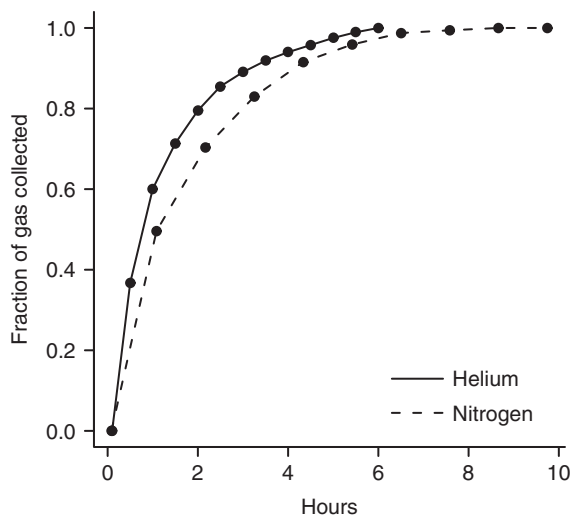


**Figure 20** Whole-body washout of helium and nitrogen. Y-axis is the fraction of total expired gas collected. Drawn from data of Behnke and colleagues (17, 69).

### Diving with nitrogen and helium

Although the kinetics of nitrogen and helium is similar in those tissues where they have both been studied (64, 66), lung washout experiments indicate that nitrogen washes out of some body tissues slower than does helium (17) (see Fig. 20). Owing to differing physicochemical properties (see Table 3), nitrogen may have a longer time constant than helium for some tissues. The perfusion time constant [Eq. (15)] depends on the tissue:blood partition coefficient ( $\alpha_{\text{tis}}/\alpha_{\text{blood}}$ ) and nitrogen will

have a longer time constant than helium in a tissue with a high lipid content such as fat. The time constant for a diffusion process is given by  $\tau = h^2/D_{\text{tis}}$ , where  $h$  is the diffusion distance, and nitrogen will have a longer time constant than helium owing to the difference in diffusivities ( $D$ ). Potentially diffusion-limited inert gas exchange appears to be important across the skin (167), in the inner ear (62) and perhaps at articular cartilage (289).

It was noted in the “Application: Ratios and  $M$  values” section that helium and nitrogen may be treated differently in decompression algorithms. Such empirical differences in latent algorithm variables could reflect the differing physicochemical properties of helium and nitrogen but may also arise because heliox diving procedures are generally developed for, and tested with, deeper dives than nitrox procedures. There are relatively few data directly comparing identical dives breathing nitrox and heliox mixtures. Following 60-fsw bounce dives (70- to 120-min duration) with ascent to surface without decompression stops, there is a nonsignificant trend toward higher DCS incidence following heliox dives than air dives (260). However, following shallow, 12 h, near-saturation dives, divers could ascend to surface without decompression stops and without DCS from deeper heliox dives than from air dives (69). This may be due to more prolonged supersaturation in slowly equilibrating tissues, perhaps those with high lipid content or substantial diffusion limitation, following nitrox dives than heliox dives. Figure 21 illustrates how faster helium washout than nitrogen uptake, such as might occur with air breathing following heliox dives, lowers total tissue partial pressures.

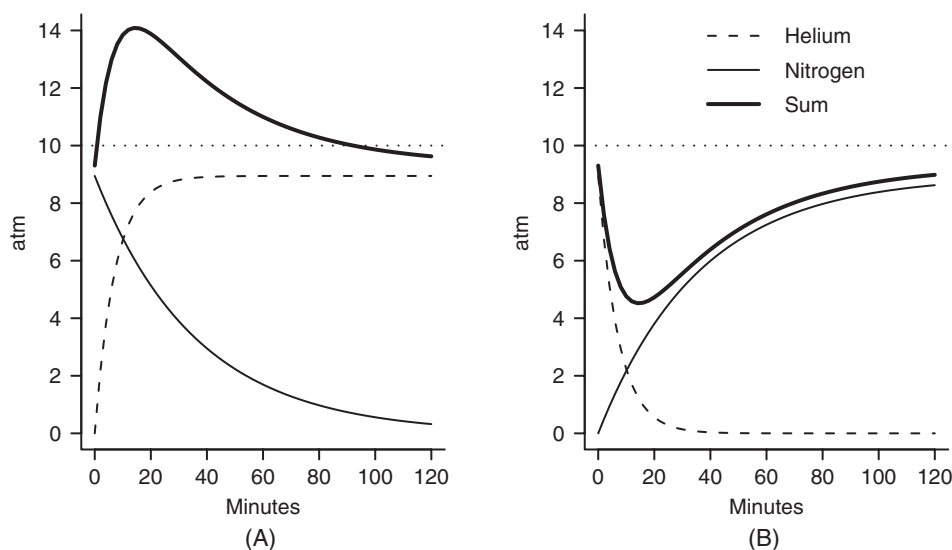


**Figure 21** Isobaric exchange of helium and nitrogen in a compartment with fivefold difference in time constants ( $\tau_{\text{He}} = 7.2$ ,  $\tau_{\text{N}_2} = 36$ ). Panel A is a simulation of a compartment at equilibrium with 90%  $\text{N}_2$ -10%  $\text{O}_2$  inspired gas at 10 atm abs ambient pressure and a switch to 90% He-10%  $\text{O}_2$  inspired gas at time zero. Dashed and thin lines indicate partial pressures of helium and nitrogen. The thick line indicates the sum of both inert gases and metabolic gases. The compartment is transiently supersaturated, while the sum of gases is above ambient pressure (dotted line). Panel B shows the reverse gas switch.

It is on the premise illustrated in Figure 21 that helium-rich to nitrogen-rich breathing gas switches can result in undersaturation and that such breathing gas switches are claimed to accelerate decompression from bounce dives. However, the often-cited work supporting accelerated decompression by switching from heliox to nitrox (151) in fact shows nothing of the sort. That work presents several manned-dives in which breathing gas mixture was changed during decompression, but changes in inert gas composition were accompanied by increases in oxygen fraction (decreases in inert gas fraction)—the latter alone can accelerate decompression. These decompression times were compared to air decompression times that were not actually (and never have been) tested. On the other hand, a larger, although still low-powered man-trial of two schedules, found a nonsignificant increase in DCS following a heliox to nitrox breathing gas switch during decompression compared to a schedule identical except for heliox breathing throughout (249).

### Isobaric counterdiffusion

Figure 21 illustrates how faster tissue uptake of helium than washout of nitrogen with an isobaric breathing gas switch at depth could result in transient supersaturation without decompression. Counterdiffusion of inert gases is thought to underlie the development of signs and symptoms of DCS and the detection of intravascular bubbles reported during sequential breathing of gas mixtures of different helium and nitrogen composition without change in ambient pressure (52, 62, 167). Vertigo, nausea, and other symptoms consistent with injury to the vestibulocochlear apparatus (“inner ear”) can occur with an isobaric switch from heliox to a nitrogen-rich breathing mixture at pressures in excess of 28 atm abs (167). A physiological model of the inner ear indicates that transient supersaturation can develop in the vascularized membranous labyrinth principally due to diffusion of helium from the endolymph and perilymph exceeding the counterdiffusion of nitrogen in the opposite direction (62). Previously, it had been conjectured that counterdiffusion across the round window could account for inner ear DCS but modeling indicates trivial gas exchange by this route (62). Inner ear symptoms are an infrequent but characteristic outcome following helium to nitrogen breathing gas switches during decompression at depths greater than about 4 atm abs (19, 25, 62, 83). The magnitude of the counterdiffusion effect is proportional to the increase in inspired  $P_{N_2}$  and is probably only modest at depths of 4 atm abs or shallower, and inner ear DCS at these depths is likely to be partly or wholly due to inadequate decompression *per se* rather than solely the breathing gas switch (62).

During transient breathing of nitrogen-rich gas in the course of dry, heliox saturation chamber dives, urticaria and pruritus has occurred where the skin is exposed to helium (167). Urticaria and eventually lethal vascular bubble formation occurs at 1 atm abs in pigs breathing nitrous oxide

with the skin exposed to a helium atmosphere (167). This is clearly due to diffusion across the skin since the pigs never breathed heliox. Local supersaturation probably arises because helium has higher skin permeability than other gases, a difference that has been found between helium and nitrogen (176), allowing faster diffusion of ambient helium across the skin than of the less permeable gas in the opposite direction from the superficial blood vessels. Bubble formation without decompression has been demonstrated in physical systems at the interface of bilayers, with differing permeabilities for helium and nitrogen where the bilayer separates reservoirs of these two gases (106).

Pruritus occurs in humans following isobaric switch of the chamber atmosphere (which is also the breathing gas) to heliox following nitrox saturation dives at 3 or 4 atm abs and does not occur if the skin is protected from contact with helium (111). Prolonged venous gas bubbling occurs following an isobaric switch to a heliox atmosphere following nitrox saturation dives at 5 or 7 atm abs in goats (52); urticaria was not reported but may not have been evident because of the animals' fur. Hydrogen, which has tissue diffusivities and solubilities different from those of helium and nitrogen (170), has been investigated as a partial substitute for helium in deep saturation diving. Following saturation at 46 atm abs with hydrogen-helium-oxygen, an isobaric switch to a heliox atmosphere resulted in venous gas bubbles in one diver (94). The latency of onset of signs and symptoms following nitrox to heliox switches appears to be inversely proportional to the magnitude of the change in inspired  $P_{N_2}$  but is of the order of hours (52, 111). If these are manifestations of a cutaneous counterdiffusion phenomenon, the source of nitrogen must be a body tissue with long perfusion time constant and is probably the subcutaneous fat. Following these gas switches, one human developed knee pain and one goat developed apparent limb pain; if these were manifestations of DCS, they would likely arise from a different mechanism than the cutaneous manifestations. Modeling of a long Krogh cylinder capillary unit with perfusion-limited axial gas partial pressure gradients suggested that an isobaric switch from nitrox to heliox breathing gas can result in supersaturation (254, 302). However, although the site of bubble formation that results in joint pain is unknown, it is tempting to speculate that these cases were due to counterdiffusion of helium and nitrogen in articular cartilage.

Photomicroscopy shows growth and dissolution of bubbles due to counterdiffusion of gases between bubble and tissue in rats. These data are interesting but difficult to interpret because partial pressures of the gases in the tissues were not measured. A switch to heliox breathing at sea level following air dives caused more rapid dissolution of air bubbles in adipose tissue and spinal white matter than continued air breathing (143, 145) and a switch to air breathing following heliox dives caused more rapid and prolonged growth of helium bubbles in adipose than continued heliox breathing (142), indicating a greater flux of nitrogen than helium across the bubble surface. For the same partial pressure gradient,

flux of gas  $j$  across the bubble surface is proportional to  $\alpha_{\text{tis}}D_j$  [Eq. (20)], which may be higher for nitrogen than for helium in tissues with high lipid content (see Table 3). However, tissues with high lipid content would be expected to have faster time constant for helium than nitrogen and therefore a faster change in helium than in nitrogen partial pressures after a breathing gas switch (see Fig. 21). Also, qualitatively similar findings on air bubble shrinking were found in aqueous tissues (144), where the relationships of  $\alpha_{\text{tis}}D_j$  and time constants for helium and nitrogen would be reversed compared to lipid-rich tissues. These data can be explained by a greater arterial-venous countercurrent exchange of helium than nitrogen so that helium uptake and washout is slower than nitrogen in the tissue surrounding the bubble (136).

## Summary

This article details gas exchange in hyperbaric environments, in particular the underwater diving environment. Increased ambient pressure results in increased density of respired gases and increased partial pressures of inspired gases. Immersion in water reduces pulmonary compliance and imposes static lung loads. The use of breathing apparatus often increases the work of breathing. Not surprisingly, there is a reduction in maximum voluntary ventilation as depth and the density of respired gas increases. There is also a propensity to hypoventilation and hypercapnia. The underlying mechanism is uncertain, but it may arise from a tendency of the respiratory controller to tolerate hypercapnia rather than drive the greater work required to maintain normocapnia in typical underwater conditions. There are multiple hypothetical disturbances of the oxygen cascade under hyperbaric conditions, but the predominant effect is an elevation of plasma and tissue  $\text{PO}_2$  because of the high inspired partial pressures of oxygen encountered in most hyperbaric situations. This can be exploited for clinical purposes but sufficient elevation of tissue  $\text{PO}_2$  can also be toxic, particularly to the lungs and brain. At depth, tissues equilibrate with high inspired partial pressures of nitrogen and helium. Subsequent ascent may reduce ambient pressure below the sum of tissue gas partial pressures, which can result in tissue injury from intracorporeal bubble formation. Despite these challenges, humans have been exposed to hyperbaric pressures of 71 atm abs and routinely work underwater at pressures up to 30 atm abs.

## References

- Ackles KN, Holness DE, Scott CA. Measurement of uptake and elimination of nitrogen in tissue, *in vivo*. In: Lambertsen CJ, editor. *Underwater Physiology V, Proceedings of the 5th Symposium on Underwater Physiology*. Bethesda, MD: Federation of American Societies for Experimental Biology, 1976, p. 349-354.
- Agostoni E, Gurtner G, Torri G, Rahn H. Respiratory mechanics during submersion and negative pressure breathing. *J Appl Physiol* 21: 251-258, 1966.
- Albin GW, Weathersby PK. *Statistically Based Decompression Tables VI. Repeat Dives on Oxygen/Nitrogen Mixes* (Technical Report 91-84). Bethesda, MD: Naval Medical Research Institute, 1991.
- Anderson D, George J, Lundgren CEG. Moderate hypercapnia: Cardiovascular function and nitrogen elimination. *Undersea Hyperb Med* 20: 225-232, 1993.
- Anthonisen NR, Utz G, Kryger MH, Urbanetti JS. Exercise tolerance at 4 and 6 atm abs. *Undersea Biomed Res* 3: 95-102, 1976.
- Arieli R. Cyclic perfusion of the lung by dense gas breathing may reduce the (A-a)D<sub>O<sub>2</sub></sub>. *J Basic Clin Physiol Pharmacol* 3: 207-221, 1992.
- Arieli R, Farhi LE. Gas exchange in tidally ventilated and non-steadily perfused lung model. *Respir Physiol* 60: 295-309, 1985.
- Aukland K, Åkre S, Leraand S. Arteriovenous counter-current exchange of hydrogen gas in skeletal muscle. *Scand J Clin Lab Invest Suppl* 99: 72-75, 1967.
- Babb TG, Viggiano R, Hurley B, Staarts B, Rodarte JR. Effect of mild to moderate airflow limitation on exercise capacity. *J Appl Physiol* 70: 223-230, 1991.
- Balldin UI. Effects of ambient temperature and body position on tissue nitrogen elimination in man. *Aerosp Med* 44: 365-370, 1973.
- Balldin UI, Lundgren CE. Effects of immersion with the head above water on tissue nitrogen elimination in man. *Aerosp Med* 43: 1101-1108, 1972.
- Barnett TB, Rasmussen B. Ventilatory responses to hypoxia and hypercapnia with external airway resistance. *Acta Physiol Scand* 80: 538-551, 1970.
- Becker HF, Polo O, McNamara SG, Bethon-Jones M, Sullivan CE. Effect of different levels of hyperoxia on breathing in healthy subjects. *J Appl Physiol* 81: 1683-1690, 1996.
- Behnke AR. The isobaric (oxygen window) principle of decompression. In: *The New Thrust Seaward, Transactions of the Third Annual Conference of the Marine Technology Society*. Washington, DC: Marine Technology Society, 1967.
- Behnke AR, Thomson RM, Motley EP. The psychological effects from breathing at 4 atmospheres pressure. *Am J Physiol* 112: 554-558, 1935.
- Behnke AR, Thomson RM, Shaw LA. The rate of elimination of dissolved nitrogen in man in relation to the fat and water content of the body. *Am J Physiol* 114: 137-146, 1935.
- Behnke AR, Willmon TL. Gaseous nitrogen and helium elimination from the body during rest and exercise. *Am J Physiol* 131: 619-626, 1940.
- Bennett M, Lehm J, Barr P. Medical support for the Sydney Airport Link Tunnel Project. *South Pacific Underwater Med Soc J* 32: 90-96, 2002.
- Bennett PB, Vann RD, Roby J, Youngblood D. Theory and development of subsaturation decompression procedures for depths in excess of 400 feet. In: Shilling CW, Beckett MW, editors. *Underwater Physiology VI, Proceedings of the 6th Symposium on Underwater Physiology*. Bethesda, MD: Federation of American Societies for Experimental Biology, 1978, p. 367-381.
- Blake RB, Morin RA. Pressure increases oxygen affinity of whole blood and erythrocyte suspensions. *J Appl Physiol* 61: 486-94, 1986.
- Boerema I, Mayne NG, Brummelkamp WK, Bouma S, Mensch MH, Kamermans F, Stern Hanf M, van Aalderen W. Life without blood: A study of the influence of high atmospheric pressure and hypothermia on dilution of the blood. *J Cardiovasc Surg* 1: 133-146, 1960.
- Boycott AE, Damant GCC, Haldane JS. The prevention of compressed-air illness. *J Hygiene (Lond)* 8: 342-443, 1908.
- Brodersen P, Sejrnsen P, Lassen NA. Diffusion bypass of xenon in brain circulation. *Circ Res* 32: 363-369, 1973.
- Bühlmann AA. Die Berechnung der risikoarmen Dekompression. *Schweiz Med Wochenschr* 118: 185-197, 1988.
- Bühlmann AA, Gehring H. Inner ear disorders resulting from inadequate decompression "vertigo bends." In: Lambertsen CJ, editor. *Underwater Physiology V, Proceedings of the 5th Symposium on Underwater Physiology*. Bethesda, MD: Federation of American Societies for Experimental Biology, 1976, p. 341-347.
- Burkard ME, Van Liew HD. Simulation of exchanges of multiple gases in bubbles in the body. *Respir Physiol* 95: 131-145, 1994.
- Cain CC, Otis AB. Some physiological effects resulting from added resistance to respiration. *J Aviat Med* 20: 149-160, 1949.
- Cain SM. Gas exchange in hypoxia, apnea, and hyperoxia. In: Farhi LE, Tenney SM, editors. *Handbook of Physiology*. Bethesda, MD: American Physiological Society, 1987, sect. 3, vol. IV, chapt. 19, p. 403-420.
- Caldwell PRB, Lee WL Jr, Schildkraut HS, Archibald ER. Changes in lung volume, diffusing capacity, and blood gases in men breathing oxygen. *J Appl Physiol* 21: 1477-1483, 1966.
- Campbell JA, Hill L. Studies in the saturation of the tissues with gaseous nitrogen, part I: Rate of saturation of goat's bone marrow *in vivo* with nitrogen during exposure to increased atmospheric pressure. *Q J Exp Biol* 23: 197-210, 1933.
- Camporesi EM, Bosco G. Ventilation, gas exchange, and exercise under pressure. In: Brubakk AO, Neuman TS, editors. *Bennett and Elliott's Physiology and Medicine of Diving* (5th ed). Edinburgh, UK: Saunders, 2003, p. 77-114.

32. Cerretelli P, Di Prampero PE. Gas exchange in exercise. In: Farhi LE, Tenney SM, editors. *Handbook of Physiology*. Bethesda, MD: American Physiological Society 1987, sect. 3, vol. IV, chapt. 16, p. 297-340.
33. Cerretelli P, Sikand SS, Farhi LE. Effect of increased airway resistance on ventilation and gas exchange during exercise. *J Appl Physiol* 27: 597-600, 1969.
34. Chavko M, Nemoto EM, Melick JA. Regional lipid composition in the rat brain. *Mol Chem Neuropathol* 18: 123-131, 1993.
35. Cherniak RM, Snidal DP. The effect of obstruction to breathing on the ventilatory response to CO<sub>2</sub>. *J Clin Invest* 35: 1286-1290, 1956.
36. Cherry AD, Forkner IF, Frederick HJ, Natoli MJ, Schinazi EA, Longphre JP, Conard JL, White WD, Freiburger JJ, Stolp BW, Pollock NW, Doar PO, Boso AE, Alford EL, Walker AJ, Ma AC, Rhodes MA, Moon RE. Predictors of increased PaCO<sub>2</sub> during immersed prone exercise at 4.7 atm abs. *J Appl Physiol* 106: 316-325, 2009.
37. Christopherson SK, Hlastala MP. Pulmonary gas exchange during altered density gas breathing. *J Appl Physiol* 52: 221-225, 1982.
38. Clark JM. Oxygen toxicity. In: Neuman TS, Thom SR, editors. *The Physiology and Medicine of Hyperbaric Oxygen Therapy*. Philadelphia: Saunders, 2008, p. 527-564.
39. Clark JM, Gelfand R, Lambertsen CJ, Stevens WC, Beck G Jr, Fisher DG. Human tolerances and physiological responses to exercise while breathing oxygen at 2.0 atm abs. *Aviat Space Environ Med* 66: 336-345, 1995.
40. Clark JM, Jackson RM, Lambertsen CJ, Gelfand R, Hiller WDB, Unger M. Pulmonary function in men after oxygen breathing at 3.0 atm abs for 3.5 hours. *J Appl Physiol* 71: 878-885, 1991.
41. Clark JM, Lambertsen CJ. Alveolar-arterial O<sub>2</sub> differences in man at 0.2, 1.0, 2.0, and 3.5 atm abs inspired Po<sub>2</sub>. *J Appl Physiol* 30: 753-763, 1971.
42. Clark JM, Lambertsen CJ, Gelfand R, Flores ND, Pisarello JB, Rossman MD, Elias JA. Effects of prolonged oxygen exposure at 1.5, 2.0, or 2.5 atm abs on pulmonary function in men (predictive studies V). *J Appl Physiol* 86: 243-59, 1999.
43. Clark JM, Thom SR. Oxygen under pressure. In: Brubakk AO, Neuman TS, editors. *Bennett and Elliott's Physiology and Medicine of Diving* (5th ed). Edinburgh, UK: Saunders, 2003, p. 358-417.
44. Clarke JR. Underwater breathing apparatus. In: Lundgren CEG, Miller JN, editors. *The Lung at Depth*. New York: Marcel Dekker, 1999, p. 429-527.
45. Clarke JR, Flook V. Respiratory function at depth. In: Lundgren CEG, Miller JN, editors. *The Lung at Depth*. New York: Marcel Dekker, 1999, p. 1-71.
46. Clarke JR, Jaeger MJ, Zumrick JL, O'Bryan R, Spaur WH. Respiratory resistance from 1 to 46 atm abs measured with the interrupter technique. *J Appl Physiol* 52: 549-555, 1982.
47. Cohen R, Bell WH, Saltzman HA, Kylstra JA. Alveolar-arterial oxygen pressure difference in man immersed up to the neck in water. *J Appl Physiol* 30: 720-723, 1971.
48. Cropp GJA. Effect of high intra-alveolar O<sub>2</sub> tensions on pulmonary circulation in perfused lungs of dogs. *Am J Physiol* 208: 130-138, 1965.
49. Dahan A, DeGoede J, Berkenbosch A, Olivevier ICW. The Influence of oxygen on the ventilatory response to carbon dioxide in man. *J Physiol* 428: 485-499, 1990.
50. Dahlback GO, Jonsson E, Liner MH. Influence of hydrostatic compression of the chest and intrathoracic blood pooling on static lung mechanics during head-out immersion. *Undersea Biomed Res* 5: 71-85, 1978.
51. D'Aoust BG, Smith KH, Swanson HT. Decompression-induced decrease in nitrogen elimination rate in awake dogs. *J Appl Physiol* 41: 348-355, 1976.
52. D'Aoust BG, Smith KH, Swanson HT, White R, Stayton L, Moore J. Prolonged bubble production by transient isobaric counter-equilibration of helium against nitrogen. *Undersea Biomed Res* 6: 109-125, 1979.
53. D'Aoust BG, Swanson HT, White R, Dunford R, Mahoney J. Central venous bubbles and mixed venous nitrogen in goats following decompression. *J Appl Physiol* 51: 1238-1244, 1981.
54. Dawson SV, Elliott EA. Wave-speed limitation on expiratory flow—a unifying concept. *J Appl Physiol* 43: 498-515, 1977.
55. Demchenko IT, Boso AE, Bennett PB, Whorton AR, Piantadosi CA. Hyperbaric oxygen reduced cerebral blood flow by inactivating nitric oxide. *Nitric Oxide* 4: 597-608, 2000.
56. Demchenko IT, Oury TD, Crapo JD, Piantadosi CA. Regulation of brain's vascular responses to oxygen. *Circ Res* 91: 1031-1037, 2002.
57. Demedts M, Anthonisen NR. Effects of increased external airway resistance during steady-state exercise. *J Appl Physiol* 35: 361-366, 1973.
58. Deming WE, Shupe LE. Some physical properties of compressed gases I. Nitrogen. *Phy Rev* 37: 638-654, 1931.
59. Derion T, Guy HJB, Tsukimoto K, Schaffartzik W, Prediletto R, Poole DC, Knight DR, Wagner PD. Ventilation-perfusion relationships in the lung during head-out immersion. *J Appl Physiol* 72: 64-72, 1992.
60. Derion T, Guy HJB. Effects of age on closing volume during head-out water immersion. *Respir Physiol* 95: 273-280, 1994.
61. Doolette DJ, Mitchell SJ. The physiological kinetics of nitrogen and the prevention of decompression illness. *Clin Pharmacokinetics* 40: 1-14, 2001.
62. Doolette DJ, Mitchell SJ. A biophysical basis for inner ear decompression sickness. *J Appl Physiol* 94: 2145-2150, 2003.
63. Doolette DJ, Upton RN, Grant C. Diffusion limited, but not perfusion limited, compartmental models describe cerebral nitrous oxide kinetics at both high and low cerebral blood flows. *J Pharmacokinetics Biopharm* 26: 649-672, 1998.
64. Doolette DJ, Upton RN, Grant C. Isobaric exchange of helium and nitrogen in the brain at high and low blood flow [abstract]. *Undersea Hyperb Med* 31: 340, 2004.
65. Doolette DJ, Upton RN, Grant C. Countercurrent compartmental models describe hind limb skeletal muscle helium kinetics at resting and low blood flows in sheep. *Acta Physiol Scand* 185: 109-121, 2005.
66. Doolette DJ, Upton RN, Grant C. Isobaric exchange of helium and nitrogen in skeletal muscle at resting and low blood flow [abstract]. *Undersea Hyperb Med* 32: 307, 2005.
67. Doolette DJ, Upton RN, Grant C. Perfusion-diffusion compartmental models describe cerebral helium kinetics at high and low cerebral blood flows in sheep. *J Physiol (Lond)* 563: 529-539, 2005.
68. Doolette DJ, Upton RN, Zheng D. Diffusion-limited tissue equilibration and arteriovenous diffusion shunt describe skeletal muscle nitrous oxide kinetics at high and low blood flows in sheep. *Acta Physiol Scand* 172: 167-177, 2001.
69. Duffner GJ, Snider HH. *Effects of Exposing Men to Compressed Air and Helium-Oxygen Mixtures for 12 Hours at Pressures of 2-2.6 Atmospheres* (Technical Report 1-59). Panama City, FL: Navy Experimental Diving Unit, 1958.
70. D'Urzo AD, Chapman KR, Rebeck AS. Effect of inspiratory resistive loading on control of ventilation during progressive exercise. *J Appl Physiol* 62: 134-140, 1987.
71. Dwyer J, Saltzman HA, O'Bryan R. Maximum physical-work capacity of man at 43.4 atm abs. *Undersea Biomed Res* 4: 359-372, 1977.
72. Dwyer JV. *Calculation of Repetitive Diving Decompression Tables* (Research Report 1-57). Washington, DC: Navy Experimental Diving Unit, 1956.
73. Eckenhoff RG, Olstad CS, Carrod G. Human dose-response relationship for decompression and endogenous bubble formation. *J Appl Physiol* 69: 914-918, 1990.
74. Eger EI. A mathematical model of uptake and distribution. In: Papper EM, Kitz RJ, editors. *Uptake and Distribution of Anesthetic Agents*. New York: McGraw-Hill, 1962, p. 72-87.
75. Ehler WJ, Marx RE, Peleo MJ. Oxygen as a drug: A dose response curve for radiation necrosis. *Undersea Hyper Med* 20 (Suppl): 94-95, 1993.
76. Eldridge F, Davis JM. Effect of mechanical factors on respiratory work and ventilatory responses to CO<sub>2</sub>. *J Appl Physiol* 14: 721-726, 1959.
77. Elliott DH. Loss of consciousness underwater. In: Bennett PB, Moon RE, editors. *Diving Accident Management. Proceedings of the 41st Undersea and Hyperbaric Medical Society Workshop*. Bethesda, MD: Undersea and Hyperbaric Medical Society, 1990, p. 301-310.
78. Epstein PS, Plesset MS. On the stability of gas bubbles in liquid-gas solutions. *J Chem Phys* 18: 1505-1509, 1950.
79. Evans A, Walder DN. Significance of gas micronuclei in the aetiology of decompression sickness. *Nature* 222: 251-252, 1969.
80. Fagraeus L, Hesser CM. Ventilatory response to CO<sub>2</sub> in hyperbaric environments. *Acta Physiol Scand* 80: 19A-20A, 1970.
81. Fagraeus L, Hesser CM, Linnarsson D. Cardiorespiratory responses to graded exercise at increased ambient air pressure. *Acta Physiol Scand* 91: 259-74, 1974.
82. Fagraeus L, Linnarsson D. Maximal voluntary and exercise ventilation at high ambient air pressures. *Forsvarmedicin* 9: 275-278, 1973.
83. Farmer JC Jr. Diving injuries to the inner ear. *Ann Otol Rhinol Laryngol Suppl* 86: 1-20, 1977.
84. Feldmeier JJ. Hyperbaric oxygen therapy for delayed radiation injuries. In: Neuman TS, Thom SR, editors. *The Physiology and Medicine of Hyperbaric Oxygen Therapy*. Philadelphia: Saunders, 2008, p. 231-256.
85. Flook V, Kelman GR. Submaximal exercise with increased inspiratory resistance to breathing. *J Appl Physiol* 35: 379-384, 1973.
86. Florio JT, Morrison JB, Butt WS. Breathing pattern and ventilatory response to carbon dioxide in divers. *J Appl Physiol* 46: 1076-1080, 1979.
87. Flynn ET, Saltzman HA, Summitt JK. Effects of head-out immersion at 19.18 atm abs on pulmonary gas exchange in man. *J Appl Physiol* 33: 113-119, 1972.
88. Forkner IF, Piantadosi CA, Scafetta N, Moon RE. Hyperoxia-induced tissue hypoxia: A danger? *Anesthesiology* 106: 1051-1055, 2007.
89. Forster RE. Diffusion of gases across the alveolar membrane. In: Farhi LE, Tenney SM, editors. *Handbook of Physiology*. Bethesda, MD: American Physiological Society, 1987, sect. 3, vol. IV, chapt. 5, p. 71-88.

90. Fothergill DM, Hedges D, Morrison JM. Effects of CO<sub>2</sub> and N<sub>2</sub> partial pressures on cognitive and psychomotor performance. *Undersea Biomed Res* 18: 1-19, 1991.
91. Fothergill DM, Joye DD, Carlson NA. Diver respiratory response to a tunable closed-circuit breathing apparatus. *Undersea Hyperb Med* 24: 91-105, 1997.
92. Francis TJR, Mitchell SJ. Manifestations of decompression disorders. In: Brubakk AO, Neuman TS, editors. *Bennett and Elliott's Physiology and Medicine of Diving* (5th ed). Edinburgh: Saunders, 2003, p. 578-599.
93. Francis TJR, Mitchell SJ. The pathophysiology of decompression sickness. In: Brubakk AO, Neuman TS, editors. *Bennett and Elliott's Physiology and Medicine of Diving* (5th ed). Edinburgh: Saunders, 2003, p. 530-556.
94. Gardette B, Fructus X, Delauze HG. First human hydrogen saturation dives at 450 msw: Hydra V. In: Bove AA, Bachrach AJ, Greenbaum LJ, editors. *Proceedings of the 9th International Symposium on Underwater and Hyperbaric Physiology*. Bethesda, MD: Undersea and Hyperbaric Medical Society, 1987, p. 375-389.
95. Gelfand R, Lambertsen CJ. Dynamic respiratory response to abrupt change of inspired CO<sub>2</sub> at normal and high PO<sub>2</sub>. *J Appl Physiol* 35: 903-913, 1973.
96. Gelfand R, Lambertsen CJ, Peterson RE. Human respiratory control at high ambient pressures and inspired gas densities. *J Appl Physiol* 48: 528-539, 1980.
97. Gelfand R, Lambertsen CJ, Strauss R, Clark JM, Puglia CD. Human respiration at rest in rapid compression and at high pressures and gas densities. *J Appl Physiol* 54: 290-303, 1983.
98. Gernhardt ML. *Development and Evaluation of a Decompression Stress Index Based on Tissue Bubble Dynamics* (Dissertation). Philadelphia: University of Pennsylvania, 1991.
99. Gerth WA. Effects of dissolved electrolytes on the solubility and partial molar volume of helium in water from 50 to 400 atmospheres at 25°C. *J Sol Chem* 12: 655-669, 1983.
100. Gerth WA. Applicability of Henry's law to hydrogen, helium, and nitrogen solubilities and water and olive oil at 37°C and pressures up to 300 atmospheres. *Arch Biochem Biophys* 241: 187-199, 1985.
101. Gerth WA, Doolette DJ, Gault KA. Deep stops and their efficacy in decompression: U.S. Navy research. In: Bennett PB, Wienke BR, Mitchell SJ, editors. *Decompression and the Deep Stop, Proceedings of the Undersea and Hyperbaric Medical Society Workshop*. Durham, NC: Undersea and Hyperbaric Medical Society, 2009, p. 165-185.
102. Gerth WA, Vann RD. *Development of Iso-DCS Risk Air and Nitrox Decompression Tables Using Statistical Bubble Dynamics Models (Final Report)*. Rockville, MD: National Oceanic and Atmospheric Administration, Office of Undersea Research, 1996.
103. Gerth WA, Vann RD. Probabilistic gas and bubble dynamics models of decompression sickness occurrence in air and N<sub>2</sub>-O<sub>2</sub> diving. *Undersea Hyperb Med* 24: 275-292, 1997.
104. Gledhill N, Froese AB, Buick FJ, Bryan AC. VA/Q inhomogeneity and AaDO<sub>2</sub> in man during exercise: Effect of SF<sub>6</sub> breathing. *J Appl Physiol* 45: 512-515, 1978.
105. Goldman S. A new class of biophysical models for predicting the probability of decompression sickness in scuba diving. *J Appl Physiol* 103: 484-493, 2007.
106. Graves DJ, Idicula J, Lambertsen CJ, Quin JA. Bubble formation resulting from counterdiffusion supersaturation: A possible explanation for isobaric inert gas 'urticaria' and vertigo. *Phys Med Biol* 18: 256-264, 1973.
107. Greenbaum R, Kelman GR, Nunn JF, Ptyes-Roberts C. Arterial oxygen tensions. *Anesthesiology* 70: 869-870, 1966.
108. Grindlay J, Mitchell SJ. Isolated pulmonary oedema associated with scuba diving. *Emerg Med* 11: 272-6, 1999.
109. Groom AC, Morin R, Farhi LE. Determination of dissolved N<sub>2</sub> in blood and investigation of N<sub>2</sub> washout from the body. *J Appl Physiol* 23: 706-712, 1967.
110. Hales JRS. Effect of exposure to hot environments on total and regional blood flow in the brain and spinal cord of the sheep. *Pflügers Arch* 344: 327-337, 1973.
111. Hamilton RW, Adams GM, Harvey CA, Knight DR. SHAD-NISAT: A Composite Study of Shallow Saturation Diving 985. Groton, CT: Naval Submarine Medical Research Laboratory, 1982.
112. Hamilton RW, Thalmann ED. Decompression practice. In: Brubakk AO, Neuman TS, editors. *Bennett and Elliott's Physiology and Medicine of Diving* (5th ed). Edinburgh, UK: Saunders, 2003.
113. Hampson NB. *Hyperbaric Oxygen Therapy: 1999 Committee Report*. Kensington, MD: Undersea & Hyperbaric Medical Society, 1999.
114. Hampson NB, Dunford RG. Pulmonary edema of scuba divers. *Undersea Hyperb Med* 24: 29-33, 1997.
115. Harabin AL, Homer LD, Bradley ME. Pulmonary oxygen toxicity in awake dogs: Metabolic and physiological effects. *J Appl Physiol* 57: 1480-1488, 1984.
116. Harvey EN, Whiteley AH, McElroy WD, Pease DC, Barnes DK. Bubble formation in animals, part II: Gas nuclei and their distribution in blood and tissues. *J Cell Comp Physiol* 24: 23-34, 1944.
117. Hashimoto A, Daskalovic I, Reddan WG, Lanphier EH. Detection and modification of CO<sub>2</sub> retention in divers. *Undersea Biomed Res* 8 (1, Suppl): 47, 1981.
118. Hawkins JA, Shilling CW, Hansen RA. A suggested change in calculating decompression tables for diving. *US Nav Med Bull* 33: 327-338, 1935.
119. Hays JR, Hart BL, Weathersby PK, Survanshi SS, Homer LD, Flynn ET. *Statistically Based Decompression Tables IV. Extension to Air and N<sub>2</sub>-O<sub>2</sub> Decompression* (Technical Report 86-51). Bethesda, MD: Naval Medical Research Institute, 1986.
120. Hemmingsen BB, Steinberg NK, Hemmingsen EA. Intracellular gas supersaturation tolerances of erythrocytes and resealed ghosts. *Biophys J* 47: 491-496, 1985.
121. Hemmingsen EA. Cavitation in gas-supersaturated solutions. *J Appl Phys* 64: 213-218, 1975.
122. Hemmingsen EA. Effects of surfactants and electrolytes on the nucleation of bubbles in gas-supersaturated solutions. *Z Naturforsch* 33a: 164-171, 1978.
123. Hemmingsen EA, Hemmingsen BB. Lack of intracellular bubble formation in microorganisms at very high gas supersaturations. *J Appl Physiol* 47: 1270-1277, 1979.
124. Hempleman HV. British decompression theory and practice. In: Bennett PB, Elliott DH, editors. *The Physiology and Medicine of Diving and Compressed Air Work*. London: Ballière Tindall & Cassell, 1969, p. 291-318.
125. Hennessy TR. The equivalent bulk-diffusion model of the pneumatic decompression computer. *Med Biol Eng* 11: 135-137, 1973.
126. Hesser CM, Adolphson J, Fagraeus L. Role of CO<sub>2</sub> in compressed air narcosis. *Aerospace Med* 42: 163-168, 1971.
127. Hesser CM, Lind F, Linnarsson D. Significance of airway resistance for the pattern of breathing and lung volumes in exercising humans. *J Appl Physiol* 68: 1875-1882, 1990.
128. Hesser CM, Linnarsson D, Fagraeus L. Pulmonary mechanics and work of breathing at maximal ventilation and raised air pressure. *J Appl Physiol* 50: 747-753, 1981.
129. Hickey DD, Norfleet WT, Pasche AJ, Lundgren CEG. Respiratory function in the upright working diver at 6.8 atm abs (190fsw). *Undersea Biomed Res* 14: 241-262, 1987.
130. Higuchi H, Adachi Y, Arimura S, Kanno M, Satoh T. The carbon dioxide absorption capacity of Amsorb is half that of soda lime. *Anesth Analg* 93: 221-225, 2001.
131. Hill L, Phillips AE. Deep sea diving. *J R Nav Med Serv* 18: 157-183, 1932.
132. Hills BA. *A Thermodynamic and Kinetic Approach to Decompression Sickness* (Dissertation). Adelaide, South Australia, Australia: The University of Adelaide, 1966.
133. Hills BA. *Decompression Sickness: The Biophysical Basis of Prevention and Treatment*. Chichester, UK: John Wiley & Sons, 1977.
134. Hills BA. Effect of decompression per se on nitrogen elimination. *J Appl Physiol* 45: 916-921, 1978.
135. Hills BA, LeMessurier DH. Unsaturation in living tissue relative to the pressure and composition of inhaled gas and its significance in decompression theory. *Clin Sci* 36: 185-195, 1969.
136. Himm JF, Homer LD. A model of extravascular bubble evolution: Effect of changes in breathing gas composition. *J Appl Physiol* 87: 1521-1531, 1999.
137. Hlastala MP. Diffusing-capacity heterogeneity. In: Farhi LE, Tenney SM, editors. *Handbook of Physiology*. Bethesda, MD: American Physiological Society, 1987, sect. 3, vol. IV, chap. 12, p. 217-232.
138. Hof IM, West VP, Younes M. Steady-state response of normal subjects to inspiratory resistive load. *J Appl Physiol* 60: 1471-1481, 1986.
139. Homer LD, Weathersby PK, Survanshi S. How countercurrent blood flow and uneven perfusion affect motion of inert gas. *J Appl Physiol* 69: 162-170, 1990.
140. Hong SK, Cerretelli P, Cruz JC, Rahn H. Mechanics of respiration during submersion in water. *J Appl Physiol* 27: 535-538, 1969.
141. Hrnčir E, Rosin J. Surface tension of blood. *Physiol Res* 46: 319-321, 1997.
142. Hyldegaard O, Jensen T. Effect of heliox, oxygen and air breathing on helium bubbles after heliox diving. *Undersea Hyperb Med* 34: 107-122, 2007.
143. Hyldegaard O, Madsen J. Influence of heliox, oxygen, and N<sub>2</sub>O-O<sub>2</sub> breathing on N<sub>2</sub> bubbles in adipose tissue. *Undersea Biomed Res* 16: 185-193, 1989.
144. Hyldegaard O, Madsen J. Effect of air, heliox, and oxygen breathing on air bubbles in aqueous tissues in the rat. *Undersea Hyperb Med* 21: 413-424, 1994.
145. Hyldegaard O, Moller M, Madsen J. Effect of He-O<sub>2</sub>, O<sub>2</sub>, and N<sub>2</sub>O-O<sub>2</sub> breathing on injected bubbles in spinal white matter. *Undersea Biomed Res* 18: 361-371, 1991.

146. Iscoe S, Fisher JA. Hyperoxia-induced hypocapnia: An underappreciated risk. *Chest* 128: 430-433, 2005.
147. Iversen PO, Standa M, Nicolaysen G. Marked regional heterogeneity in blood flow within a single skeletal muscle at rest and during exercise hyperaemia in the rabbit. *Acta Physiol Scand* 136: 17-28, 1989.
148. Jacoby I. Clostridial myositis, necrotizing fasciitis, and zygomycotic infections. In: Neuman TS, Thom SR, editors. *The Physiology and Medicine of Hyperbaric Oxygen Therapy*. Philadelphia: Saunders, 2008, p. 397-418.
149. Jarrett AS. Alveolar carbon dioxide tension at increased ambient pressures. *J Appl Physiol* 21: 158-162, 1966.
150. Johnston AJ, Steiner LA, Gupta AK, Menon DK. Cerebral oxygen vasoreactivity and cerebral tissue oxygen reactivity. *Br J Anaesth* 90: 774-786, 2003.
151. Keller H, Bühlmann AA. Deep diving and short decompression by breathing mixed gases. *J Appl Physiol* 20: 1267-1270, 1965.
152. Kerem D, Daskalovic YI, Arieli R, Shupak A. CO<sub>2</sub> retention during hyperbaric exercise while breathing 40/60 nitrox. *Undersea Hyperbaric Med* 22: 339-346, 1995.
153. Kerem D, Melamed Y, Moran A. Alveolar Pco<sub>2</sub> during rest and exercise in divers and non-divers breathing O<sub>2</sub> at 1 atm abs. *Undersea Biomed Res* 7: 17-26, 1980.
154. Kety SS. The theory and applications of the exchange of inert gas at the lungs and tissues. *Pharmacol Rev* 3: 1-40, 1951.
155. Kiesow LA. Hyperbaric inert gases and the hemoglobin-oxygen equilibrium in red blood cells. *Undersea Biomed Res* 1: 29-43, 1974.
156. Kindwall EP. Compressed air work. In: Brubakk AO, Neuman TS, editors. *Bennett and Elliott's Physiology and Medicine of Diving* (5th ed). Edinburgh, UK: Saunders, 2003, p. 17-28.
157. Kindwall EP, Baz A, Lightfoot EN, Lanphier EH, Seireg A. Nitrogen elimination in man during decompression. *Undersea Biomed Res* 2: 285-297, 1975.
158. Kjellmer I, Lindberg I, Prerovsky I, Tønnesen H. The relation between blood flow in an isolated muscle measured with the Xe<sup>133</sup> clearance and a direct recording technique. *Acta Physiol Scand* 69: 69-78, 1967.
159. Klein B, Kuschinsky W, Schrock H, Vetterlein F. Interdependency of local capillary density, blood flow, and metabolism in rat brains. *Am J Physiol* 251: H1333-H1340, 1986.
160. Koulouris NG, Valta P, Lavoie A, Corbeil C, Chassé M, Braidy J, Milic-Emili J. A simple method to detect expiratory flow limitation during spontaneous breathing. *Eur Respir J* 8: 306-313, 1995.
161. Krichevsky IR, Kasarnovsky JS. Thermodynamical calculations of solubilities of nitrogen and hydrogen in water at high pressures. *J Am Chem Soc* 57: 2168-2171, 1935.
162. Kurss DI, Lundgren CEG, Päsche AJ. Effect of water temperature on vital capacity in head-out immersion. In: Bachrach AJ, Matzen MM, editors. *Underwater Physiology VII. Proceedings of the 5th Symposium on Underwater Physiology*. Bethesda, MD: Federation of American Societies for Experimental Biology, 1981, p. 297-301.
163. Kvale PA, Davis J, Schroter RC. Effect of gas density and ventilatory pattern on steady-state CO uptake by the lung. *Respir Physiol* 24: 385-398, 1975.
164. Kylastra JA, Paganelli CV, Lanphier EH. Pulmonary gas exchange in dogs ventilated with hyperbarically oxygenated liquid. *J Appl Physiol* 21: 177-184, 1966.
165. Lally DA, Zechman FW, Tracy RA. Ventilatory responses to exercise in divers and non-divers. *Respir Physiol* 20: 117-129, 1974.
166. Lambertsen CJ, Ewing JH, Kough RH, Gould R, Stroud MW. Oxygen toxicity. Arterial and internal jugular blood gas composition in man during inhalation of air, 100% O<sub>2</sub> and 2% CO<sub>2</sub> in O<sub>2</sub> at 3.5 atmospheres ambient pressure. *J Appl Physiol* 8: 255-263, 1955.
167. Lambertsen CJ, Idicula J. A new gas lesion syndrome in man, induced by "isobaric gas counterdiffusion". *J Appl Physiol* 39: 434-443, 1975.
168. Lambertsen CJ, Kough RH, Cooper DY, Emmel GL, Loeschcke HH, Schmidt CF. Oxygen toxicity: Effects in man of oxygen inhalation at 1 and 3.5 atmospheres upon blood gas transport, cerebral circulation and cerebral metabolism. *J Appl Physiol* 5: 471-86, 1953.
169. Lambertsen CJ, Owen SG, Wendel H, Stroud MW, Lurie AA, Lochner W, Clark GF. Respiratory and circulatory control during exercise at 0.21 and 2.0 atmospheres inspired Po<sub>2</sub>. *J Appl Physiol* 14: 966-982, 1959.
170. Lango T, Morland T, Brubakk AO. Diffusion coefficients and solubility coefficients for gases in biological fluids: A review. *Undersea Hyperb Med* 23: 247-272, 1996.
171. Lanphier EH. *Nitrogen-Oxygen Mixture Physiology Phases 1 and 2* (Research Report 7-55). Washington, DC: Navy Experimental Diving Unit, 1955.
172. Lanphier EH. *Nitrogen-Oxygen Mixture Physiology Phases 4 and 6* (Research Report 7-58). Washington, DC: Navy Experimental Diving Unit, 1958.
173. Lanphier EH, Bookspan J. Carbon dioxide retention. In: Lundgren CEG, Miller JN, editors. *The Lung at Depth*. New York: Marcel Dekker, 1999, p. 211-236.
174. Lassen NA. Blood flow of the cerebral cortex calculated from <sup>85</sup>krypton-beta-clearance recorded over the exposed surface; evidence of inhomogeneity of flow. *Acta Neurol Scand Suppl* 14: 24-28, 1965.
175. Lee YC, Wu YC, Gerth WA, Vann RD. Absence of intravascular bubble nucleation in dead rats. *Undersea Hyperb Med* 20: 289-296, 1993.
176. Lin YC, Kakitsuba N, Watanabe DK, Mack GW. Influence of blood flow on cutaneous permeability to inert gas. *J Appl Physiol* 57: 1167-1172, 1984.
177. Linnarsson D, Hesser CM. Dissociated ventilatory and central respiratory responses to CO<sub>2</sub> at raised N<sub>2</sub> pressure. *J Appl Physiol* 45: 756-761, 1978.
178. Linnarsson D, Ostlund A, Lind F, Hesser CM. Hyperbaric bradycardia and hypoventilation in exercising med: Effects of ambient pressure and breathing gas. *J Appl Physiol* 87: 1428-1432, 1999.
179. Lippmann J, Mitchell SJ. *Deeper into Diving* (2nd ed). Melbourne, Victoria, Australia: Submariner Publications, 2005.
180. Lumb AB. *Nunn's Applied Respiratory Physiology* (6th ed). Philadelphia: Elsevier, 2005.
181. Lundgren C, Bergoe G, Olszowka A, Tyssebotn I. Tissue nitrogen elimination in oxygen-breathing pigs is enhanced by fluorocarbon-derived intravascular micro-bubbles. *Undersea Hyperb Med* 32: 215-226, 2005.
182. Lundgren CEG. Respiratory function during simulated wet dives. *Undersea Biomed Res* 11: 139-147, 1984.
183. Lundgren CEG. Immersion effects. In: Lundgren CEG, Miller JN, editors. *The Lung at Depth*. New York: Marcel Dekker, 1999, p. 91-128.
184. Lundgren CEG, Harabin A, Bennett PB, Van Liew HD, Thalman ED. Gas physiology in diving. In: Fregly MJ, Blatteis CM, editors. *Handbook of Physiology*: Bethesda, MD: American Physiological Society, 1987, sect. 4, vol. II, chapt. 43, p. 999-1022.
185. Lundin G. Nitrogen elimination during oxygen breathing. *Acta Physiol Scand* 30 (Suppl 111): 130-143, 1953.
186. Macklem PT, Mead J. Resistance of central and peripheral airways measured by a retrograde catheter. *J Appl Physiol* 22: 395-401, 1967.
187. Mahon RT, Kerr S, Amundson D, Parrish JS. Immersion pulmonary edema in special forces combat swimmers. *Chest* 122: 383-384, 2002.
188. Maio DA, Farhi LE. Effect of gas density on mechanics of breathing. *J Appl Physiol* 23: 687-693, 1967.
189. Mapleson WW. Quantitative prediction of anesthetic concentrations. In: Papper EM, Kitz RJ, editors. *Uptake and Distribution of Anesthetic Agents*. New York: McGraw-Hill, 1962, p. 104-119.
190. Marshall JM. Nitrogen narcosis in frogs and mice. *Am J Physiol* 166: 699-710, 1951.
191. McClaran SR, Wetter TJ, Pegelow DF, Dempsey JA. Role of expiratory flow limitation in determining lung volumes and ventilation during exercise. *J Appl Physiol* 86: 1357-1366, 1999.
192. McDonough PM, Hemmingsen EA. Bubble formation in crustaceans following decompression from hyperbaric gas exposure. *J Appl Physiol* 56: 513-519, 1984.
193. McMahon TJ, Moon RE, Luschinger BP, Carraway MS, Stone AE, Stolp BW, Gow AJ, Pawloski JR, Watke P, Singel DJ, Piantadosi CA, Stamler JS. Nitric oxide in the human respiratory cycle. *Nature Med* 8: 711-717, 2002.
194. Menn SJ, Sinclair RD, Welch BE. Effect of inspired CO<sub>2</sub> up to 30mmHg on response of normal man to exercise. *J Appl Physiol* 28: 663-671, 1970.
195. Miller JN. Physiological limits to breathing dense gas. In: Lundgren CEG, Warkander DE, editors. *Physiological and Human Engineering Aspects of Underwater Breathing Apparatus. Proceedings of the 40th Undersea and Hyperbaric Medical Society Workshop*. Washington, DC: Undersea & Hyperbaric Medical Society, 1989, p. 5-18.
196. Mitchell SJ. Immersion pulmonary oedema. *South Pacific Underwater Med Soc J* 32: 200-204, 2002.
197. Mitchell SJ, Bennett MH. Clearance for diving and fitness for work. In: Neuman TS, Thom SR, editors. *The Physiology and Medicine of Hyperbaric Oxygen Therapy*. Philadelphia: Saunders, 2008, p. 65-94.
198. Mitchell SJ, Cronje F, Meintjes WAJ, Britz HC. Fatal respiratory failure during a technical rebreather dive at extreme pressure. *Aviat Space Environ Med* 78: 81-86, 2007.
199. Momson C. *Report on the Use of Helium Oxygen Mixtures for Diving* (Research Report 2). Washington, DC: Navy Experimental Diving Unit, 1939.
200. Moon RE, Cherry AD, Stolp BW, Camporesi EM. Pulmonary gas exchange in diving. *J Appl Physiol* 106: 668-677, 2009.
201. Moon RE, Gorman DF. Treatment of decompression disorders. In: Brubakk AO, Neuman TS, editors. *Bennett and Elliott's Physiology and Medicine of Diving* (5th ed). Edinburgh, UK: Saunders, 2003, p. 600-650.
202. Moon RE, Gorman DF. Decompression sickness. In: Neuman TS, Thom SR, editors. *The Physiology and Medicine of Hyperbaric Oxygen Therapy*. Philadelphia: Saunders, 2008, p. 283-320.
203. Morrison JB, Florio JT, Butt WS. Observations after loss of consciousness underwater. *Undersea Biomed Res* 5: 179-187, 1978.

204. Moulder PV, Lancaster JR, Harrison RW, Michel SL, Snyder M, Thompson RG. Pulmonary arterial hyperoxia producing increased pulmonary vascular resistance. *J Thorac Cardiovasc Surg* 40: 588-601, 1960.
205. Mummery HJ, Stolp BW, Dear G deL, Doar PO, Natoli MJ, Boso AE, Archibold JD, Hobbs GW, El-Moalem HE, Moon RE. Effects of age and exercise on physiological dead space during simulated dives at 2.8 atm abs. *J Appl Physiol* 94: 507-517, 2003.
206. Nairn JR, Power GG, Hyde RW, Forster RE, Lambertsen CJ, Dickson J. Diffusing capacity and pulmonary capillary blood flow at hyperbaric pressures. *J Clin Invest* 44: 1591-1599, 1965.
207. Naval Sea Systems Command. *U.S. Navy Diving Manual*. Arlington, VA: Naval Sea Systems Command, 2008.
208. Navy Department. *Diving Manual*. Washington, DC: Navy Department, 1916.
209. Neuman TS, Thom SR. *The Physiology and Medicine of Hyperbaric Oxygen Therapy*. Philadelphia: Saunders, 2008.
210. Nishi RY, Lauckner GR. *Development of the DCIEM 1983 Decompression Model for Compressed Air Diving* (Report 84-R-88). Downsview, Ontario, Canada: Defence and Civil Institute of Environmental Medicine, 1984.
211. Novotny JA, Mayers DL, Parsons Y-FJ, Survanshi SS, Weathersby PK, Homer LD. Xenon kinetics in muscle are not explained by a model of parallel perfusion-limited compartments. *J Appl Physiol* 68: 876-890, 1990.
212. Ohta Y, Farhi LE. Cerebral gas exchange: Perfusion and diffusion limitations. *J Appl Physiol* 46: 1164-1168, 1979.
213. Paiva M, Engel LA. Pulmonary interdependence of gas transport. *J Appl Physiol* 47: 296-305, 1979.
214. Peacher DF, Pecorella SRH, Freiburger JJ, Natoli MJ, Schinazi EA, Doar O, Boso AE, Walker AJ, Gill M, Kernagis D, Ugucioni D, Moon RE. Effects of hyperoxia on ventilation and pulmonary hemodynamics during immersed prone exercise at 4.7 atm abs: Possible implications for immersion pulmonary edema. *J Appl Physiol* 109: 68-78, 2010.
215. Pedley TJ, Schroter RC, Sudlow MF. The prediction of pressure drop and variation of resistance within the human bronchial airways. *Resp Physiol* 9: 387-405, 1970.
216. Pendergast DR, Lindholm P, Wylegala J, Warkander D, Lundgren CEG. Effects of respiratory muscle training on respiratory sensitivity in SCUBA divers. *Undersea Hyperb Med* 33: 447-453, 2006.
217. Perl W, Rackow H, Salanitro E, Wolf GL, Epstein RM. Intertissue diffusion effect for inert fat-soluble gases. *J Appl Physiol* 20: 621-627, 1965.
218. Piantadosi C. Pulmonary gas exchange, oxygen transport, and tissue oxygenation. In: Neuman TS, Thom SR, editors. *The Physiology and Medicine of Hyperbaric Oxygen Therapy*. Philadelphia: Saunders, 2008, p. 133-158.
219. Piiper J, Scheid P. Diffusion and convection in intrapulmonary gas mixing. In: Farhi LE, Tenney SM, editors. *Handbook of Physiology*. Bethesda, MD: American Physiological Society, 1987, sect. 3, vol. IV, chapt. 4, p. 51-70.
220. Poon CS. Ventilatory control in hypercapnia and exercise: Optimization hypothesis. *J Appl Physiol* 62: 2447-2459, 1987.
221. Poon CS. Effects of inspiratory elastic load on respiratory control in hypercapnia and exercise. *J Appl Physiol* 66: 2400-2406, 1989.
222. Poon CS. Effects of inspiratory resistive load on respiratory control in hypercapnia and exercise. *J Appl Physiol* 66: 2391-2399, 1989.
223. Pope H, Holloway R, Campbell EJM. The effects of elastic and resistive loading of inspiration on the breathing of conscious man. *Respir Physiol* 4: 363-372, 1968.
224. Prausnitz JM. *Molecular Thermodynamics of Fluid-Phase Equilibria*. Englewood Cliffs, NJ: Prentice-Hall, 1969.
225. Prefaut C, Dubois F, Roussos C, Amaral-Marques R, Macklem PT, Ruff F. Influence of immersion to the neck in water on airway closure and distribution of perfusion in man. *Respir Physiol* 37: 313-323, 1979.
226. Prefaut C, Lupi-H E, Anthonisen NR. Human lung mechanics during water immersion. *J Appl Physiol* 40: 320-323, 1976.
227. Puy RJM, Hyde RW, Fisher AB, Clark JM, Dickson J, Lambertsen CJ. Alterations in the pulmonary capillary bed during early O<sub>2</sub> toxicity in man. *J Appl Physiol* 24: 537-543, 1968.
228. Reeves RB, Morin RA. Pressure increases oxygen affinity of whole blood and erythrocyte suspensions. *J Appl Physiol* 61: 486-494, 1986.
229. Ringqvist T. The ventilatory capacity in healthy subjects. *Scand J Clin Lab Invest* 18 (Suppl 88): 1-179, 1966.
230. Saltzman HA. Rational normobaric and hyperbaric oxygen therapy. *Ann Intern Med* 67: 843-852, 1967.
231. Saltzman HA, Salzano JV, Blenkarn GD, Kylstra JA. Effects of pressure on ventilation and gas exchange in man. *J Appl Physiol* 30: 443-449, 1971.
232. Salzano J, Rausch DC, Saltzman HA. Cardiorespiratory responses to exercise at a simulated seawater depth of 1,000 feet. *J Appl Physiol* 28: 34-41, 1970.
233. Salzano JV, Camporesi EM, Stolp BW, Moon RE. Physiological responses to exercise at 47 and 66 atm abs. *J Appl Physiol* 57: 1055-1068, 1984.
234. Sapoval B, Filoche M, Weibel ER. Smaller is better—but not too small: A physical scale for the design of the mammalian pulmonary acinus. *Proc Natl Acad Sci U S A* 99: 10411-10416, 2002.
235. Sejrnsen P. Shunting by diffusion of gas in skeletal muscle and brain. In: Johansen K, Burggren W, editors. *Cardiovascular Shunts: Phylogenetic, Ontogenic, and Clinical Aspects. Proceedings of the Alfred Benzon Symposium 21*. Copenhagen, Denmark: Munksgaard, 1985, p. 452-462.
236. Sejrnsen P, Tønnesen KH. Inert gas diffusion method for measurement of blood flow using saturation techniques. *Circ Res* 22: 679-693, 1968.
237. Sejrnsen P, Tønnesen KH. Shunting by diffusion of inert gas in skeletal muscle. *Acta Physiol Scand* 86: 82-91, 1972.
238. Shepard RH, Campbell EJM, Martin HB, Enns T. Factors affecting the pulmonary dead space as determined by single breath analysis. *J Appl Physiol* 11: 241-244, 1957.
239. Shepard RJ. The maximum sustained voluntary ventilation in exercise. *Clin Sci* 32: 167-76, 1967.
240. Sherman D, Eilender E, Shefer A, Kerem D. Ventilatory and occlusion-pressure responses to hypercapnia in divers and non-divers. *Undersea Biomed Res* 7: 61-74, 1980.
241. Shupak A, Weiler-Ravell D, Adir Y, Daskalovic YI, Ramon Y, Kerem D. Pulmonary oedema induced by strenuous swimming: a field study. *Respir Physiol* 121: 25-31, 2000.
242. Slade JB Jr, Hattori T, Ray CS, Bove AA, Cianci P. Pulmonary edema associated with scuba diving: Case reports and review. *Chest* 120: 1686-1694, 2001.
243. Slutsky AS. Gas mixing by cardiogenic oscillations: A theoretical quantitative analysis. *J Appl Physiol* 51: 1287-1293, 1981.
244. Smart DR, Bennett MH, Mitchell SJ. Transcutaneous oximetry, problem wounds and hyperbaric oxygen therapy. *Diving Hyperb Med* 36: 72-86, 2006.
245. Srinivasan RS, Gerth WA, Powell MR. Mathematical models of diffusion-limited gas bubble dynamics in tissue. *J Appl Physiol* 86: 732-741, 1999.
246. Srinivasan RS, Gerth WA, Powell MR. Mathematical model of diffusion-limited gas bubble dynamics in unstirred tissue with finite volume. *Ann Biomed Eng* 30: 232-246, 2002.
247. Srinivasan RS, Gerth WA, Powell MR. Mathematical model of diffusion-limited evolution of multiple gas bubbles in tissue. *Ann Biomed Eng* 31: 471-481, 2003.
248. Stolp BW, Moon RE, Salzano JV, Camporesi EM. 2,3 DPG levels during saturation diving to 650 msw. *Undersea Biomed Res* 12: 21, 1985.
249. Survanshi SS, Parker EC, Gummin DD, Flynn ET, Toner CB, Temple DJ, Ball R, Homer LD. *Human Decompression Trial with 1.3 ATA Oxygen in Helium* (Technical Report 98-09). Bethesda, MD: Naval Medical Research Institute, 1998.
250. Taunton JE, Banister EW, Patrick TR, Oforsagd P, Duncan WR. Physical work capacity in hyperbaric environments and conditions of hyperoxia. *J Appl Physiol* 28: 421-427, 1970.
251. Taylor NAS, Morrison JB. Effects of breathing-gas pressure on pulmonary function and work capacity during immersion. *Undersea Biomed Res* 17: 413-428, 1990.
252. Taylor NAS, Morrison JB. Static respiratory muscle work during immersion with positive and negative respiratory loading. *J Appl Physiol* 87: 1397-1403, 1999.
253. Teorell T. Kinetics of distribution of substances administered to the body, part II: The intravascular modes of administration. *Arch Int Pharmacodyn Ther* 57: 226-240, 1937.
254. Tepper RS, Lightfoot EN, Baz A, Lanphier EH. Inert gas transport in the microcirculation: Risk of isobaric supersaturation. *J Appl Physiol* 46: 1157-1163, 1979.
255. Thalmann ED. *Phase II Testing of Decompression Algorithms for Use in the U.S. Navy Underwater Decompression Computer* (Technical Report 1-84). Panama City, FL: Navy Experimental Diving Unit, 1984.
256. Thalmann ED. *Development of a Decompression Algorithm for Constant 0.7 ATA Oxygen Partial Pressure in Helium Diving* (Technical Report 1-85). Panama City, FL: Navy Experimental Diving Unit, 1985.
257. Thalmann ED. Rebreather basics. In: Richardson D, editor. *Proceedings of Rebreather Forum 2.0*. Redondo Beach, CA: Diving Science and Technology, 1996, p. 23-30.
258. Thalmann ED, Parker EC, Survanshi SS, Weathersby PK. Improved probabilistic decompression model risk predictions using linear-exponential kinetics. *Undersea Hyperb Med* 24: 255-274, 1997.
259. Thalmann ED, Sponholtz DK, Lundgren GEG. Effects of immersion and static lung loading on submerged exercise at depth. *Undersea Biomed Res* 6: 259-290, 1979.
260. Thalmann ED, Survanshi SS, Flynn ET. Direct comparison of the effects of He, N<sub>2</sub>, and wet or dry conditions on the 60 fsw no-decompression limit [abstract]. *Undersea Biomed Res* 16: 67, 1989.

261. Thavasothy M, Broadhead M, Elwell C, Peters M, Smith M. A comparison of cerebral oxygenation as measured by the NIRO 300 and the INVOS 5100 near-infrared spectrophotometers. *Anesthesia* 57: 999-1006, 2002.
262. Tikuisis P, Gault KA, Nishi RY. Prediction of decompression illness using bubble models. *Undersea Hyperb Med* 21: 129-143, 1994.
263. Tikuisis P, Gerth WA. Decompression theory. In: Brubakk AO, Neuman TS, editors. *Bennett and Elliott's Physiology and Medicine and Diving* (5th ed). Edinburgh: Saunders, 2003, p. 419-454.
264. Tikuisis P, Nishi RY, Weathersby PK. Use of the maximum likelihood method in the analysis of chamber air dives. *Undersea Biomed Res* 15: 301-313, 1988.
265. Trytko B, Mitchell SJ. Extreme survival: A deep technical diving accident. *South Pacific Underwater Med Soc J* 35: 23-7, 2005.
266. Van Der Aue OE, Kellar RJ, Brinton ES, Barron G, Gilliam HD, Jones RJ. *Calculation and Testing of Decompression Tables for Air Dives Employing the Procedure of Surface Decompression and the Use of Oxygen* (Research Report 13-51). Washington, DC: Navy Experimental Diving Unit, 1951.
267. Van Liew HD. Mechanical and physical factors in lung function during work in dense environments. *Undersea Biomed Res* 10: 255-264, 1983.
268. Van Liew HD. Simulation of the dynamics of decompression sickness bubbles and the generation of new bubbles. *Undersea Biomed Res* 18: 333-345, 1991.
269. Van Liew HD, Bishop B, Walder-D P, Rahn H. Effects of compression on composition and absorption of tissue gas pockets. *J Appl Physiol* 20: 927-933, 1965.
270. Van Liew HD, Conkin J, Burkard ME. The oxygen window and decompression bubbles: Estimates and significance. *Aviat Space Environ Med* 64: 859-865, 1993.
271. Van Liew HD, Hlastala MP. Influence of bubble size and blood perfusion on absorption of gas bubbles in tissue. *Resp Physiol* 7: 111-121, 1969.
272. Van Liew HD, Thalmann ED, Sponholtz DK. Hindrance to diffusive gas mixing in the lung in hyperbaric environments. *J Appl Physiol* 51: 243-247, 1981.
273. Verstappen FT, Bernards JA, Kreuzer F. Effects of pulmonary gas embolism on circulation and respiration in the dog, part II: Effects on respiration. *Pflugers Arch* 368: 97-104, 1977.
274. von Kummer R, Herold S. Hydrogen clearance method for determining local cerebral blood flow, part I: Spatial resolution. *J Cereb Blood Flow Metab* 6: 486-491, 1986.
275. von Kummer R, von Kries F, Herold S. Hydrogen clearance method for determining local cerebral blood flow, part II: Effect of heterogeneity in cerebral blood flow. *J Cereb Blood Flow Metab* 6: 492-498, 1986.
276. Vorosmarti J Jr, Barnard EE, Williams J, de GH. Nitrogen elimination during steady-state hyperbaric exposures. *Undersea Biomed Res* 5: 243-252, 1978.
277. Wagner PD. Insensitivity of  $\dot{V}O_2$ max to hemoglobin- $P_{50}$  at sea level and altitude. *Respir Physiol* 107: 205-212, 1997.
278. Wagner PD, Laravuso RB, Uhl RR, West JB. Continuous distributions of ventilation-perfusion ratios in normal subjects breathing air and 100%  $O_2$ . *J Clin Invest* 54: 54-68, 1974.
279. Wagner PD, Saltzman HA, West JB. Measurement of continuous distributions of ventilation-perfusion ratios: Theory. *J Appl Physiol* 36: 588-589, 1974.
280. Ward CA, Balakrishnan A, Hooper FC. On the thermodynamics of nucleation in weak gas-liquid solutions. *J Basic Eng* 92: 695-704, 1970.
281. Warkander DE. Development of a scrubber gauge for closed-circuit diving [abstract]. *Undersea Hyper Med* 34: 251, 2007.
282. Warkander DE, Lundgren CEG. Effects of graded combinations of resistance and elastance on divers' respiratory performance. *Undersea Hyper Med* 21, (Suppl): 96-97, 1994.
283. Warkander DE, Lundgren CEG. Effects of combinations of resistance and elastance on divers' respiratory performance during exposure to a negative static lung load [abstract]. *Undersea Hyper Med* 22 (Suppl): 71, 1995.
284. Warkander DE, Nagasawa GK, Lundgren CEG. Effects of inspiratory and expiratory resistance in divers' breathing apparatus. *Undersea Hyper Med* 28: 63-73, 2001.
285. Warkander DE, Norfleet WT, Nagasawa GK, Lundgren CE.  $CO_2$  retention with minimal symptoms but severe dysfunction during wet simulated dives to 6.8 atm abs. *Undersea Biomed Res* 17: 515-523, 1990.
286. Warkander DE, Norfleet WT, Nagasawa GK, Lundgren CEG. Physiologically and subjectively acceptable breathing resistance in divers' breathing gear. *Undersea Biomed Res* 19: 427-445, 1992.
287. Wasserman K. Testing regulation of ventilation with exercise. *Chest* 70 (Suppl): 173-178, 1975.
288. Weathersby PK, Mendenhall KG, Barnard EEP, Homer LD, Survanshi S, Vieras F. Distribution of xenon gas exchange rates in dogs. *J Appl Physiol* 50: 1325-1336, 1981.
289. Weathersby PK, Meyer P, Flynn ET, Homer LD, Survanshi S. Nitrogen gas exchange in the human knee. *J Appl Physiol* 61: 1534-1545, 1986.
290. Weibe R, Gaddy VL, Heins C. The compressibility isotherms of helium at temperatures from  $-70$  to  $200^\circ C$  and at pressures to 1000 atmospheres. *J Am Chem Soc* 53: 1721-1725, 1931.
291. Weibel ER, Sapoval B, Filoche M. Design of peripheral airways for efficient gas exchange. *Respir Physiol Neurobiol* 148: 3-21, 2005.
292. Whalen RE, Saltzman HA, Holloway DH, McIntosh HD, Sieker HO, Brown IW. Cardiovascular and blood gas responses to hyperbaric oxygenation. *Am J Cardiol* 15: 638-646, 1965.
293. Whitelaw WAJ, Derenne JP, Milic-Emili J. Occlusion pressure as a measure of respiratory centre output in conscious man. *Respir Physiol* 23: 181-199, 1975.
294. Willmon TL, Behnke AR. Nitrogen elimination and oxygen absorption at high barometric pressure. *Am J Physiol* 131: 633-638, 1940.
295. Wilmshurst PT, Crowther A, Nuri M, Webb-Peploe MM. Cold-induced pulmonary oedema in scuba divers and swimmers and subsequent development of hypertension. *Lancet* i: 62-65, 1989.
296. Wilmshurst PT, Nuri M, Crowther A, Webb-Peploe MM. Forearm vascular responses in subjects who develop recurrent pulmonary edema when scuba diving; a new syndrome. *Br Heart J* 45 (Suppl): A349, 1982.
297. Wolpers HG, Hoefl A, Korb H, Lichtlen PR, Hellige G. Transport of inert gases in mammalian myocardium: Comparison with a convection-diffusion model. *Am J Physiol* 259: H167-H173, 1990.
298. Wood LDH, Bryan AC. Effect of increased ambient pressure on flow-volume curve of the lung. *J Appl Physiol* 27: 4-8, 1969.
299. Wood LDH, Bryan AC. Exercise ventilatory mechanics at increased ambient pressure. *J Appl Physiol* 44: 231-237, 1978.
300. Wood LDH, Bryan AC, Bau SK, Weng TR, Levison H. Effect of increased gas density on pulmonary gas exchange in man. *J Appl Physiol* 41: 206-210, 1976.
301. Workman RD. *Calculation of Decompression Schedules for Nitrogen-Oxygen and Helium-Oxygen Dives* (Research Report 6-65). Washington, DC: Navy Experimental Diving Unit, 1965.
302. Young C, D' Aoust BG. Factors determining temporal pattern of isobaric supersaturation. *J Appl Physiol* 51: 852-857, 1981.
303. Yount DE, Hoffman DC. On the use of a bubble formation model to calculate diving tables. *Aviat Space Environ Med* 57: 149-156, 1986.
304. Yount DE, Lally DA. On the use of oxygen to facilitate decompression. *Aviat Space Environ Med* 51: 544-550, 1980.
305. Yount DE, Maiken EB, Baker EC. Implications of the varying permeability model for reverse dive profiles. In: Lang MA, Lehner CE, editors. *Proceedings of the Reverse Dive Profiles Workshop*. Washington, DC: Smithsonian Institution, 2000, p. 29-60.
306. Zechman F, Hall FG, Hull WE. Effects of graded resistance to tracheal air flow in man. *J Appl Physiol* 10: 356-362, 1957.